THE UNIVERSITY OF CHICAGO

HOST AND VIRAL REGULATION OF INNATE IMMUNITY TO INFECTION

A DISSERTATION SUBMITTED TO

THE FACULTY OF THE DIVISION OF THE BIOLOGICAL SCIENCES

AND THE PRITZKER SCHOOL OF MEDICINE

IN CANDIDACY FOR THE DEGREE OF

DOCTOR OF PHILOSOPHY

COMMITTEE ON MICROBIOLOGY

BY

REBECCA ANNE REIS

CHICAGO, ILLINOIS

AUGUST 2023

TABLE OF CONTENTS

LIST OF FIGURES V

ACKNOWLEDGMENTS VI

ABSTRACT VII

1 INTRODUCTION 1

1.1 Innate Immune PRRs Sense Viral Infetion 1
1.1.1 PRRs detect conserved PAMPs to initiate a rapid and effective innate immune response 1
1.1.2 The RLRs initiate an antiviral signaling pathway in response to cytoplasmic RNA 2
1.1.3 Dephosphorylation by PP1 is necessary for RLR activity 4
1.1.4 R12C is a PP1 subunit that regulates cytoskeleton dynamics 5
1.1.5 Perturbation of the host cytoskeleton during viral infection 6
1.2 IFNs produced in response to infection induce a STAT1-mediated antiviral response 8
1.2.1 Identification and classification of IFNs 8
1.2.2 IFNs induce ISGs via the JAK-STAT pathway 9
1.2.3 Activation of STAT1 10
1.2.4 STAT1 targeting by viral proteins 14
1.3 Noroviruses and the innate immune response to their infection 15
1.3.1 Norovirus discovery and disease burden 15
1.3.2 MNV as a model for human noroviruses 16
1.3.3 Norovirus NS5 has multiple functions 17
1.3.3 TAG-dependent and -independent IFN-γ immune responses 19

2 THE PHOSPHATASE REGULATORY SUBUNIT PPP1R12C MEDIATES VIRUS-INDUCED DEPHOSPHORYLATION OF THE RIG-I-LIKE RECEPTORS BY PP1 21

2.1 Abstract 21
2.2 Introduction 22
2.3 Results 24
2.3.1 R12C is an important component of the RLR pathway 24
2.3.2 A complete RLR-mediated antiviral response requires R12C 27
2.3.3 R12C is critical for inhibition of viral restriction 33
2.3.4 The function of R12C in the innate immune response is to target PP1 to the RLRs, inducing their dephosphorylation 35
2.3.5 Virus-induced actin perturbations trigger R12C relocalization and targeting of PP1 to the RLRs 41
2.4 Discussion 47
2.5 Materials and Methods 49

3 INHIBITION OF IFN-γ-MEDIATED STAT1 ACTIVATION BY NOROVIRUS 59

3.1 Abstract 59
3.2 Introduction 60
3.3 Results 62

3.3.1 MNV actively inhibits the TAG-independent IFN-γ antiviral pathway..... 62
3.3.2 The MNV protein NS5 antagonizes the IFN-γ-induced antiviral response 63
3.3.3 Complete STAT1 activation is inhibited in the presence NS5..... 68
3.3.5 NS5 prevents the nuclear accumulation of STAT1 in response to IFN . 75
3.4 Discussion..... 80
3.5 Materials and Methods 81
4 CONCLUSIONS 91
4.1 Overview of Results..... 91
4.2 Concluding remarks and perspectives..... 92
4.2.1 Regulation of R12C activity in actin dynamics and innate immune signaling..... 92
4.2.2 Actin perturbation as a potential regulator of multiple sensors in response to infection with diverse pathogens..... 94
4.2.3 Implications of different types of virus-induced actin rearrangement of the activation of RLRs 95
4.2.4 RLR dephosphorylation by R12C in autoimmune disorders and vaccine development 96
4.2.5 Not all ISGs are created equal: only a subset of ISGs are needed for viral restriction..... 96
4.2.6 The potential regulation of STAT1 by human noroviruses..... 98
REFERENCES 99

LIST OF FIGURES

2.1 The phosphatase regulatory subunit R12C plays a critical role in type I interferon induction by contributing to RLR activation
2.2 Depletion of R12C inhibits IFN-β induction in response to viral infection
2.3 Knockout of R12C in HEK 293T reduces IFN-β protein production upon infection with SeV
2.4 Virus-induced IFN-β and ISG expression is reduced in HAP1 R12C knockout cells
2.5 ISG upregulation is reduced in Ppp1r12C knockout primary mouse dermal fibroblasts stimulated with poly(I:C) or viral infection
2.6 R12C knockout HEK 293T cells support viral replication to higher titers than WT cells
2.7 R12C expression is not upregulated during viral infection
2.8 The C-terminal domain of R12C interacts with the RLR CARD domains
2.9 PP1 binding to the RLRs is ablated by the loss of R12C
2.10 R12C-mediated IFN-β induction is dependent on RLR dephosphorylation
2.11 Viral infection triggers actin remodeling and R12C relocalization
2.12 The actin perturbing agent CytoD induces RLR dephosphorylation but not IFN-β induction
2.13 Transfection reagents induce RLR dephosphorylation but not IFN-β transcription
3.1 IFN-ɣ-mediated inhibition of several RNA viruses is not dependent on TAG
3.2 Norovirus NS5 inhibits INFɣ-mediated viral restriction
3.3 Mass spectrometry analysis of NS5 binding partners
3.4 NS5 inhibits the induction of a subset of ISGs
3.5 Norovirus NS5 inhibits STAT1 serine phosphorylation
3.6 Loss of STAT1 serine phosphorylation does not prevent IFN-ɣ restriction of viral replication
3.7 Norovirus infection inhibits nuclear accumulation of STAT1
3.8 Norovirus infection inhibits nuclear accumulation of phosphorylated STAT1
3.9 Nuclear accumulation of STAT1 and STAT2 during MNV infection after IFNβ stimulation
3.10 NS5 inhibits nuclear accumulation of STAT1

ACKNOWLEDGMENTS

I have had the privilege of working with not one, but two mentors on my dissertation research. Firstly, I would like to thank Dr. Michaela Gack for her guidance and training for the first part of my PhD. From my time working with Michaela, I learned the precision and perseverance that make me the researcher I am today.

I am incredibly thankful for the mentorship of my second advisor Dr. Glenn Randall. Glenn has always advocated for me and supported me through even the most difficult situations. Your unwavering support and mentorship continues to inspire me as a scientist.

I would additionally like to thank my thesis committee—Dr. Raymond Roos, Dr. Dominique Missiakas, and Dr. Jueqi Chen—for their expertise, insightful questions, and support both academically and personally.

The work presented here would not have been possible without Dr. Dhiraj Acharya and Dr. Soowon Kang, two postdoctoral fellows who contributed significantly to these projects. Thank you for generously sharing your expertise and always being willing to offer help and answer questions.

Finally, I am deeply thankful to the friends and family who have supported me personally throughout all the trials and triumphs of my PhD. Thank you.

ABSTRACT

The outcome of a viral infection is determined by the balance between host antiviral defenses and viral evasion strategies. To achieve the best possible outcome during infection the host utilizes pattern recognition receptors (PRRs) to rapidly and specifically detect the presence of an invading virus. One class of PRRs, the RLRs, integrate two distinct signals; cytoplasmic RNA and virus-induced cytoskeletal changes to reliably and quickly promote an antiviral response mediated by interferons (IFNs), which induce the expression of interferon stimulated genes (ISGs). On the other hand, viruses such as murine norovirus (MNV) have evolved to combat the host immune response by encoding multifunction proteins, such as NS5, which can inhibit the host's IFN response by preventing the activation of the critical signal transducer STAT1. An understanding of the interplay between the host immune response and the corresponding mechanisms of viral subversion can help us tip the balance in favor of host survival by developing therapeutics that bolster the immune response or inhibit viral immune antagonists.

CHAPTER 1

INTRODUCTION

1.1 Innate immune PRRs sense viral infection

1.1.1 PRRs detect conserved PAMPs to initiate a rapid and effective innate immune response

During viral infection, the host's quickest means of defense is the innate immune response. To mount a rapid antiviral innate immune response, the host cell must first be able to quickly and reliably detect an infection. For this specific purpose, the host employs an array of proteins that act as pattern recognition receptors (PRRs), which identify and respond to conserved pathogen motifs known as pathogen-associated molecular patterns (PAMPs). One commonly detected PAMP is the presence of nucleic acids in unusual cellular compartments or with atypical modifications (Hartman, 2017; Paludan & Bowie, 2013). For example, the cyclic GMP–AMP synthase (cGAS)/ stimulator of interferon genes (STING) pathway senses cytosolic DNA, while virus and host-derived RNAs produced during infection can be detected by the Toll-like receptors (TLRs) or the retinoic acid-inducible gene I (RIG-I)-like receptors (RLR) depending on their location (Goubau et al., 2013; Paludan & Bowie, 2013; Kawai & Akira, 2010; Meylan et al., 2006). In response to the detection of nucleic acid PAMPs, host PRRs trigger the secretion of cytokines, notably interferons (IFNs), which bind to specialized receptors and initiate antiviral defenses in the infected and neighboring cells (Meylan et al., 2006; Goubau et al., 2013; Paludan & Bowie, 2013).

1.1.2 The RLRs initiate an antiviral signaling pathway in response to cytoplasmic RNA

The RLRs are the primary sensors of cytoplasmic RNA during viral infection. This family consists of three members: RIG-I, melanoma differentiation-associated protein 5 (MDA5), and laboratory of genetics and physiology 2 (LGP2). Of these three members, the functions of RIG-I and MDA5 have been well characterized; however, the role of LGP2 is less clear. From what is currently known, LGP2's primary function seems to be regulating the function of RIG-I and MDA5 rather than signaling on its own (Venkataraman et al., 2007; Yoneyama et al., 2005). Because of this difference, LGP2 will not be discussed further here, and 'the RLRs' will be used to refer to RIG-I and MDA5 specifically.

In uninfected cells, RIG-I and MDA5 reside as inactive monomers in the cytoplasm. The RLRs can become activated after exposure to virus- or host-derived RNAs with key features not typically found in the absence of infection (Rehwinkel & Gack, 2020; Loo & Gale, 2011; Goubau et al., 2013). RIG-I recognizes shorter RNAs, particularly ones with di- or tri-phosphates at their 5' end (Yoneyama & Fujita, 2008). MDA5, on the other hand, recognizes longer dsRNAs and has no specificity for 5' phosphorylated RNAs (Yoneyama et al., 2005). RNA recognition requires the direct interaction of the helicase domain of RIG-I or MDA5 with a suitable RNA ligand (Reikine et al., 2014; Yoneyama & Fujita, 2008). In addition, the C-terminal domain (CTD) of RIG-I also forms contacts with 5′ triphosphate (5′-ppp) moieties present on stimulatory RNAs; however, the CTD of MDA5 does not (Reikine et al., 2014; Yoneyama & Fujita, 2008). Because RIG-I and MDA5

recognize distinct RNA ligands, they have the capacity to respond to different but overlapping families of viruses. This may explain in part why cells encode both RIG-I and MDA5 when both sensors detect the same PAMP.

The binding of an RNA ligand to the helicase domain of RIG-I or MDA5 activates the ATPase activity of these sensors and triggers a conformational change in RIG-I (Jiang et al., 2011; Yoneyama & Fujita, 2008). This activity, as well as RNA binding itself, facilitates the oligomerization of the RLR caspase activation and recruitment domains (CARDs), which are responsible for signaling transduction in response to infection (Peisley et al., 2013; Yu et al., 2018). In addition, RLR multimerization is also dependent on several post-translational modifications. In uninfected cells, CARD domain interaction is prevented by serine phosphorylation at serine 8 (S8) of RIG-I and serine 88 (S88) of MDA5 (Gack et al., 2010; Wies et al., 2012). In order for RIG-I and MDA5 to oligomerize during viral infection, this modification must be removed by the phosphatases PP1α and PP1γ (Wies et al., 2012). The ubiquitination and ISGylation of RIG-I and MDA5, respectively, also contribute to the formation and stability of RLR oligomers (Peisley et al., 2014; Liu et al., 2021). CARD oligomerization is necessary for their activation of the corresponding CARD domains of the downstream adaptor mitochondrial antiviral-signaling protein (MAVS) to promote the initiation of an antiviral signaling cascade. Activated MAVS also oligomerizes forming prion-like structures which act as a scaffold for the activation of signaling molecules immediately downstream (Wu & Hur, 2015). MAVS filaments promote the activation of TANK-binding kinase 1 (TBK1) and IκB kinase-ε (IKKε), which in turn activate the transcription factors interferon regulatory factor 3

(IRF3), IRF7, and nuclear factor-κB (NF-κB) which promote the transcription of cytokines, including interferons (Liu et al., 2015).

1.1.3 Dephosphorylation by PP1 is necessary for RLR activity

While all steps in the activation of the RLRs are important for their full antiviral activity, dephosphorylation of the RLRs by PP1 is unique because PP1 is the only described enzyme that positively regulates the activation of both RIG-I and MDA5. RLR CARD domain dephosphorylation is also particularly important because it allows for the signaling domains to oligomerize and interact with additional, downstream factors. If the dephosphorylation of RIG-I and MDA5 is prevented, either by substituting the phosphorylated residues with phosphomimetic amino acids or by knocking down the phosphatase, the RLR-mediated antiviral response is inhibited (Weis et al., 2012). Despite how important this component of the RLR pathway is, we still do not fully understand how the dephosphorylation of RIG-I and MDA5 by PP1 is regulated.

The human genome encodes upwards of 400 kinases that specifically phosphorylate a wide range of proteins (Cohen, 2002). In contrast, there are only about 150 known phosphatases, of which only a few are needed to accomplish most cellular dephosphorylation reactions (Virshup & Shenolikar, 2009; Moorhead et al., 2007; Cohen, 2002). PP1α and PP1γ belong to the superfamily of serine-threonine phosphatases known as the phosphoprotein phosphatases (PPPs), which together are responsible for the majority of dephosphorylation reactions in the cell (Moorhead et al., 2007). PP1 is a holoenzyme composed of a catalytic subunit (PP1c), which dephosphorylates a wide

range of substrates, and one or more PP1 regulatory subunits (Virshup & Shenolikar, 2009; Heroes et al., 2012). While there are only three isoforms of the PP1 catalytic subunit, to date there are more than 200 PP1 regulatory subunits have been identified or predicted (Cohen, 2002; Korrodi-Gregório et al., 2014). These regulatory subunits are largely unrelated at the level of sequence and structure, although many contain a conserved RVxF PP1 binding motif (Cohen, 2002; Heroes et al., 2012). Association with a particular regulatory subunit can positively or negatively regulate PP1's activity toward different cellular targets and allow PP1 to catalyze a multitude of reactions without being completely promiscuous (Heroes et al., 2012; Cohen, 2002; Korrodi-Gregório et al., 2014).

Despite catalyzing the dephosphorylation of a plethora of proteins at any given time in the cells, PP1 only dephosphorylates the RLRs specifically during infection. PP1's activity in this case cannot be attributed to the presence of the protein alone as PP1 is ubiquitously expressed and its expression is not enhanced during viral infection (Wies et al., 2012). Rather, based on previously established principles of PP1 activity, it is likely that specific PP1 regulatory subunits are needed to direct PP1's activity toward the RLRs. However, the identity of these regulatory subunits has not previously been characterized.

1.1.4 R12C is a PP1 subunit that regulates cytoskeleton dynamics

PPP1R12C (hereafter 'R12C') was first identified in 2001 as part of a screen for kinase substrates (Tan et al., 2001). Based on its similarity to other PP1 regulatory subunits, R12C was hypothesized to regulate PP1 activity toward myosin light chain (Tan

et al., 2001). R12C itself has not been well characterized; however, it is part of a group of PP1 regulatory subunits termed myosin phosphatase targeting subunits (MYPTs), which we know a little more about (Ito et al., 2004; Grassie et al., 2011). The MYPTs target PP1 to myosin regulatory light chain inducing its dephosphorylation at serine 19 (S19). Phosphorylation at this site is an activating modification that facilitates the ATPase activity of myosin and enhances myosin-dependent cytoskeleton changes (Vicente-Manzanares, et al., 2009, Ito et al., 2004). Therefore, MYPT-directed PP1 dephosphorylation of the regulatory light chain inhibits myosin activity and reduces its association with actin (Grassie et al., 2011; Vicente-Manzanares, et al., 2009). R12C association with PP1 and myosin light chain was confirmed and its ability to induce myosin dephosphorylation was shown to be regulated by phosphorylation at two sites: threonine 560 (T560) and serine 452 (S452) (Tan et al., 2001; Ito et al., 2004; Grassie et al., 2011; Banko et al., 2011). Aside from what little is known about its function in regulating the cytoskeleton, no other functions or substrates have previously been attributed to R12C.

1.1.5 Perturbation of the host cytoskeleton during viral infection

Viruses have evolved to exploit and remodel the host cell's actin cytoskeleton to facilitate many stages of their lifecycle, such as entry, intracellular transport, virion assembly, and egress (Döhner & Sodeik, 2005; Taylor et al., 2011). During viral entry, the cortical actin network acts as a physical barrier that the virus must cross during endocytosis or membrane fusion. However, viruses have adapted to also use the cortical actin network to their own advantage by coopting the host's cytoskeleton to facilitate various entry processes (Taylor et al., 2005). Actin can be used by viruses such as

hepatitis C virus (HCV), human immunodeficiency virus (HIV), and vesicular stomatitis virus (VSV) to move across the cell surface, or to cluster virus receptors to promote receptor-mediated entry (Grove & Marsh, 2011; Taylor et al., 2005). In addition, actin has some involvement in every known endocytic process used for viral entry (Mercer et al., 2012; Taylor et al., 2005). After entry, viruses often utilize the cytoskeleton as a means of transporting viral proteins and genomes to sites of replication, assembly, and egress (Radtke et al., 2006; Sodeik, 2000; Ploubidou & Way, 2001). When newly synthesized viral particles are ready, they again encounter the same actin barrier that they overcame during entry; however, actin is also critical to many viral egress strategies such as budding and formation of actin comets (Taylor et al., 2005).

Because changes in the actin cytoskeleton are such a ubiquitous feature of the viral life cycle, changes in actin dynamics are an attractive target for PRRs; however, it is little studied. Previous studies have demonstrated that actin perturbation by bacterial effectors or by pharmacological means resulted in NOD-like receptor (NLR) activation of NF-κB (Legrand-Poels et al., 2007; Bielig et al., 2014). Activation of the NLRs was shown to be mediated by cytoskeleton-associated small Rho GTPases, providing a link between actin perturbation and activation of the innate immune response (Legrand-Poels et al., 2007; Bielig et al., 2014; Keestra et al., 2013). However, a thorough investigation of the effects of virus-specific actin disturbances on the activation of PRRs, particularly the RLRs has not been conducted.

1.2 IFNs produced in response to infection induce a STAT1-mediated antiviral response

1.2.1 Identification and classification of IFNs

Interferons were first discovered as secreted factors that inhibit viral replication and were named because they 'interfered' with viral replication (Isaacs & Lindenmann, 1957; Isaacs et al., 1957). There are three known classes of interferons (IFNs); type I, II, and III. Type I interferons in humans include thirteen α interferons, IFN-β, IFN-ε, IFN-κ, and IFN-ω. Mice have an additional IFN-α as well as IFN-ζ. In both mice and humans, type I interferons share significant structural similarities (Lazear et al., 2019; Platanias, 2005). In contrast, type II interferons consist of only a single member in mammals; IFN-γ, which, unlike type I interferons, forms a dimer (Platanias, 2005). The most recently discovered class of IFN, type III, consists of IFN-λ1, IFN-λ2, IFN-λ3, and IFN-λ4 in humans, but only IFN-λ2 and IFN-λ3 exist in mice (Lazear et al. 2019). All three classes of IFNs inhibit viral replication by binding to specific cellular receptors and triggering signaling pathways leading to the upregulation of interferon stimulated genes (ISGs), which are responsible for the virus-restricting phenotype initially observed.

One question that has arisen is, why do mammals have all three types of IFN instead of just one when all of them lead to the production of ISGs? While it is true that there is some redundancy between the three IFN types, they each also have their own unique functions. Although type I and type III IFN both activate the same signaling pathway downstream of their individual receptors, studies have shown that these two types of IFN are produced by different cell types. While type I IFN is expressed ubiquitously, type II IFN is expressed primarily in epithelial cells, suggesting IFN-λs

provide additional antiviral protection at epithelial barriers (Wack et al., 2015; Lazear et al. 2019). Additionally, despite sharing overlapping pathways, type III IFN induces less of an inflammatory response than type I IFN, which may be beneficial in some circumstances (Wack et al., 2015; Lazear et al. 2019). Unlike type I and type III IFN, type II IFN utilizes a slightly different pathway downstream of its receptor. This allows IFN-γ to upregulate an overlapping but slightly different set of ISGs with different antiviral functions (Platanias, 2005; Liu et al., 2012; Begitt et al., 2014). INF-γ is also the only IFN that can upregulate the class II antigen-presenting pathway, suggesting a unique role for type II IFN in the implementation of an adaptive immune response (Platanias, 2005; Schroder et al., 2003). Finally, having partial redundancy between all three IFN pathways may be beneficial to the host since it creates the potential for compensation if one of the IFN pathways is antagonized during viral infection.

1.2.2 IFNs induce ISGs via the JAK-STAT pathway

While each class of IFN may have multiple members, all IFNs of a particular type are recognized by the same receptor. Type I IFNs bind to and signal through the interferon-alpha receptor (IFNAR), a heterodimer composed of IFNAR1 and IFNAR2 (Lazear et al., 2019; Platanias, 2005). IFN-γ is recognized by the interferon-gamma receptor (IFNGR) comprised of IFNGR1 and IFNGR2 (Platanias, 2005). Type III IFNs also bind to their own specific receptor, the interferon-lambda receptor (INFLR), which like the other IFN receptors, is a dimer, in this case of IFNLR1 and IL10Rβ (Lazear et al. 2019). Binding of IFNs to their receptors results in receptor rearrangement and dimerization which acts as a signal for downstream proteins.

The binding of interferons to their receptors initiates a signaling cascade culminating in an antiviral response. The first step in this pathway is the activation of receptor-associated tyrosine kinases. Type I and type III IFN binding induce receptor dimerization which triggers the autophosphorylation of tyrosine kinase 2 (TYK2) and Janus activated kinase 1 (JAK1) (Platanias, 2005; Lazear et al. 2019). Type II IFN also induces conformational changes and receptor dimerization but this results in the activation of JAK1 and JAK2 (Platanias, 2005). The phosphorylated forms of TYK2, JAK1, and JAK2 are active and subsequently phosphorylate signal transducers and activators of transcription (STATs) at conserved tyrosine residues, which is critical for JAK-STAT mediated signaling (Villarino et al., 2017). Once phosphorylated, STATs can form homo- or heterodimer complexes, which are translocated to the nucleus where they upregulate genes with antiviral activities (Villarino et al., 2017).

1.2.3 Activation of STAT1

In mammals, there are seven known STATs (STAT1, 2, 3, 4, 5A, 5B, and 6). All the STATs share a similar domain architecture consisting of an N-terminal domain, which mediates protein-protein interactions, a central core domain comprising 1) a coiled-coil domain, 2) a DNA binding domain which also contains noncanonical nuclear import and export signals, 3) linker domain, and 4) SH2 domain, which is important for dimerization, a transactivation domain necessary for promoting transcription, and a C-terminal domain (Villarino et al., 2017; Levy & Darnell, 2002). The most well-characterized STAT is STAT1, which is activated by all three types of IFNs. In unstimulated cells, STAT1 is unphosphorylated and resides predominantly in the cytoplasm as a dimer (Mao et al.

2005; Zhong et al. 2005; Wenta et al. 2008). Some STAT1 is found in the nucleus of uninfected cells and is necessary for the constitutive expression of genes unrelated to the antiviral response (Meyer et al., 2002). Non-phosphorylated STAT1 dimers adopt primarily an antiparallel conformation, mediated by an interaction between the coiled-coil domain and DNA binding domains of opposing monomers, but can also form parallel conformation with the N-terminal domains forming a connection between the monomers (Mao et al. 2005; Zhong et al. 2005). Dimerization between the unphosphorylated forms of STAT1 and STAT2 has also been described in an analogous antiparallel orientation (Wang et al. 2020).

Upon IFN stimulation, STAT1 is phosphorylated by activated JAKs at tyrosine 701 (Y701) within the transactivation domain. Phosphorylation of STAT1 at this tyrosine site stabilizes parallel STAT1 dimers via reciprocal interactions between the phosphorylated domains (Chen et al. 1998; Zhong et al. 2005; Wang et al. 2020). In the case of type I and type III IFN signaling, STAT1 primarily forms heterodimers with STAT2 which also associate with interferon regulatory factor 9 (IRF9) as part of a heterotrimeric complex known as IFN-stimulated gene factor 3 (ISGF3) (Platanias, 2005; Rengachari et al. 2017). Exposure to type II IFN; however, promotes the formation of STAT1 homodimers (Platanias, 2005).

Once phosphorylated and dimerized, STAT1 complexes must translocate to the nucleus to carry out their transcription-activating functions. Nuclear import of activated STAT1 dimers is dependent on tyrosine phosphorylation and proceeds through a mechanism independent of the import of nonphosphorylated STAT1 (Meyer et al., 2002). While phosphorylation-dependent dimer stabilization precedes nuclear import, only one

functional NLS is required per dimer for import (McBride et al. 2002). Therefore, it is likely that STAT1 dimerization induces a conformational change that promotes the accessibility of the NLS to import factors. Import of phospho-STAT1 complexes is dependent on a noncanonical nuclear localization signal (NLS) within the DNA binding domain of STAT1, which interacts directly with the import factor importin-α5 (Sekimoto et al. 1997; McBride et al. 2002; McBride & Reich 2003; Fagerlund et al. 2002). As a member of the Importin-α family, Importin-α5 acts as an adaptor for Importin-β by directly binding to cargo for transport (Tessier et al., 2019). Once the Importin-α/Importin-β/phospho-STAT1 complex is formed in the cytoplasm it can be shuttled into the nucleus through the nuclear pore complex (Tessier et al., 2019). Inside the nucleus, the STAT import complex associates with the GTPase Ran in its GTP-bound form inducing the dissolution of the importin complex and releasing STAT1 so that it can associate with DNA (Tessier et al., 2019; McBride & Reich, 2003).

Even after nuclear translocation, STAT1 requires additional steps to achieve full transcriptional activity. Within the nucleus, STAT1 can be subsequently phosphorylated at serine 727 (S727) of the C-terminal domain (Zhang et al., 1998; Bancerek et al. 2013; Sadzak et al). Serine phosphorylation of STAT1 modulates its transcriptional activity and is necessary for full activation but depends on tyrosine phosphorylation and nuclear accumulation (Sazak et al. 2008; Bancerek et al. 2013). In addition, STAT1 mutants that do not impact STAT1 tyrosine phosphorylation or nuclear localization prevent STAT1 serine phosphorylation, but it remains unclear if this is due to a loss of STAT1 chromatin binding (Sadzak et al. 2008; Begitt et al. 2014). When STAT1 serine phosphorylation is lost due to mutation of the serine 727 to a non-phosphorylatable residue, a specific subset

of ISGs are no longer upregulated by IFNg treatment and mice are unable to control *Listeria monocytogenes* infection (Bancerek et al. 2013; Varinou et al. 2003). Several kinases, including CDK8, CDK19, PCKδ, p38, and CaMKII phosphorylate STAT1 in response to IFN (Bancerek et al. 2013; Steinparzer et al., 2019; Uddin et al. 2002; Nair et al. 2002; Pilz et al. 2003). CDK8 has been most extensively studied among that STAT1 serine kinases; however, particular kinases may play cell type-dependent or context-specific roles in regulating STAT1 phosphorylation.

Fully activated STAT1 complexes within the nuclear compartment bind to specific DNA sequences via their DNA binding domain and activate the transcription of IFN-stimulated genes (ISGs). ISGs are a large class of diverse genes with numerous different functions, many of which can directly or indirectly inhibit viral replication. After type I or type III IFN exposure, ISGF3 containing STAT1 binds to IFN-sensitive response elements (ISREs) located in the promotors of many ISGs (Villarino et al., 2017; Platanias, 2005; Lazear et al. 2019). ISG promoters may also have gamma IFN-activated sequences (GAS), which are recognized by the STAT1 homodimer formed after type II IFN stimulation (Platanias, 2005; Begitt et al., 2014). The presence of one or both of these sequences within ISG promoters allows different types of IFN to activate unique but overlapping portions of ISGs (Platanias, 2005; Liu et al., 2012; Begitt et al., 2014).

After signaling, STAT1 is rapidly deactivated and shuttled back to the cytosol. Before transport, STAT1 dimers must first be dephosphorylated at Y701 by the nuclear phosphatase T-cell protein tyrosine phosphatase (Tc45) (ten Hoeve et al., 2002). Export can then be mediated by chromosome region maintenance 1 (CRM1) which binds to GTP-Ran to shuttle STAT1 back to the cytoplasm (McBride & Reich, 2003; Tessier et al.,

2019). Hydrolysis of GTP-Ran to GDP-Ran releases STAT1 from the nuclear export complex, completing the STAT1 activation cycle (McBride & Reich, 2003; Tessier et al., 2019).

1.2.4 STAT1 targeting by viral proteins

Because STAT1 is such a critical component of the IFN response, it is often targeted by viral proteins. The mechanisms by which viruses inhibit STAT1 primarily fall into one of three categories: 1) degradation of STAT1, 2) inhibition of STAT1 post-translational modification, or 3) inhibition of STAT1 nuclear accumulation (Tolomeo et al., 2022; Najjar & Fagard, 2010). For example, the V protein of many members of the *Paramyxoviridae* family of viruses induces proteasomal degradation of STAT1 through various mechanisms (Horvath, 2004). A wide variety of viruses reduce the tyrosine phosphorylation of STAT1 either by preventing phosphorylation in the first place or by inducing dephosphorylation (Tolomeo et al., 2022; Najjar & Fagard, 2010). Finally, several viruses inhibit the nuclear accumulation of STAT1 such as foot-and-mouth disease virus which inhibits the nuclear import of STAT1 by degrading STAT1 nuclear import factors (Du et al., 2014). Alternatively, Nipa virus and Hendra virus inhibit STAT1 nuclear import by preventing the formation of STAT1 dimer complexes (Sugai et al., 2017). Additional viruses including coronavirus, rabies virus, and Ebola virus prevent STAT1 nuclear translocation by interfering with various nuclear import machinery or through unknown mechanisms (Tolomeo et al., 2022). The fact that so many different families of viruses have evolved to inhibit STAT1 activation underscores the importance

of STAT1 in mediating an effective innate immune response and restricting viral replication.

1.3 Noroviruses and the innate immune response to their infection

1.3.1 Norovirus discovery and disease burden

Noroviruses represent one genera of the *Caliciviridae* family of RNA viruses. They have positive-sense single-stranded RNA genomes that reside within a small, non-enveloped virion (Green, 2013). Noroviruses can be further divided into ten genogroups, with GI, GII, and GIV containing viruses that infect humans (Chhabra et al., 2019). While norovirus infection can cause a range of different diseases in its various hosts, in humans, norovirus primarily causes acute but self-limiting infections resulting in nausea, vomiting, and diarrhea (Kapikian et al., 1972).

The first human norovirus characterized, Norwalk virus, was identified from an outbreak of gastroenteritis in Norwalk, Ohio in 1972 (Kapikian et al., 1972). Since its initial discovery, noroviruses have been established as the predominant cause of epidemics of acute gastroenteritis, resulting in approximately 700 million cases each year (Glass et al., 2009; Bartsch et al., 2016). Norovirus is the second leading cause of all acute viral gastroenteritis, not just epidemic gastroenteritis, behind rotavirus (Glass et al., 2009; Bartsch et al., 2016; McAtee et al., 2016). However, with the development and implementation of a rotavirus vaccine, norovirus is surpassing rotavirus as the primary viral cause of acute gastroenteritis in many locations (Koo et al., 2012; McAtee et al., 2016).

1.3.2 MNV as a model for human noroviruses

Unlike rotavirus, there are currently no vaccines or therapeutics for norovirus (Netzler et al., 2018; Straub et al., 2007; Mboko et al., 2022; Chan et al., 2007). One of the challenges associated with developing effective norovirus treatments is our lack of understanding of norovirus biology and the immune response to norovirus infection. A major contributing factor to this knowledge gap is the absence of traditional cell culture and small animal models to study human norovirus (Duizer et al., 2004; Netzler et al., 2018; Vashist et al., 2009).

Human noroviruses have been successfully cultured in specific B cell lines and enteric organoids; however, in these systems, human norovirus did not achieve high tiers, and even limited replication in these systems has been difficult to reproduce (Jones et al., 2015; Papafragkou et al., 2013). Human norovirus proteins and RNA can also be produced from cell lines expressing a human norovirus replicon; however, this does not fully recapitulate infection (Chang et al., 2006). *In vivo*, most of our understanding of norovirus biology comes from human volunteer studies, which have their own limitations (Vashist et al., 2009).

Because of the difficulties associated with studying human noroviruses, researchers have turned to animal noroviruses as a model to investigate the mechanism of basic norovirus biology. In 2003 a novel mouse calicivirus from the *Norovirus* genus was identified in immunocompromised mice (Karst et al., 2003). This murine norovirus (MNV-1) was similar to human noroviruses in several key respects. Both viruses share a

similar icosahedral virion structure composed primarily of the viral protein VP1 (Green, 2013; Wobus et al. 2006). They also have a very similar genome organization. In both human and murine noroviruses, six nonstructural proteins are encoded within the N-terminal ORF1, which is translated as a single polyprotein and then subsequently cleaved into its constituent parts (Green, 2013). ORF2 and ORF3 encode the structural proteins VP1 and VP2, respectively, which form the virion capsid and are highly similar between human and murine noroviruses (Green, 2013; Snowden et al., 2020). The only major difference in the genome organization of human and murine noroviruses is that MNV includes an additional open reading frame, ORF4, which codes for virulence factor 1 (VF-1) that is unique to MNV (McFadden et al., 2011; Green, 2013).

Despite the similarities between MNV and human noroviruses, an important advantage of studying MNV is that this virus readily replicates in many cell culture systems. While MNV was initially identified in immunocompromised mice where it can be lethal, MNV can also infect immunocompetent mice but do not cause disease (Karst et al., 2003). Therefore, MNV can also be used to study norovirus infection *in vivo* using a mouse model where MNV infection naturally occurs via the fecal-oral route, leading to infection of the gastrointestinal tract, just as human noroviruses do in humans (Kapikian et al., 1972; Wobus et al., 2006; Vashist et al., 2009).

1.3.3 Norovirus NS5 has multiple functions

Using MNV as a model to study noroviruses, researchers have already discovered key aspects of MNV biology which have been related back to human noroviruses. Of

particular interest to this study is what has been discovered about the MNV protein encoded by NS5. The nonstructural protein NS5 encodes a protein known as viral protein, genome linked (VPg), which is covalently linked to the viral genomic and subgenomic RNAs (Green, 2013). The structure of the core region of MNV NS5 has been determined by nuclear magnetic resonance spectroscopy. While the N- and C-terminal regions of NS5 are highly disordered, the central domain consists of two compact helices, with the residue that is covalently linked to the genome (Y26) residing in the first helix (Leen et al., 2013). One advantage of possessing a VPg is that it mimics the cap structure found on eukaryotic mRNAs and can therefore prevent the recognition of viral RNAs by innate immune sensors such as RIG-I, which detect triphosphorylated RNAs (Yoneyama & Fujita, 2008). As in picornaviruses, the VPg of *caliciviridae* also functions as a protein primer to facilitate RNA transcription (Goodfellow, 2011; Thorne & Goodfellow, 2014). However, unlike picornavirus VPg, MNV NS5 also has a critical function in protein translation, which is uncommon for VPgs from vertebrate viruses (Goodfellow, 2011; Thorne & Goodfellow, 2014; Chung et al., 2014). For noroviruses, the ability of NS5 to initiate viral RNA translation depends on its binding to the eIF4F complex, a critical component of host translation (Chung et al., 2014; Goodfellow et al., 2005; Chaudhry et al., 2006). Human, mouse, and feline norovirus VPgs have all been demonstrated to interact directly with eIF4E, a component of the eIF4F complex that directly binds the eukaryotic mRNA cap (Goodfellow et al., 2005; Chaudhry et al., 2006).

In addition to its functions in transcription and translation, MNV NS5 has other functions associated with an N-terminal polybasic region that do not require covalent linkage of VPg to the viral genome (McSweeny et al., 2021). This region of NS5 has

nonspecific RNA binding activity, which was also shown *in vitro* for human norovirus VPg (McSweeny et al., 2021). Additionally, the polybasic region is associated with NS5's ability to induce a G0/G1 phase cell cycle arrest which favors viral replication, although a mechanism has not yet been identified (Davies & Ward, 2016; McSweeny et al., 2021). It remains unclear if NS5 RNA-binding and induction of cell cycle arrest are linked or if they merely map to the same region of NS5. However, it is interesting to note that RNA-binding proteins have previously been implicated in the modulation of cell cycle progression by regulating the localization, and translation of critical host factors.

1.3.3 TAG-dependent and -independent IFN-γ immune responses

MNV has also been used as a model to study the immune response to norovirus infection. Mice lacking a B- and T-cell-mediated adaptive immune response did not succumb to norovirus infection (Karst et al., 2003), suggesting that the adaptive immune response plays little or no role in inhibiting MNV-associated mortality. In contrast, the innate immune system was found to be critical for controlling MNV infection (Karst et al., 2003; Hwang et al., 2012). MNV has been shown to be sensed by MDA5 resulting in the activation of IFN-dependent innate immune pathways (McCartney et al., 2008). While the loss of either the type I or type II interferon response individually had minimal effect on the mortality of mice infected with MNV, impairment of both type I and type II signaling together, resulted in 100% fatality of mice infected with MNV (Karst et al., 2003; Hwang et al., 2012). While not completely redundant, these data suggest that the type I and type II interferon have overlapping functions in the inhibition of MNV pathogenesis.

Type II interferon restriction of MNV was found to be dependent on a specific set of proteins that have important functions in autophagy as part of a system termed targeting by autophagy (TAG) (Park et al., 2016; Hwang et al., 2012). Loss of one of these components, Atg5, in mice that also lack the type I interferon receptor, resulted in high susceptibility to MNV infection (Hwang et al., 2012). This phenocopies what is observed in mice lacking both type I and type II interferon receptors, suggesting that Atg5 is necessary for type II interferon restriction of MNV. In the TAG pathway, Atg5 functions as part of an E3 ligase complex with Atg12 and Atg16l1 to conjugate LC3 to phosphatidylethanolamine (PE) in the membranes surrounding the norovirus replication compartment (Hwang et al., 2012, Park et al., 2016). The LC3-tagged membranes are then recognized by INF-inducible GTPases leading to disruption of the replication complex's membranes, exposing the pathogen within to immune detection (Park et al., 2016; Biering et al., 2017). Depletion of ATG5 or ATG16l1 prevents targeting by autophagy (TAG) and allows MNV to effectively escape restriction by IFN-γ (Biering et al., 2017).

CHAPTER 2

THE PHOSPHATASE REGULATORY SUBUNIT PPP1R12C MEDIATES VIRUS-INDUCED DEPHOSPHORYLATION OF THE RIG-I-LIKE RECEPTORS BY PP1

This chapter is adapted from the following publication:

Acharya, D., **Reis, R.,** Volcic, M., Liu, G., Wang, M. K., Chia, B. S., Nchioua, R., Groß, R., Münch, J., Kirchhoff, F., Sparrer, K. M. J., and Gack, M. U. Actin cytoskeleton remodeling primes RIG-I-like receptor activation. Cell 2022, 185(19):3588-3602.e2. doi: 10.1016/j.cell.2022.08.011.

Attributions: RAR performed and analyzed all experiments with the exception of the following: MW performed and analyzed Figure 2.1 A. KMJS performed and analyzed Figures 2.3 B and C. MV performed and analyzed Figure 2.11 A and 2.12 B. DA performed and analyzed Figures 2.8 A, 2.11 B, 2.12 C and 2.13 A. BSC performed and analyzed Figure 2.8 C.

2.1 Abstract

Our current understanding of how the RIG-I-like receptor (RLR) family of pattern recognition receptors functions is that they detect viral infection by directly binding to cytoplasmic RNA and in response activate an antiviral signaling pathway. However, it has

also been well-established that RLR activation requires the addition and removal of an array of post-translational modifications. One of these modifications is the phosphorylation of the CARD domains of two of the RLRs; RIG-I and MDA5, which must be removed in order for the RLRs to interact with their signaling adaptor. Dephosphorylation at these sites is achieved by the phosphatases PP1α and PP1γ; however, it is unclear how these enzymes are regulated to ensure that the RLR CARD domains are dephosphorylated specifically during infection and not in uninfected cells. Here we report the identification of the PP1 regulatory subunit PPP1R12C as a critical regulator of PP1α/γ's activity toward the RLRs. Viral infection results in changes in the filamentous actin cytoskeleton, resulting in a redistribution of R12C from the cytoskeleton where it normally resides to the cytosol so that it can form a complex including PP1α/γ and the RLRs. Thus, R12C allows for the integration of a second signal, actin cytoskeleton disturbance, into the activation of RLR-mediated innate immunity.

2.2 Introduction

Activation of innate immunity during viral infection is triggered by specialized sensor proteins called pattern-recognition receptors (PRRs), which respond to molecular patterns absent from uninfected cells. One type of pattern commonly detected by PRRs is viral or host-derived nucleic acids outside of their typical cellular compartments (Hartman, 2017; Paludan & Bowie, 2013). The RIG-I-like receptor (RLR) family of cytosolic RNA sensors detects and responds to the presence of cytoplasmic RNA (Rehwinkel & Gack, 2020). Two important members of the RLR family, RIG-I and MDA5, directly interact with stimulatory RNAs through their central DExD/H box RNA helicase

domain and carboxy-terminal domain (Reikine et al., 2014; Yoneyama & Fujita, 2008). After RNA binding, the RLRs initiate a signaling cascade via an interaction between their caspase activation and recruitment domains (CARDs) and the CARDs of mitochondrial antiviral signaling protein (MAVS) (Wu & Hur, 2015; Liu et al., 2015).

Stimulatory RNA binding is absolutely critical for RLR activation; however, there are also a number of other regulators of RIG-I and MDA5 activity. Both the addition and removal of post-translational modifications can be used as a means for other proteins and pathways to modulate RLR activity. Phosphorylation of RIG-I at serine 8 (S8) (and other residues) and of MDA5 at serine 88 (S88) prohibits RLR activation prior to infection, whereas dephosphorylation of these sites by the cellular protein phosphatase-1 PP1α or PP1γ is crucial for RLR activation in response to virus infection (Gack et al., 2010; Maharaj et al., 2012; Nistal-Villán et al., 2010; Wies et al., 2013). Thus, PP1α/γ is a key upstream activator of both RIG-I and MDA5; however, how PP1α/γ itself is activated upon viral infection is unknown. Moreover, as PP1 catalyzes not only dephosphorylation of RLRs but also of many other cellular substrates, it remains unclear what determines its specificity toward RLRs. Substrate specificity of PP1, the catalytic core, is conferred by complex formation with one of >200 PP1-regulatory proteins (Peti et al., 2013; Terrak et al., 2004), many of which have not been characterized functionally. In particular, it is unknown which PP1-regulatory protein(s) mediate RLR-targeting by PP1α/γ.

Here, we show that PP1α/γ's specificity toward RLRs is mediated by the F-actin-residing PP1-regulatory protein PPP1R12C (hereafter called "R12C"). R12C is necessary for the complete activation of an RLR-mediated antiviral response, and in its absence, IFN and ISG production is reduced, while viral replication is enhanced. We further identify

that virus-mediated actin cytoskeleton disturbance triggers RLR dephosphorylation by the PP1-R12C phosphatase complex contributing to the RLRs activation by RNA ligands.

2.3 Results

2.3.1 R12C is an important component of the RLR pathway

A previously published screen of 257 phosphatases and phosphatase regulatory subunits indicated that siRNA-mediated knockdown of PP1α and PP1γ inhibited IFN-β promoter activity in response to the constitutively active MDA5(2CARD) mutant (Wies et al., 2013). In this screen, eight PP1 regulatory subunits also inhibited MDA5(2CARD)-mediated IFN-β promoter-driven luciferase expression. These data suggest that each of these PP1 regulatory subunit has a potential function in the RLR pathway between MDA5 activation and IFN-β expression, and one or more of these candidates may be involved in regulating the dephosphorylation of the RLRs by PP1α/γ.

To narrow down the role of each regulatory subunit in the RLR pathway, we determined if each subunit was necessary for RLR- and MAVS-induced type I interferon upregulation by individually depleting each protein in HEK 293T cells with specific pooled siRNA and verified by qPCR (Fig 2.1 B). In the phosphatase regulatory subunit knockdown cells, IFN-β induction was assessed by luciferase promoter assay in response to activation of the RLR pathway by transfection of the active 2CARD forms of RIG-I or MDA5 or transfection of the common adaptor protein MAVS. In comparison to cells transfected with a non-targeting control siRNA (si.C), loss of each one of the PP1 regulatory subunits inhibited both RIG-I and MDA5-induced IFN-β promoter activity to

varying degrees (Fig 2.1 A). However, unlike the other PP1 regulatory subunits, only silencing of PPP1R12C failed to inhibit MAVS-induced IFN-β upregulation. These data suggest that, while all the teste PP1 regulatory subunits potentially contribute to RLR-mediated IFN-β induction, seven of them either affect fundamental cellular processes or play a role in the RLR pathway downstream of MAVS activation and RLR dephosphorylation. Only PPP1R12C's (hereafter referred to as 'R12C') function is specific to the activation of RIG-I and MDA5 and is not necessary for any downstream steps in the RLR-activated pathway.

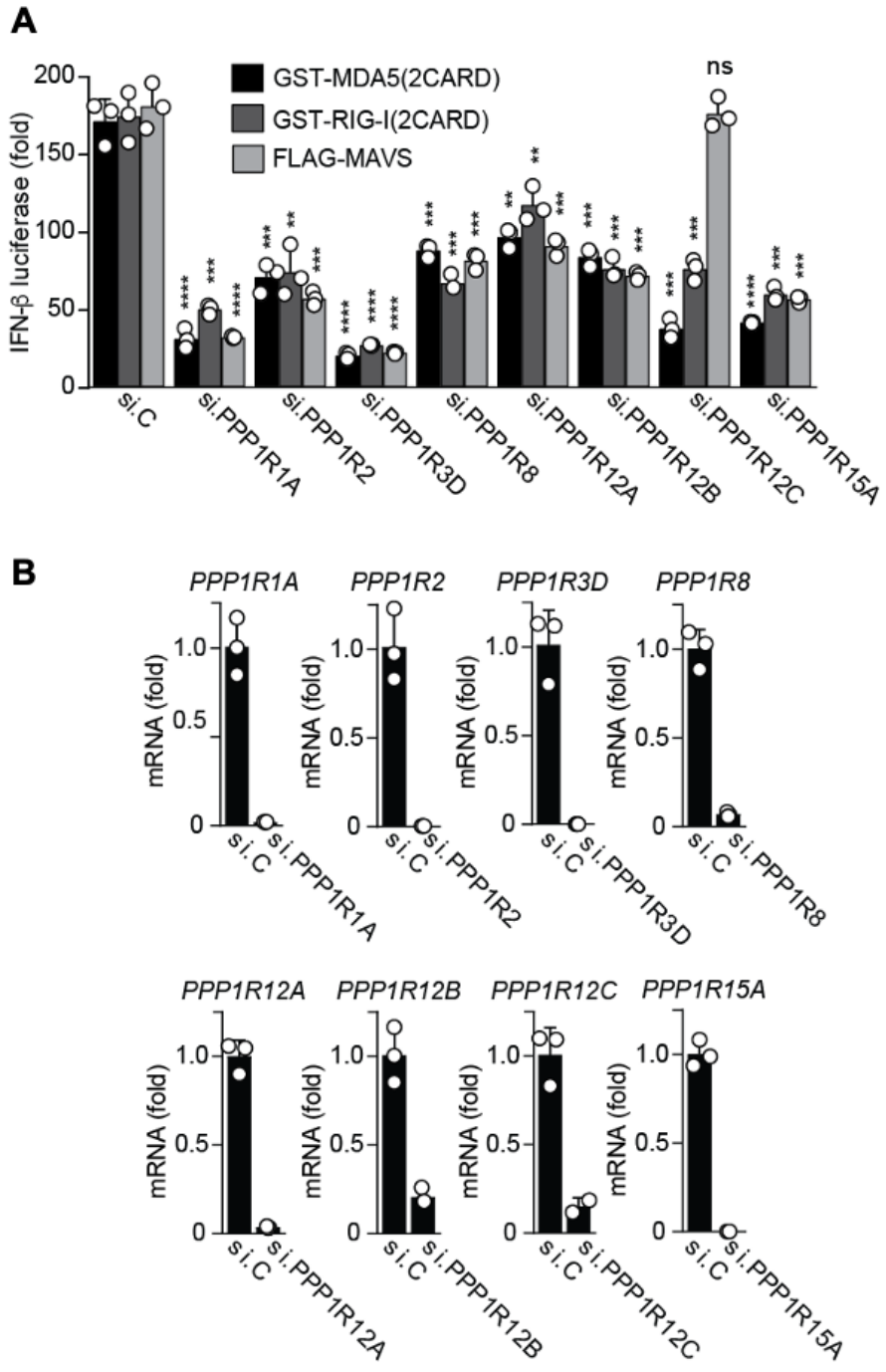

Figure 2.1: The phosphatase regulatory subunit R12C plays a critical role in type I interferon induction by contributing to RLR activation

Figure 2.1 continued: A) IFN-β luciferase reporter activity in HEK293T cells depleted of the indicated PP1-regulatory proteins using specific siRNAs and transfected with an IFN-β luciferase plasmid along with GST-MDA5(2CARD), GST-RIG-I(2CARD) or FLAG-MAVS, determined at 48 h post-transfection and normalized to co-transfected β-galactosidase. si.C, non-targeting control siRNA. **B)** Representative knockdown efficiency of the indicated genes for the experiment shown in Figure 1A, determined by qRT-PCR analysis at 48 h after siRNA transfection.

2.3.2 A complete RLR-mediated antiviral response requires R12C

To validate the importance of R12C for RLR-mediated antiviral gene activation, we used qRT-PCR to quantify the transcription-level upregulation of several ISGs known to be upregulated in response to RIG-I or MDA5 signaling in cells lacking R12C. In addition to the pooled siRNA used in Fig 2.1, each of the four siRNAs in the pool was also tested individually, and the knockdown of R12C by each siRNA was verified by qRT-PCR (Fig 2.2 B). mRNA levels of *IFNB1*, *CCL5*, *RSAD2*, and *IL8* after infection with a mutant strain of influenza A virus (IAV) lacking the NS1 protein (IAV∆NS1), which has been established to activate RIG-I, were significantly lower in primary normal human lung fibroblasts (NHLF) lacking R12C compared to control siRNA treated cells (Fig 2.2 A). This indicates that R12C is critical for the RLRs to induce ISG transcription in response to viral infection. In addition, the magnitude of the decrease in ISG expression after the R12C knockdown was similar to what was observed after the knockdown of RIG-I (Fig 2.2 A-B), emphasizing the importance of R12C in the RLR pathway.

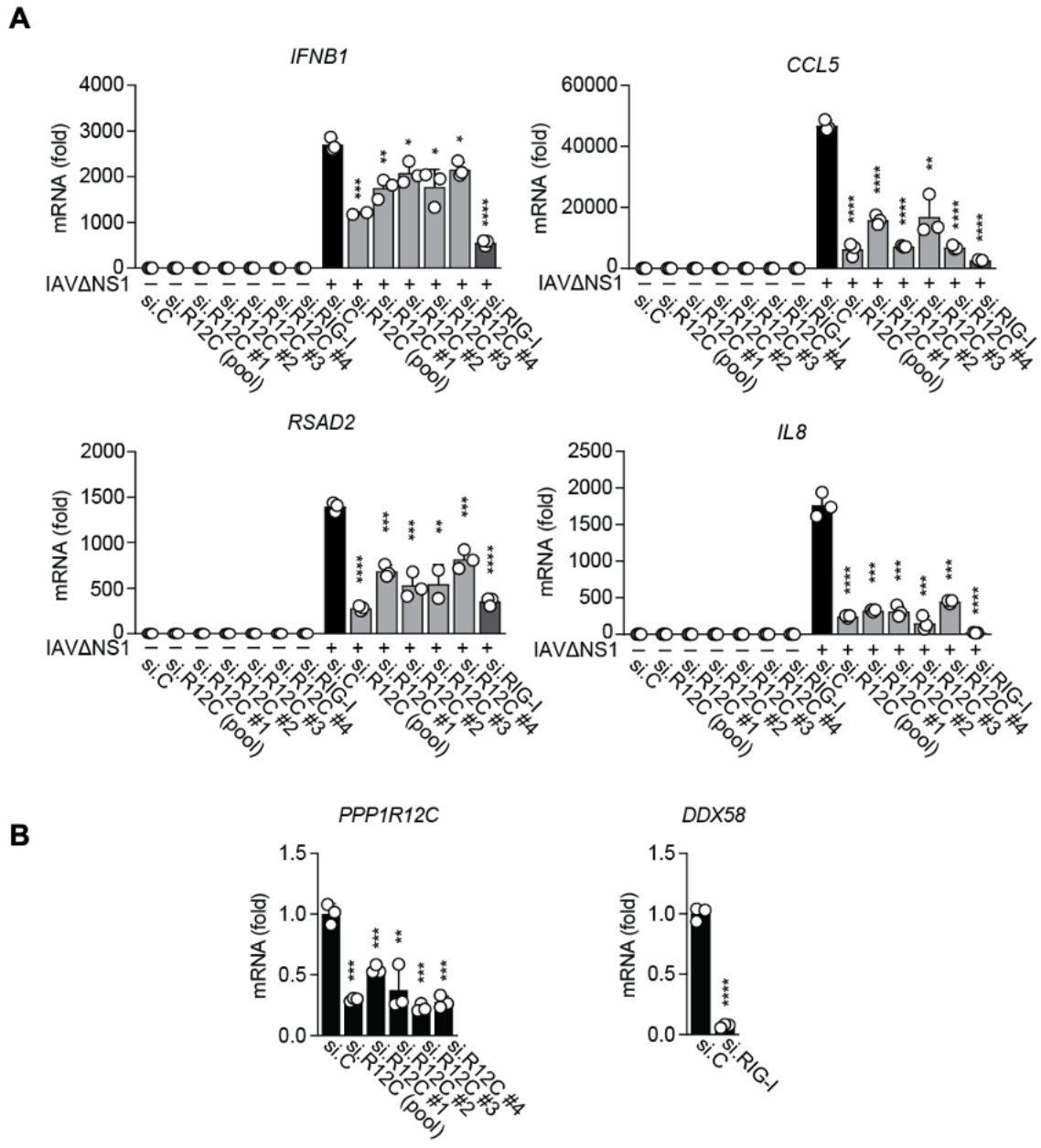

Figure 2.2: Depletion of R12C inhibits IFN-β induction in response to viral infection. **A)** qRT-PCR analysis of IFNB1, CCL5, RSAD2, and IL8 transcripts in NHLF cells that were transfected for 30 h with si.C, si.R12C (pool of 4 siRNAs), the four individual siRNAs targeting R12C (si.R12C #1–#4), or si.RIG-I (control) and then infected with IAVΔNS1 (MOI 0.1) for 18 h. **B)** Representative knockdown efficiency of the indicated genes for the experiment shown in A, determined by qRT-PCR analysis at 48 h after siRNA transfection.

To further corroborate the role of R12C in RLR-mediated antiviral response, we generated two clonal R12C knockout HEK 293T cell lines using CRISPR-Cas9 technology to disrupt R12C by removing a portion of the second exon of *PPP1R12C* and replacing it with a Blasticidin resistance gene (Fig 2.3 A). Insertion of the resistance cassette was initially verified via PCR with extracted genomic DNA using primers that bind only within the inserted sequence or sets of primers that amplify either the 5' or 3' junction of the insert and the rest of the genome (Fig 2.3 B). Loss of R12C in these cells was also validated at the protein level by western blot using antibodies targeting endogenous R12C (Fig 2.3 C). At the DNA and protein levels, both R12C KO HEK 293T clones were shown to have successful insertion of the Blasticidin resistance cassette and ablation of R12C protein expression.

Using the R12C KO HEK 293T cells, we assessed the function of the RLR signaling in the absence of R12C. R21C KO or passage-matched WT control cells were infected with Sendai virus (SeV), a virus known to be sensed by RIG-I (Baum & García-Sastre, 2011), and the production of IFN-β protein in response to infection was measured by ELISA. While WT HEK 293T secreted robust levels of IFN-β into the cell culture media after SeV infection, IFN-β production by R12C KO was significantly diminished (Fig 2.3 D). These data suggest that R12C is necessary for the RIG-I antiviral pathway to be fully functional and is critical for RLR-mediated induction of IFN-β.

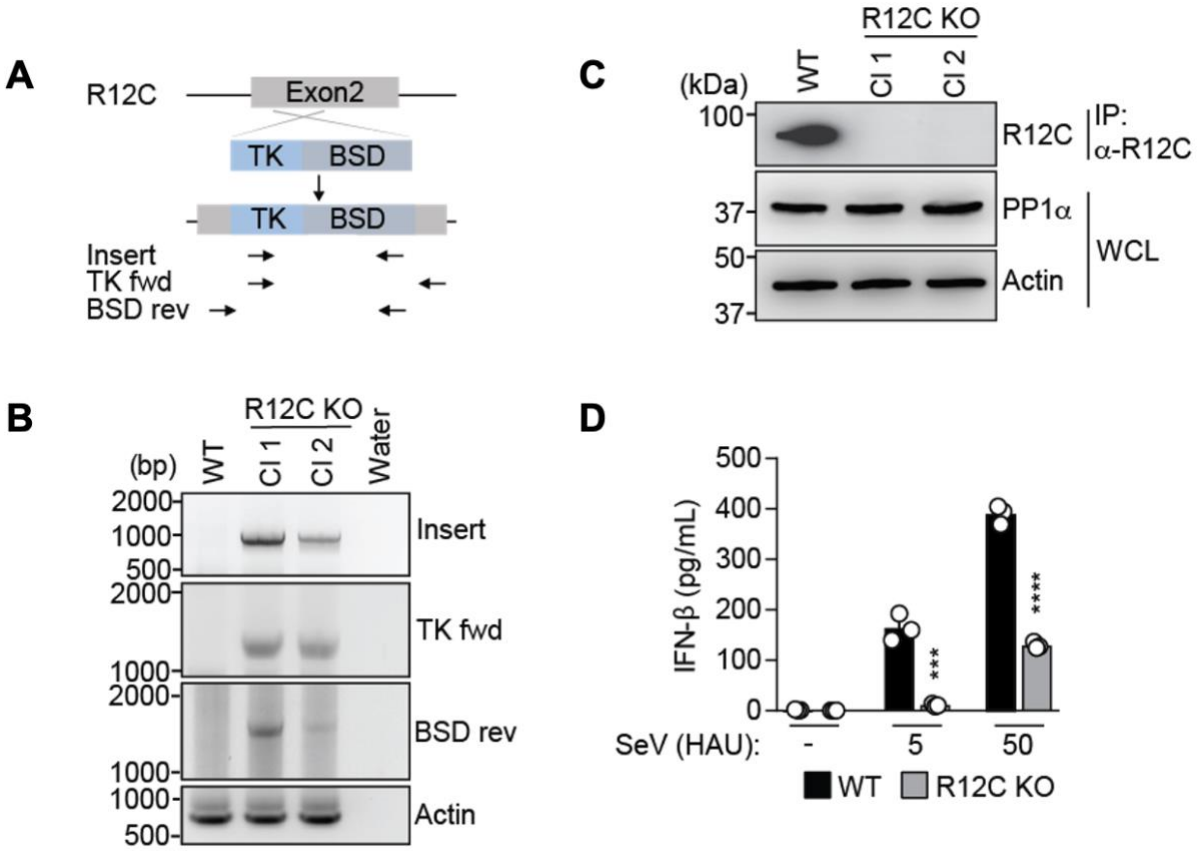

Figure 2.3: Knockout of R12C in HEK 293T reduces IFN-β protein production upon infection with SeV. A) R12C-KO HEK293T cells were generated using Cas9-mediated induction of a dsDNA break and homologous insertion (crossed lines) of a cassette encoding for a Blasticidin resistance gene (BSD) controlled by the HSV-1 thymidine kinase (TK) promoter into the second exon of R12C gene through homologous recombination disrupting R12C expression. Upon selection of resistant cell clones using Blasticidin, single clones were isolated and propagated. **B)** Presence of the TK-BSD insert was confirmed by PCR using genomic DNA extracted from two independent R12C KO HEK293T clonal cell lines and from WT control cells. Primers were used that target the TK promotor (fwd) and the BSD resistance cassette (rev). Actin was amplified as a control. Target location of primers used for each PCR reaction are indicated. H2O, water control. **C)** Loss of R12C protein expression in R12C KO HEK293T clonal cell lines (Cl-1 and Cl-2), determined by IP and IB with anti-R12C. WCLs of R12C KO and WT control HEK293T cells were further immunoblotted with anti-PP1a and anti-actin (controls). **D)** ELISA of IFN-β in the supernatant of WT and R12C KO HEK293T cells that were infected with SeV for 18 h.

As an additional means of validating our findings in R12C KO HEK 293T cells, we also acquired R12C KO HAP1 cells, a fibroblast-like myeloid cell line. Similar to what we observed in R12C KO HEK 293T, when R12C was knocked out in Hap1 cells, the transcription of ISGs including *IFNB1*, *IL8*, *RSAD2*, and *MX1* was significantly lower in comparison to ISG expression in WT HAP1 cells (Fig 2.4 A). Because ISG upregulation in response to viral infection is diminished in both HEK 293T and HAP1 R12C KO cells, and also after R12C knockdown in primary fibroblasts, it is unlikely that R12C has a cell type-specific function but rather is a general requirement for the RIG-I-mediated innate immune response.

We also used R12C KO HAP1 to demonstrate a role for R12C in not just the RIG-I-mediated but also the MDA5-mediated antiviral pathway. In comparison to WT HAP1 cells, R12C KO HAP1s had substantially lower levels of ISG mRNAs, across multiple different time points, after infection with an MDA5-triggering mutant strain of encephalomyocarditis virus (EMCV) (Fig 2.4 B). What these data indicate is that R12C is important for both RIG-I and MDA5 signaling and may also suggest that R12C's function in the antiviral response is related to a common component of both RLR-signaling pathways.

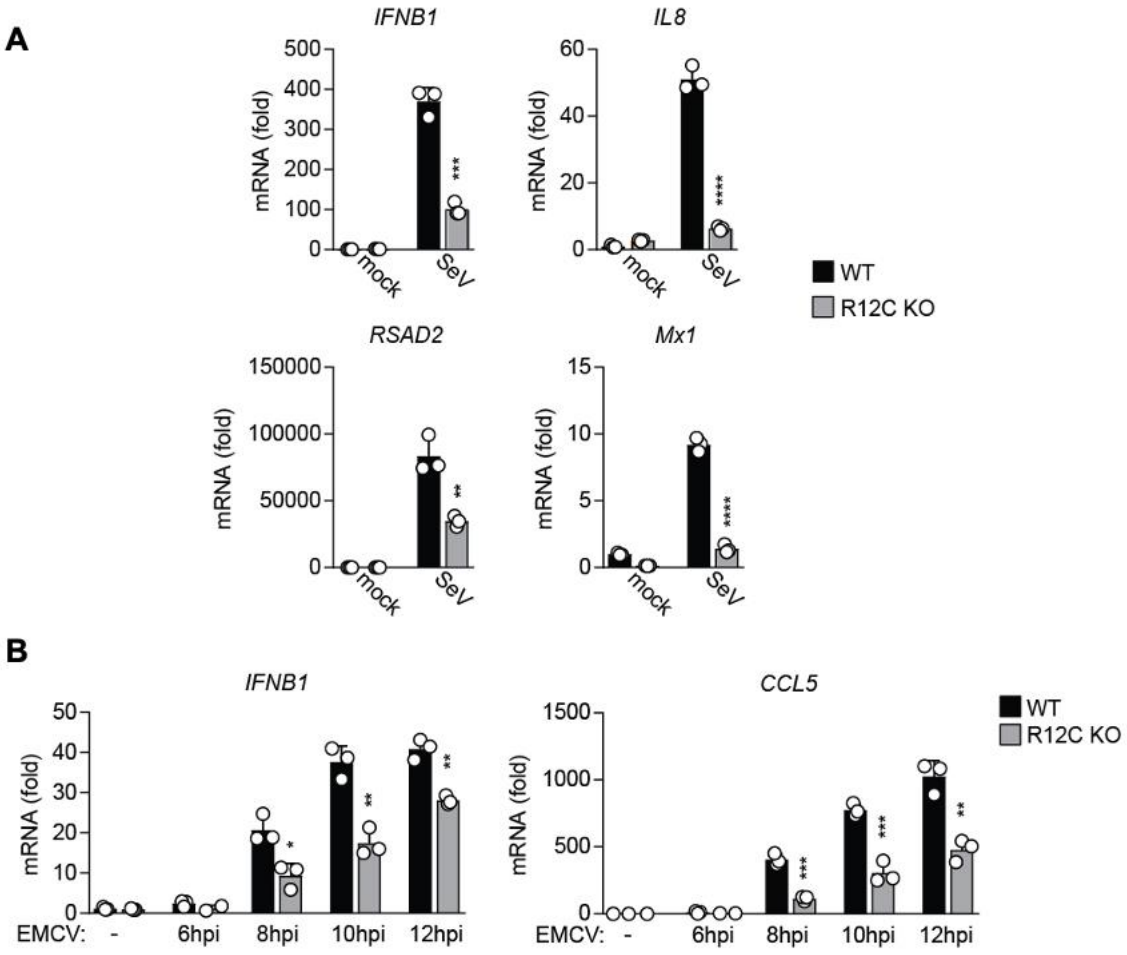

Figure 2.4: Virus-induced IFN-β and ISG expression is reduced in HAP1 R12C knockout cells. A) qRT-PCR analysis of the *IFNB1*, *IL8*, *RSAD2*, and *MX1* in WT and R12C KO Hap1 cells that were either mock-treated or infected with SeV (50 HAU/mL) for 18 h. **B)** qRT-PCR analysis of IFNB1 and *CCL5* transcripts in WT and R12C KO HAP1 cells that were either mock-treated or infected with EMCV (MOI 0.25) for the indicated times.

Primary mouse dermal fibroblasts were isolated from *Ppp1r12C*$^{-/-}$ C57BL/6NJ mice to assess the contribution of R12C to the antiviral response *ex vivo*. When *Ppp1r12C*$^{-/-}$ fibroblasts and fibroblasts derived from WT control mice were stimulated with the high molecular weight (HMW) double-stranded RNA mimic poly(I:C) which activates signaling through MDA5, *Ppp1r12C*$^{-/-}$ cells had significantly lower levels of *Ifnb1* and *Oas1* mRNA

compared to WT cells (Fig 2.5 A). In addition, the production of IFN-β by *Ppp1r12C*$^{-/-}$ fibroblasts after infection with SeV was also substantially reduced compared to WT cells when assessed by ELISA (Fig 2.5 B). Both RIG-I and MDA5 signaling in R12C deficient primary mouse cells is impaired, in agreement with our data from cell culture systems, and in primary human cell lines.

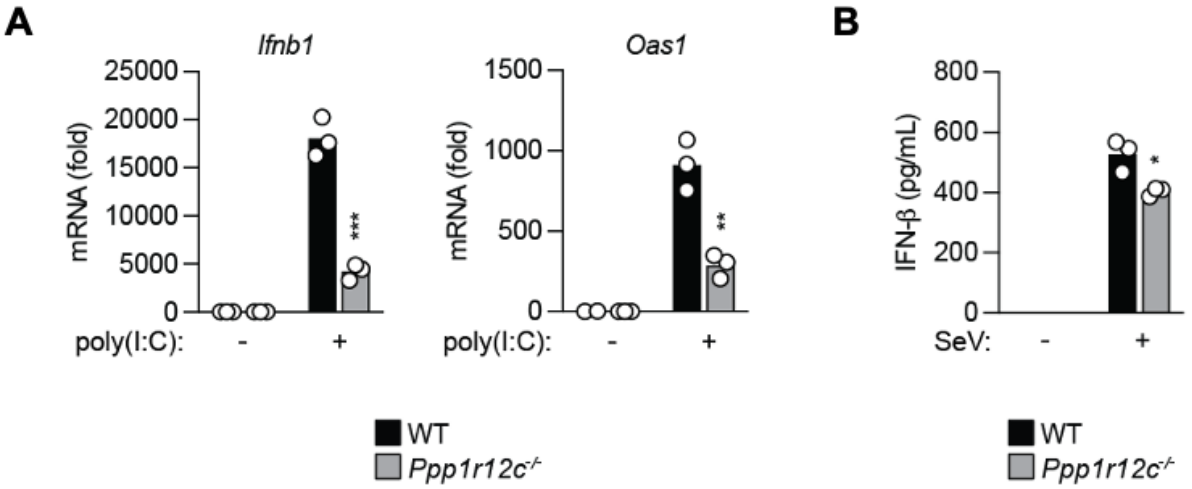

Figure 2.5: ISG upregulation is reduced in *Ppp1r12C* knockout primary mouse dermal fibroblasts stimulated with poly(I:C) or viral infection. A) qRT-PCR analysis of the *Ifnb1*, *Oas1*, and *Il6* in dermal fibroblasts from *Ppp1r12c*$^{-/-}$ and WT mice that were treated ex vivo with poly(I:C) (100 ng/mL, 20 h). **B)** ELISA of IFN-β in the supernatant of WT and *Ppp1r12c*$^{-/-}$ mouse dermal fibroblasts that were infected with SeV for 18 h.

2.3.3: R12C is critical for inhibition of viral restriction

Because we observe significant reductions in the antiviral response at the level of INF-β production and ISG upregulation in the absence of R12C, we hypothesized that viral replication would be enhanced in R12C KO cells. We first measure the replication of the RIG-I-sensed virus IAVΔNS1 in R12C KO HEK 293T. After 72 hours of infection, IAV replication in R12C KO cells was increased by a log in comparison to WT control cells

(Fig 2.6 A). Such a significant increase in the production of infectious virions after knockout of R12C indicates that the observed reduction of ISG expression in these cells has a significant impact on the outcome of viral infection.

To ensure that R12C was not only important for restricting the replication of viruses detected by RIG-I, the replication of MDA5-sensed viruses in R12C KO cells was also measured by TCID50 assay after infection with the representative virus EMCV. At several time points during infection, the replication of EMCV in R12C KO cells was significantly higher than in WT cells (Fig 2.6 B). This strongly suggests that R12C is important for the full induction of antiviral factors by RIG-I and MDA5 and importantly, without the complete RLR-mediated innate immune response, the restriction of viral replication is impaired.

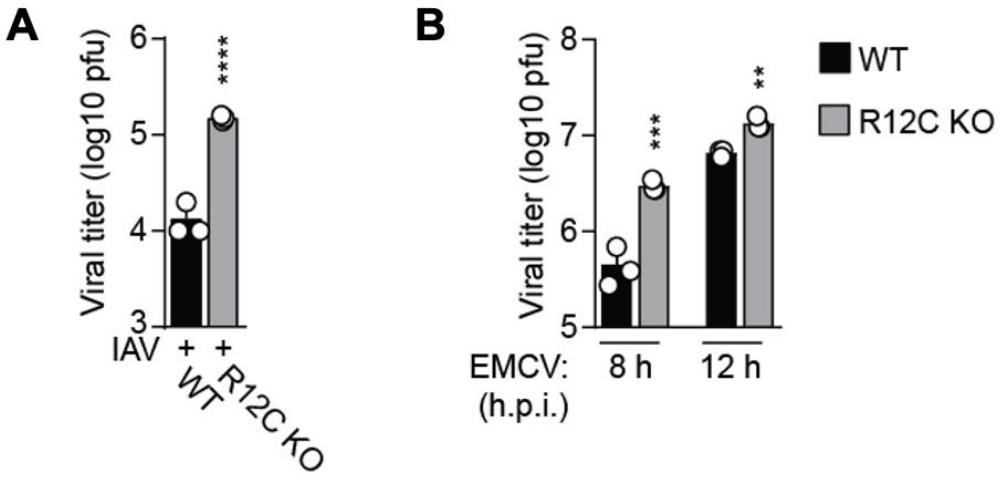

Figure 2.6: R12C knockout HEK 293T cells support viral replication to higher titers than WT cells. A) viral titers in the supernatant of WT and R12C KO HEK293T cells that were infected with IAV (MOI 0.001) for 72 h, determined by plaque assay. **B)** EMCV titers in the supernatant of WT and R12C KO HEK293T cells that were infected with EMCV (MOI 0.01) for 8 h, determined by TCID50 assay.

2.3.4: The function of R12C in the innate immune response is to target PP1 to the RLRs, inducing their dephosphorylation

We next wanted to gain a mechanistic understanding of R12C's role in the innate immune response controlled by the RLRs. Many antiviral factors fall into the broad class of ISGs; their activity is regulated by transcriptional upregulation in response to IFNs produced during viral infection. To determine if R12C is upregulated during viral infection, the expression of R12C was quantified by qRT-PCR after cells were exposed to IFN-β or infected with SeV. Unlike the mRNA levels of RIG-I and MDA5 which were also tested, there were no significant changes in the transcription of R12C after either infection of IFN treatment, as is also the case for PP1α and PP1γ transcription (Fig 2.7). Therefore, it is unlikely that R12C's function in the antiviral response is not due to transcriptional upregulation.

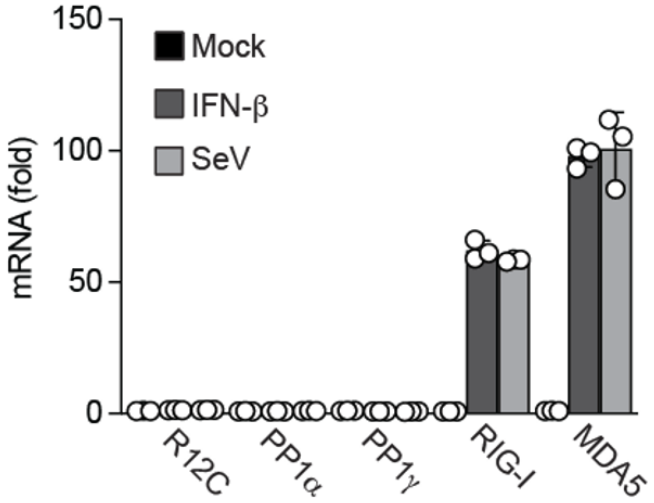

Figure 2.7: R12C expression is not upregulated during viral infection.

Figure 2.7 continued: qRT-PCR analysis of the PPP1R12C, PPP1CA, PPP1CC, DDX58, and IFIH1 in primary NHLF cells that were mock-treated, stimulated with IFN-β (1,000 U/mL) for 8 h, or infected with SeV (50 HAU/mL) for 8 h.

Since R12C expression is not increased during viral infection, we next assessed the binding of R12C to RIG-I and MDA5. For these experiments we used two flaviviruses; Zika virus (ZIKV), and dengue virus (DENV2), which can activate both RIG-I and MDA5. After viral infection, R12C's interaction with RIG-I and MDA5 was determined by co-immunoprecipitation. In both infected and uninfected cells, R12C was able to pull down the α isoform of PP1; however, this interaction was increased after viral infection. In addition, both RIG-I and MDA5 bound to R12C only after infection with ZIKV or DENV2 (Fig 2.8 A). It is unclear if this interaction is direct or mediated through the formation of a larger complex; however, because this interaction is dependent on viral infection, we chose to further investigate this interaction to determine if it is important for R12C's antiviral function.

We assessed the interaction between R12C and the RLRs by mapping the domains of each protein involved in this interaction. Because the CARD domains of both RIG-I and MDA5 are necessary for their ability to interact with the adaptor proteins MAVS, immediately downstream of the RLRs, we tested the interaction of R12C with truncated mutants of RIG-I and MDA5 consisting of only the CARD domains (2CARD). By co-immunoprecipitation, R12C was revealed to interact with both RLR 2CARD mutants, indicating that the CARD domains are sufficient for R12C to interact with (Fig 2.8 B). In contrast, R12C did not immunoprecipitated with the control protein interferon regulatory factor 3 (IRF3) (Fig 2.8 B).

Similarly, we determined the domains of R12C necessary for RIG-I and MDA5 interaction using truncated R12C mutants containing only the N-terminal domains (R12C N), only the C-terminal domains (R12C C), or lacking its PP1 binding site (R12C ∆95) (Fig 2.8 C). While both R12C N and R12C ∆95 were able to bind to RIG-I just like full-length R12C, when the N terminal domains are absent, R12C is no longer able to interact with RIG-I (Fig 2.8 C). The N-terminal fragment of R12C contains the ankyrin repeats, a protein motif known to be involved in protein-protein interactions, which could be responsible for mediating the interaction with the CARD domains of the RLRs (Tan et al., 2001).

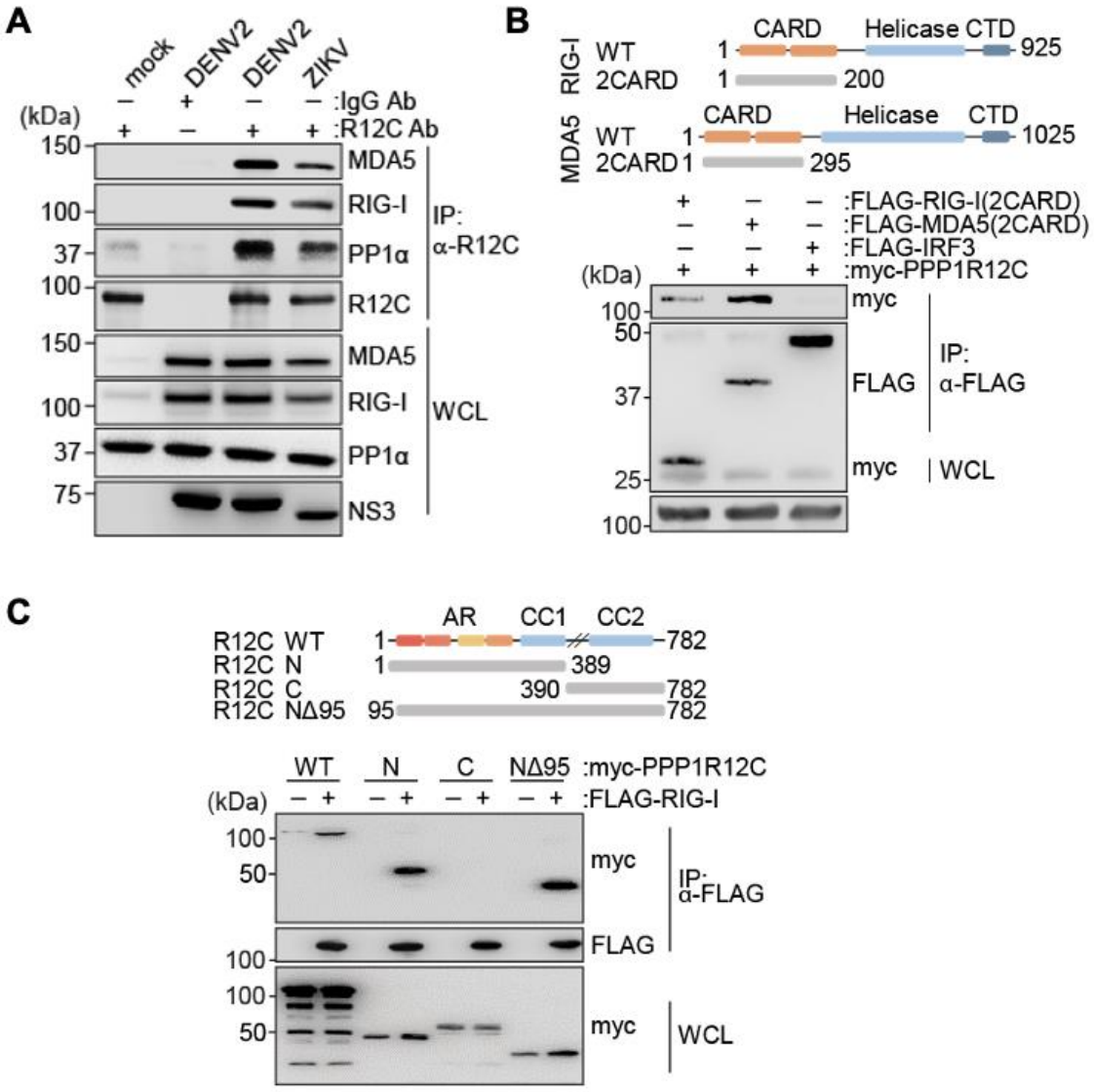

Figure 2.8: The C-terminal domain of R12C interacts with the RLR CARD domains. **A)** Binding of endogenous R12C to MDA5, RIG-I and PP1α/γ in NHLF cells that were either mock treated or infected with DENV or ZIKV (each MOI 1) for 40 h, determined by IP with anti-R12C (or an IgG isotype control) and IB with the indicated antibodies. **B)** Top: schematic representation of the RLR truncation mutant constructs used in the experiments. Bottom: binding of FLAG-RIG-I(2CARD), FLAG-MDA5(2CARD), or FLAG-IRF3 (negative control) to myc-R12C in transiently transfected HEK293T cells, determined by IP with anti-FLAG and IB with anti-myc. **C)** Top: schematic representation of the domain organization of R12C and of its truncation mutant constructs used in the mapping experiments. AR1–4, ankyrin repeats 1–4; CC, coiled coil. Bottom: binding of FLAG-RIG-I to the indicated myc-tagged R12C mutant proteins in transiently transfected HEK293T cells, determined by IP with anti-FLAG.

R12C was originally pulled out of a siRNA screen to identify the phosphatase responsible for dephosphorylating the CARD domains of the RLRs, the same region where R12C binding is localized. R12C was a particularly interesting candidate because its only previously characterized function is the regulation of PP1 toward myosin light chain, and PP1α/γ happens to be a positive regulator of both RIG-I and MDA5. Our data shows that R12C is important for both RIG-I and MDA5 signaling, suggesting R12C has a similar function in the signaling of both or has a function related to a common component of both pathways. From these observations, we hypothesized that R12C's function in the RLR pathway might be to target PP1 specifically to the RLR card domains during infection in a manner analogously to its previously described targeting of PP1 to myosin light chain.

If R12C is involved in targeting PP1 to the RLRs, we would expect that in the absence of R12C PP1 can no longer interact with RIG-I and MDA5. In WT cells, the interaction between PP1 and RIG-I can be detected by co-immunoprecipitation (Fig 2.9 A). However, when PP1 is immunoprecipitated from the lysate of R12C KO HEK 293T, PP1γ was unable to bind to the RLR (Fig 2.9 A). Similarly, when R12C is ablated, PP1γ was no longer detected among MDA5 binding partners even though it was readily detected in WT control cells (Fig 2.9 B). From our data showing that PP1 binding to the RLRs is dependent on R12C, it is plausible to predict that R12C is also necessary for PP1 to dephosphorylate the RLR CARD domains.

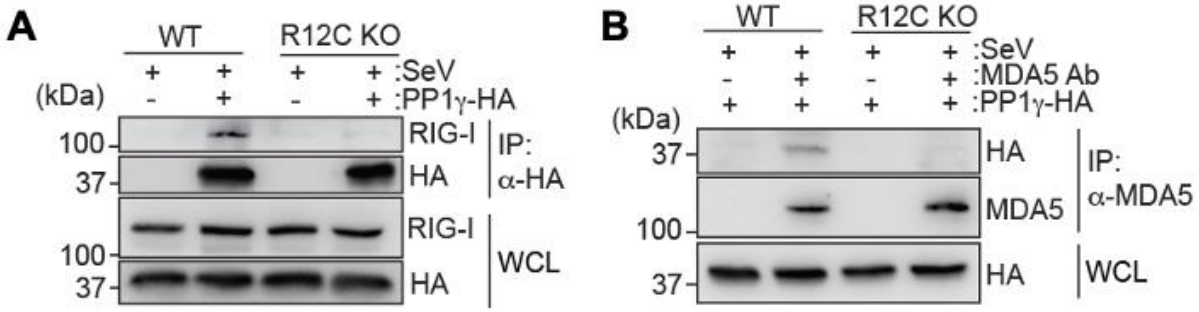

Figure 2.9: PP1 binding to the RLRs is ablated by the loss of R12C. A) Binding of endogenous RIG-I to PP1γ-HA in WT and R12C KO HEK293T cells that were infected with SeV (100 HAU/mL) for 18 h, determined by IP with anti-HA. **B)** Binding of endogenous MDA5 to PP1γ-HA in WT and R12C KO HEK293T cells that were infected with EMCV (MOI 1) for 6 h, determined by IP with anti-MDA5.

To test if R12C is important specifically for the dephosphorylation of the RLRs and not just PP1 binding, we utilized a nonphosphorylatable MDA5 mutant in which the S88 residue is substituted with alanine (S88A). The S88A MDA5 mutant cannot be phosphorylated at the critical CARD domain site and therefore is constitutively dephosphorylated, independent of PP1 activity. When MDA5 is exogenously expressed in WT or R12C KO cells, IFN-β is highly induced, and ablation of R12C results in a significant decrease in IFN-β expression (Fig 2.10). However, when the nonphosphorylated MDA5 mutant is expressed in R12C deficient cells, IFN-β mRNA levels are comparable to what is observed in WT cells expressing MDA5 S88A (Fig 2.7). Therefore, R12Cs function in the RLR-activated innate immune response is highly dependent on the sensitivity of the RLRs to PP1 dephosphorylation, supporting our theory that R12C mediates PP1s activity toward RIG-I and MDA5.

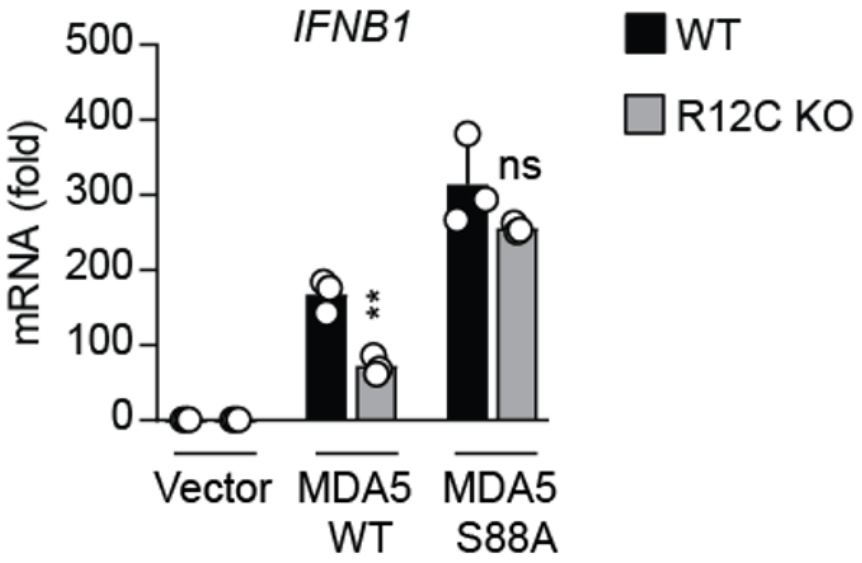

Figure 2.10: R12C-mediated IFN-β induction is dependent on RLR dephosphorylation. qRT-PCR analysis of IFNB1 transcripts in WT and R12C KO HEK293T cells that were transfected for 48 h with either empty vector or myc-tagged MDA5 WT or S88A mutant.

2.3.5 Virus-induced actin perturbations trigger R12C relocalization and targeting of PP1 to the RLRs

Although the biological function of R12C is largely unknown, it has been shown that R12C regulates actomyosin cytoskeleton dynamics as part of the myosin phosphatase complex (Tan et al., 2001). Most viruses modulate the cellular actin cytoskeleton during their lifecycles (Taylor et al., 2011), and our data showed that RLRs interact with the R12C ankyrin repeats, which also mediate R12C binding to actin components (Tan et al., 2001). Thus, we hypothesized that virus-induced actin cytoskeleton disturbance may trigger displacement of R12C from actin, thereby promoting cytoplasmic PP1-R12C-RLR complex formation and RLR dephosphorylation. To test this

theory, we assessed the localization of R12C in uninfected cells and cells infected with GFP-tagged vesicular stomatitis virus (VSV). In unperturbed primary fibroblasts, R12C formed filament-like structures which also colocalized with actin staining, suggesting R12C is associated with the filamentous actin cytoskeleton (Fig 3.11 A). In contrast, R12C was distributed throughout the cytoplasm in cells infected with VSV-GFP (Fig 3.11 A). R12C localization is clearly responsive to viral infection, which suggests that R12C's spatial localization determines the targeting of PP1 and explains the specific dephosphorylation of the RLRs during viral infection.

Our theory is that the trigger inducing R12C relocalization from the cytoskeleton to the cytosol is changes in the actin network that occur during viral infection. To determine if this theory is valid, we checked for general actin remodeling during viral infection using cofilin phosphorylation at serine 3 as a readout for changes in actin dynamics. In both WT and R12C KO cells, infection with VSV-GFP resulted in dephosphorylation of cofilin indicating the occurrence of changes in the cytoskeleton (Fig 3.11 B). Therefore, viral infection induces concurrent R12C cytoplasmic localization and actin remodeling.

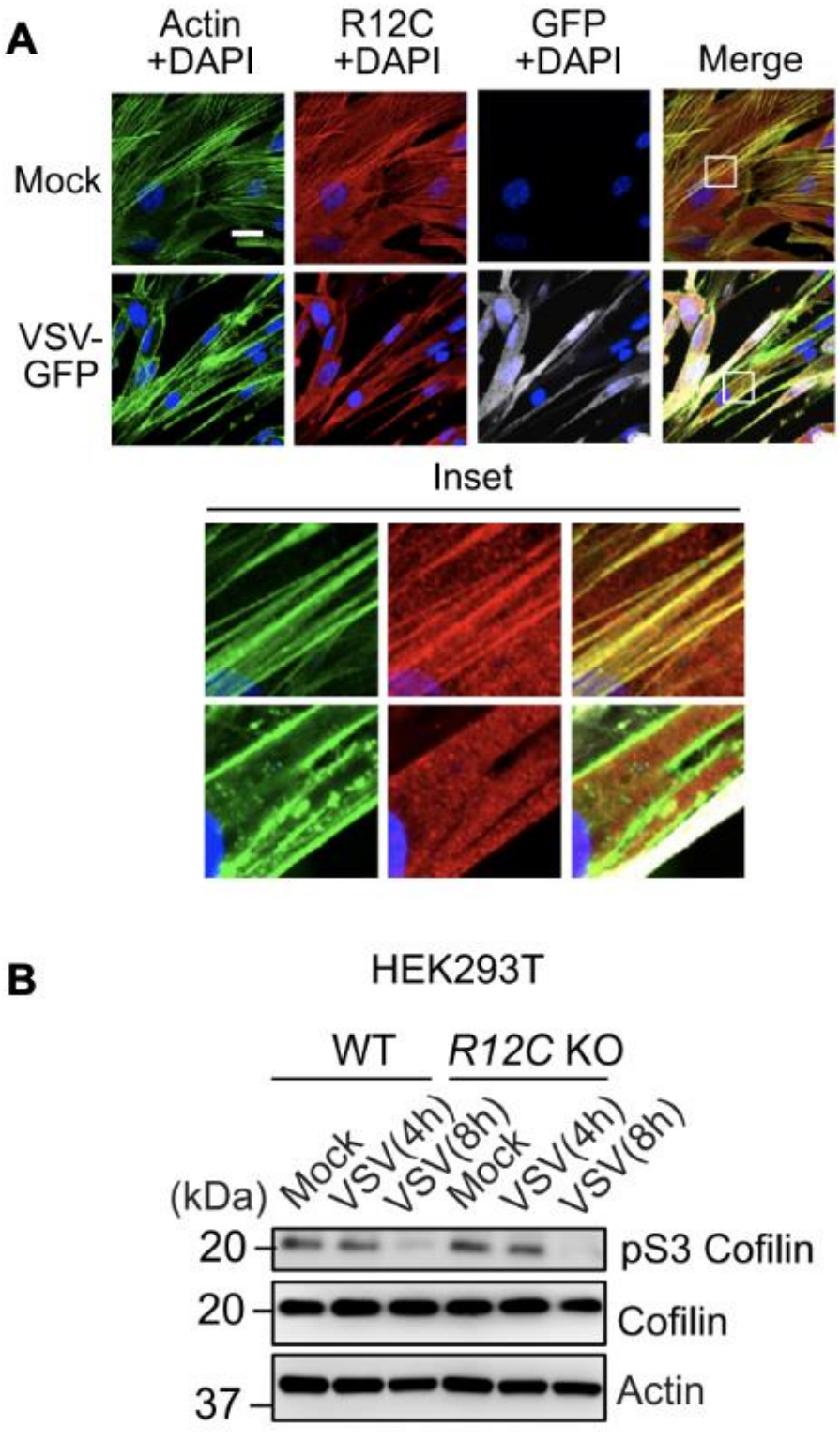

Figure 2.11: Viral infection triggers actin remodeling and R12C relocalization.

Figure 2.11 continued: A) Representative confocal microscopy images showing colocalization of endogenous R12C (red) with F-actin (green) in NHLF cells that were either mock-treated or infected with VSV-GFP (MOI 2) for 16 h. Nuclei (DAPI), blue. Scale bars, 10 μm. **B)** Phosphorylation of endogenous cofilin (at S3) in WT and *R12C KO* HEK293T cells that were either mock-treated or infected with VSV (MOI 0.5) for the indicated times, determined in the WCLs by IB with the indicated antibodies.

To show a more direct link between actin perturbation and R12C's function toward the RLRs, we used Cytochalasin D (CytoD), a commonly used actin-perturbing drug that inhibits cytoskeleton polymerization resulting in significant changes to the organization of actin filaments (Fig 2.12 A). Like what was observed during viral infection, when cells were treated with CytoD, the distribution of R12C shifted from mostly actin filament associated to mostly cytoplasmic with little colocalization between actin and R12C (Fig 2.12 B). In addition, when cells were treated with increasing concentrations of CytoD, it resulted in a marked dephosphorylation of RIG-I at S8 (Fig 2.12 C). Interestingly, CytoD treatment did not result in RLR-mediated ISG induction. Treatment of cells with concentrations of CytoD sufficient to induce actin remodeling and RIG-I dephosphorylation failed to increase IFN-β transcription relative to mock treatment (Fig 2.12 D). When these data are considered together, it suggests that actin remodeling is sufficient to trigger RLR dephosphorylation but is not sufficient for RLR signaling. This is in agreement with previously published data which has demonstrated that RIG-I and MDA5 signaling requires the presence of stimulatory RNA. We therefore propose that complete RLR activation requires two signals: 1) binding of cytoplasmic RNA, and 2) dephosphorylation as a result of actin perturbation. Both signals should be present during viral infection; however, if either one of these signals is absent, we would expect that the RLR-activated antiviral program would not be implemented.

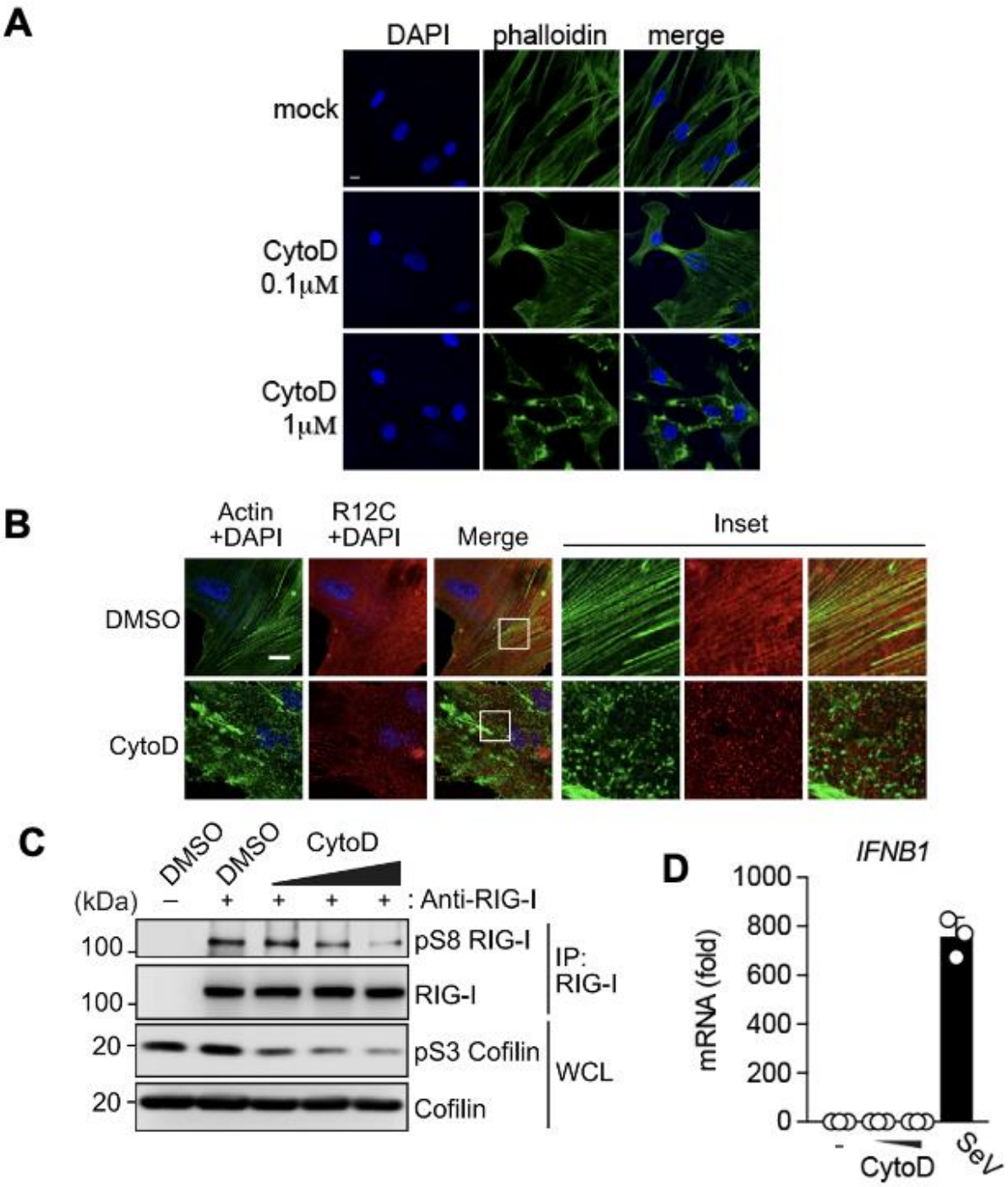

Figure 2.12: The actin perturbing agent CytoD induces RLR dephosphorylation but not IFN-β transcription. A) Representative confocal microscopy images showing endogenous F-actin (green) in primary NHLF cells that were treated with 0.1 μM or 1 μM cytoD for 4 h. Nuclei (DAPI), blue. Scale bar, 10 mm.

Figure 2.12 continued: B) Representative confocal microscopy images showing colocalization of endogenous R12C (red) with F-actin (green) in NHLF cells treated with CytoD (10 μM) or DMSO (control) for 10 min. Nuclei (DAPI), blue. Scale bars, 10 μm. **C)** Dephosphorylation of endogenous RIG-I in NHLFs that were either mock-treated, treated with 10μg/mL of poly(I:C) for 30 min, 3 h, or 6 h, or with 0.1 μM CytoD for the same amounts of time, determined by IP with anti-RIG-I and IB with anti-pS8-RIG-I. **D)** qRT-PCR analysis of IFNB1 transcripts in NHLF cells that were mock treated, treated with CytoD (0.1 or 1 μM) for 16 hours, or infected with SeV (5 HAU/mL) (control) for 16 h.

While it has been well established that viral infection, particularly entry and egress, can induce significant changes in the cellular cytoskeleton, it is less clear how delivery of stimulatory RNA molecules directly to the cell via transfection induces RLR activation if both RNA and cytoskeletal reorganization are necessary signals for complete activation of RIG-I and MDA5. Successful RNA transfections with commonly used transfection reagents are known to require cellular uptake and fusion (Cardarelli et al., 2016; Coppola et al., 2013), which we hypothesize may trigger actin cytoskeleton disturbance, providing the second signal needed for RLR activation. We first tested if lipid/polymer-based transfection reagents induce actin remodeling by assessing cofilin S3 phosphorylation—an indicator of actin reorganization. Treatment of cells with PEI, LyoVec, or Lipo2000 induced the dephosphorylation of cofilin at S3 (Fig 3.13 A), indicating that the process of transfection alone induces changes in the actin cytoskeleton. Transfection reagent treatment also induced the dephosphorylation of MAD5 at S88 even in the absence of stimulatory RNA (Fig 3.13 A). However, because no RLR-activating RNAs were present, transfection reagents alone did not activate an antiviral response. Unlike infection with SeV, neither PEI, LyoVec, nor Lipo2000 induced the transcriptional upregulation of IFNB1 (Fig 13.2 B).

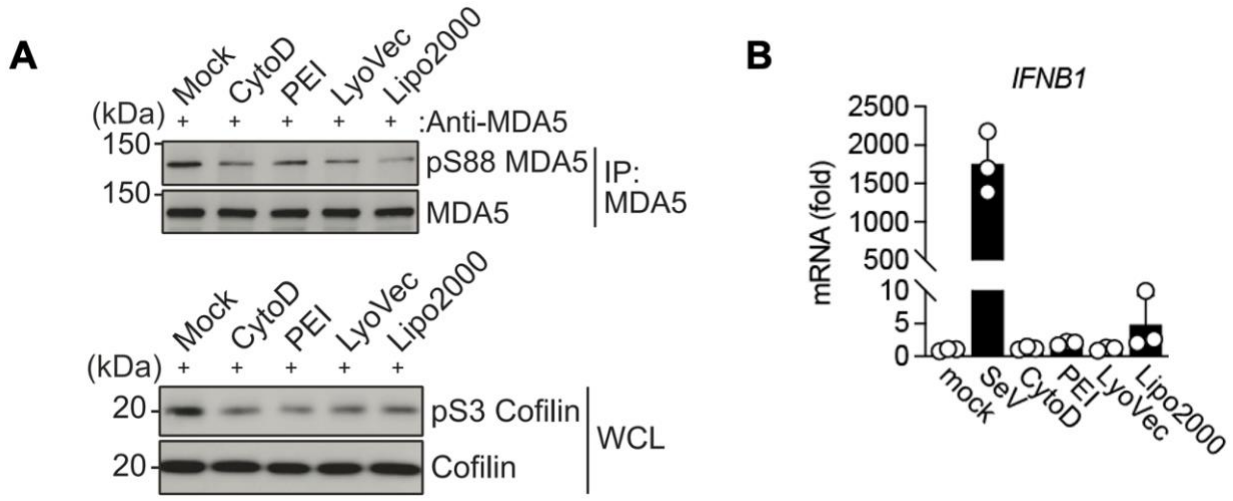

Figure 2.13: Transfection reagents induce RLR dephosphorylation but not IFN-β induction. A) Upper: dephosphorylation of endogenous MDA5 in IFN-β-stimulated (500 U/mL for 18 h) NHLF cells that were treated with CytoD (4 mM), PEI (25 mg/ mL), LyoVec (25 mg/mL), or Lipo2000 (20 mL/mL) for 4 h, determined by IP with anti-MDA5 and IB with anti-pS88-MDA5. Lower: dephosphorylation of cofilin at S3 in WCLs after treatment as described in A, determined by IB probed with the indicated antibodies. **B)** qRT-PCR analysis of IFNB1 transcripts in NHLF cells that were either mock-treated or treated with PEI (50 μg/mL), LyoVec (25 μg/mL) or Lipo2000 (20 μL/mL) for 16 h. Cells infected with SeV (5 HAU/mL) for 16 h served as control.

2.4 Discussion

Being able to effectively detect viral infection is the first step in mounting an innate immune response. Distinguishing viral infection is a complex process that requires the cell to be able to recognize cues that occur only during viral infection. To do this, cells employ pattern recognition receptors, such as the RLRs which detect a specific pathogen-associated pattern in this case cytoplasmic RNA. In addition to pattern recognition, the activity of the RLRs and other PRRs can be regulated by other cellular components, often via post-translational modification. An area that warrants further investigation is determining how additional factors that regulate PRRs are attuned to viral infection.

In this study we characterize a novel regulator of the RLRs; R12C. R12C is a PP1 regulatory subunit, whose function in uninfected cells pertains to the regulation of actin cytoskeleton dynamics. We show that R12C is critical for targeting PP1 to the CARD domains of the RLRs and mediating their dephosphorylation. In the absence of R12C, PP1 is not properly targeted to the RLRs, which translates into reduced IFN-β and ISG induction downstream of RIG-I and MDA5 and enhanced viral replication. What is particularly interesting about R12C's role in the RLR pathway is that its function is both upstream of the RLRs and dependent on viral infection. This raises the question: how does R12C detect and respond to viral infection?

To answer this question we looked for changes in the expression and localization of R12C. We found that R12C is redistributed from the filamentous actin cytoskeleton in uninfected cells to the cytosol after infection. Based on R12C's known function, we hypothesized that R12C might be responding to changes in actin dynamics. Actin remodeling is a ubiquitous feature of the viral lifecycle (Taylor et al., 2011), making it an attractive candidate for detecting the presence of viral infection. We also confirmed that viral infection produces detectable changes in global actin dynamics. Furthermore, perturbing actin dynamics in the absence of virus infection was sufficient to promote dephosphorylation of the RLRs by R12C and PP1.

In contrast to the classical model of RLR activation which requires only a stimulatory RNA ligand, our work suggests that RLR-RNA binding is not sufficient for RIG-I and MDA5 activation. Indeed, Acharya and colleagues (2022) showed that when an RLR ligand is inducibly expressed from cells in the absence of actin remodeling associated with viral infection or treatment with transfection reagents, little or no RLR

signaling is activated. This is not; however, because the RNA ligand lacked the ability to stimulate the RLRs. When changes in the actin cytoskeleton were induced by treating the cells with transfection reagents or viral particles in conjunction with the expression of the inducible RIG-I ligand, a robust RLR-mediated immune response was observed (Acharya at al., 2022). This changes our understanding of how the RLRs are activated, which has previously been attributed solely to the presence of stimulatory RNA. Not only is a stimulatory RNA necessary for RIG-I and MDA5 activation but a second signal in the form of cytoskeleton remodeling is also required for RLR dephosphorylation and downstream signaling.

2.5 Materials and Methods

Cells. Human embryonic kidney cells (HEK293T, ATCC), normal human lung fibroblasts (NHLF, Lonza), and African green monkey kidney epithelial cells (Vero, ATCC) were cultured in Dulbecco's modified Eagle media (DMEM, Gibco) supplemented with 10% (vol/vol) fetal bovine serum (FBS; Gibco), 100 U ml^{-1} penicillin-streptomycin (Pen-Strep, Gibco), 1 mM sodium pyruvate (Gibco), and 2 mM L-glutamine (Gibco). Madin-Darby canine kidney cells (MDCK, kindly provided by B. Manicassamy, University of Iowa) were grown in Eagle's minimum essential media (MEM; Gibco) supplemented with 10% (vol/vol) FBS, 100 U ml −1 Pen-Strep, and 2 mM L-glutamine. PPP1R12C knockout (KO) and control HAP1 cells (both Horizon Discovery) were grown in Iscove's modified Dulbecco's media (IMDM; Gibco) supplemented with 10% (vol/vol) FBS and 100 U ml −1 Pen-Strep. All cell cultures were maintained at 37 °C in a humidified 5% CO2 atmosphere. All commercially obtained cells were authenticated by the vendor (ATCC, Lonza, or

Horizon Discovery) and not further validated by our laboratory. Cell lines obtained and verified by other groups were not further validated. The *PPP1R12C* KO HEK293T cells generated in this study were validated as described in detail below. All cell lines used in this study were regularly checked for the presence of mycoplasma by PCR.

Adult mouse dermal fibroblasts derived from ear tissue of *Ppp1r12c*$^{+/+}$ or *Ppp1r12c*$^{-/-}$ mice (C57BL/6NJ mice, 6 weeks old) were generated after mincing and then treatment with 1000 U ml^{-1} collagenase (Gibco) followed by trypsinization. Cells were cultured in DMEM supplemented with 10% (vol/vol) FBS, 2 mM L-glutamine (Gibco), 1% (vol/vol) non-essential amino acids (NEAA; Gibco), 1 mM sodium pyruvate (Gibco), and 100 U ml^{-1} Pen-Strep.

Viruses. Sendai virus (SeV; Cantell strain) was purchased from Charles River Laboratories. Recombinant IAVΔNS1 (strain H1N1, A/PR/8/34) was a kind gift from A. García-Sastre (Icahn School of Medicine at Mount Sinai). Encephalomyocarditis virus (EMCV; strain EMC) was purchased from ATCC. mutEMCV (Deddouche et al., 2014; Hato et al., 2007), which encodes two point mutations in the zinc domain of the L protein (ZnC19A/C22A), was kindly provided by F. J. M. van Kuppeveld (Utrecht University). VSV-eGFP was a gift from S. Whelan (Washington University St. Louis). ZIKV strain Brazil Paraiba 2015 (BRA/2015) is described elsewhere (Braun et al., 2019; Sapparapu et al., 2016). DENV2 serotype 2 (strain 16681) was a gift from Lee Gehrke (Harvard/M.I.T.).

DNA constructs and transfection reagents. pEBG-GST-RIG-I(2CARD), pEBG-GST-MDA5(2CARD), pEF-BOS-FLAG-RIG-I, pEF-BOS-FLAG-MDA5, pEF-BOS-FLAG-MAVS, and pCMV2-FLAG-IRF3 were previously described (Gack et al., 2010; Gack et al., 2007; Maharaj et al., 2012; Wies et al., 2013). pIRES-PP1α-HA and pIRES-PP1γ-HA were previously described (Wies et al., 2013). pXJ40-R12C-FLAG was a gift from T. Leung (Agency for Science, Technology and Research, Connexis, Singapore) and was subcloned into the pEF-IRES-Puro between EcoRI and MluI and pCMV6 between EcoRI and XhoI containing a myc tag. pCMV6-R12C-myc was used as a template for around-the-horn PCR to generate R12C N (aa 1-389), R12C C (aa 390-782), and R12C NΔ95 (aa 95-782), which were then subcloned into pEF-IRES-Puro. pCDNA3-MLV Gag-YFP was a kind gift from W. Mothers (Addgene #1813). pMD2.G was described previously (Dull et al., 1998). pCas9 GFP was a kind gift from K.-K. Conzelmann (Ludwig-Maximilian-University Munich). pMH3-TK-BSD and pKF274 to generate CRISPR/Cas9 KO cells are described elsewhere (Bottcher et al., 2014). The sequence of all constructs was confirmed as correct by DNA sequencing.

Transient DNA transfections were performed using linear polyethylenimine (PEI; Polysciences) prepared as 1 mg/mL solution in 10 mM Tris (pH 6.8), calcium phosphate (Clontech), Lipofectamine and PLUS reagent (Invitrogen), or Lipofectamine2000 (Invitrogen) as per the manufacturer's instructions.

Antibodies and other reagents. The following antibodies were used for immunoblotting at the indicated concentrations: anti-GST (1:2000, GST-2, Sigma), anti-HA (1:2000, HA-7, Sigma), anti-FLAG (1:2000, M2, Sigma), anti-myc (1:2000, 71D10, Invitrogen), anti-

RIG-I (1:2000, Alme-1, AdipoGen), anti-PP1α (1:2000, Bethyl laboratories), anti-PP1γ (1:2000, Bethyl laboratories), anti-phospho-cofilin (Ser3) (1:1000, 3311S, CST), and anti-cofilin (1:1000, D3F9, CST). The monoclonal anti-MDA5 antibody was purified from clone 17 of a mouse hybridoma cell line provided by J. Rehwinkel (University of Oxford) (Hertzog et al., 2018). The anti-pS8-RIG-I and anti-pS88-MDA5 antibodies have been previously described (Gack et al., 2010; Maharaj et al., 2012; Wies et al., 2013). The custom-generated anti-R12C antibody (1:2000, GeneScript) was produced in rabbits immunized with the peptide Cys-CRKVGKEWRGPAEGE covalently linked to keyhole limpet hemocyanin. Sera were collected from the immunized rabbits and the presence of R12C-specific antibodies was detected by enzyme-linked immunosorbent assay (ELISA) and subsequently affinity purified. Secondary horseradish peroxidase-conjugated anti-mouse and anti-rabbit were purchased from CST.

Anti-FLAG M2 magnetic beads (MilliporeSigma), anti-FLAG agarose beads (MilliporeSigma), anti-HA magnetic beads (Pierce), Glutathione Sepharose 4B resin (GE Healthcare) and Protein A, G or A/G conjugated agarose beads (Invitrogen) or Dynabeads (Invitrogen) were used for immunoprecipitations.

Protease inhibitor cocktail (P2714) and phosphatase inhibitor cocktail 3 (P0044) were purchased from MilliporeSigma. Calyculin A (PHZ1044) and Cytochalasin D (CytoD) were purchased from Gibco and Tocris Bioscience, respectively. High-molecular weight (HMW) poly(I:C) complexed with LyoVec, and uncomplexed LyoVec, were purchased from Invivogen and used according to manufacturer's instructions. Human IFN-β was purchased from PBL Biomedical Laboratories.

Generation of CRISPR knockout cells. To generate R12C KO HEK293T cells, a dsDNA template was synthesized using overlap extension PCR with the following primers: 5′-GGA AGA GGG CCT ATT TCC CAT GAT TCC TTC AT-3′, 5′-tgg aaa gga cga aac acc cCC AAG AAG CGC ACC ACC TCC gtt taa gag cta tgc tg-3′, 5′ -GTT TAA GAG CTA TGC TGG AAA CAG CAT AGC AAG TTT AAA TAA GGC TAG TCC GTT ATC AAC TTG AAA AAG TGG CAC CGA GTC GGT GC-3′, 5′-GCA CCG ACT CGG TGC CAC T-3′ and the plasmid pKF274 (Bottcher et al., 2014) (provided by K. Förstemann, Ludwig-Maximilians-University of Munich) as a template to generate an sgRNA template which contains the U6 snRNA promoter, followed by the R12C gRNA (5′-CCA AGA AGC GCA CCA CCT CC-3′) and the sgRNA scaffold. Similarly, a double-stranded homologous recombination (HR) donor construct was synthesized using the plasmid pMH3-TK-BSD (Bottcher et al., 2014) as a template with the forward primer 5′-AGT GGC GTC CAG CCC TCG TTG TCT GCC TGG TTC ACA GTG GCG CCC TGC TCC ACC AAG AAG CGC ACC ACC TAA TGA GTC TTC GGA CCT CGC GGG GGC CG-3′ and reverse primer 5′-GAC ACC GTG GCT GGG GTA GGT GCG GCT GAC GGC TGT TTC CCA CCC CCA GGC CTG CAT TGA TGA GAA CTG ACA TAT GTT AGA AAC AAA TTT ATT TTT AAA G-3′. HEK293T cells were transfected with the sgRNA template, the HR template, and Cas9 (pCas9_GFP). Three days after transfection, cells were selected using 10 µg/mL blasticidin (Thermo Fisher Scientific). Knockout of R12C was confirmed by IB to confirm the absence of R12C protein expression as well as by PCR to confirm insertion of the blasticidin resistance cassette.

siRNA-mediated gene silencing. Transient gene knockdown was achieved by using gene-specific siGenome SMARTpool siRNA or individual siGENOME siRNAs (Horizon Discovery). siRNA was transfected into cells seeded into 12-well plates (~1 x 10^5 cells per well) via Lipofectamine RNAiMAX (Invitrogen) at a final concentration of 80 to 120 nM according to the manufacturer's instructions. The siGENOME SMARTpool siRNAs used in this study are: si.PPP1R1A (D-001210-03-05), si.PPP1R2 (D-001210-03-05), si.PPP1R3D (M-021439-01-0005), si.PPP1R8 (M-010903-01-0005), si.PPP1R12A (M-011340-01-0005), si.PPP1R12B (M-013547-01-0005), si.PPP1R12C (M-013547-01-0005), si.PPP1R15A (D-013775-04-0002), si.PP1α (M-008927-01-0005), si.PPP1γ (M-008927-01-0005), si.IRF3 (M-008927-01-0005), si.MDA5 (M-013041-00), and si.RIG-I (M-008927-01-0005). The following individual siGENOME siRNAs were used: si.PPP1R12C #1 (D-013775-01-0002), si.PPP1R12C #2 (D-013775-01-0002), si.PPP1R12C #3 (D-013775-03-0002), and si.PPPR12C #4 (D-013775-04-0002). Non-targeting siRNAs (D-001210-03-05 or D-001206-14) were used as controls. Knockdown efficiency was determined by measuring mRNA abundance of the respective gene by qRT-PCR using gene-specific predesigned PrimeTime qPCR Probe Assays (Integrated DNA Technologies) as indicated.

Luciferase reporter assay. HEK293T, seeded into 12-well plates (~1 x 10^5 cells per well) were transfected with 200 ng IFN-β luciferase reporter plasmid, 300 ng β-galactosidase (β-gal)-expressing pGK-β-gal plasmid, and the following amounts of effector plasmid: 400 ng GST-MDA5(2CARD), 2 ng GST-RIG-I(2CARD), 15 ng FLAG-MAVS, 500 ng FLAG-MDA5, or 50 ng FLAG-RIG-I. Luciferase and β-gal activities were determined at the

indicated times after transfection using the Luciferase Assay System (Promega) and β-Galactosidase Enzyme Assay System (Promega), respectively. Luminescence and absorbance were measured using a Synergy HT Microplate Reader (BioTek). Luciferase activity was normalized to β-gal values and luciferase fold induction was calculated relative to mock-transfected samples, set to 1.

Immunoprecipitation and immunoblotting. Immunoprecipitation of endogenous proteins or overexpressed tagged proteins was performed as previously described (Wies et al., 2013) Briefly, cells that were infected or transfected were lysed at the indicated times in Nonidet P-40 (NP-40) buffer (50 mM HEPES pH 7.4, 150 mM NaCl, 1% (vol/vol) NP-40, 1 mM EDTA) or radioimmunoprecipitation assay (RIPA) buffer (50 mM Tris-HCl; pH 7.4, 150 mM NaCl, 1% (vol/vol) NP-40, 0.5% (wt/vol) deoxycholic acid (DOC), 0.1% (wt/vol) SDS) with protease inhibitor cocktail. Cell lysates were then cleared of cellular debris via centrifugation at 21,000 g for 20 min at 4°C. A portion of the cleared lysate was reserved for analysis of the whole cell lysate (WCL), while the remaining lysate was subjected to protein immunoprecipitation. Lysates were incubated with anti-FLAG M2 magnetic beads (MilliporeSigma), anti-FLAG agarose beads (MilliporeSigma), anti-HA magnetic beads (Pierce), or GST magnetic or agarose beads (Pierce) at 4 °C for 4-16 h. For immunoprecipitation of endogenous protein, cell lysates were probed overnight at 4°C with 1-2 µg/mL of primary antibody, followed by coupling to protein A, G, or A/G conjugated agarose or magnetic beads for an additional 2 h at 4°C. To detect the phosphorylation of RIG-I and MDA5, cells were treated with 50 nM Calyculin A (Invitrogen) for 45 min prior to harvesting and cell lysis was carried out in the presence of

protease inhibitor cocktail (MilliporeSigma), phosphatase inhibitor cocktail 3 (MilliporeSigma) and Calyculin A (Invitrogen).

Beads were extensively washed with NP-40 or RIPA buffer and the immunoprecipitated proteins were eluted by heating samples in Laemmli SDS sample buffer at 95°C for 5 min. Proteins were resolved on 7-12% Bis-Tris SDS-PAGE gels, transferred onto polyvinylidene difluoride (PVDF) membranes (Bio-Rad), probed with the specified antibodies, and visualized as previously described (Wies et al., 2013).

RT-qPCR analysis. Total RNA was extracted using the E.Z.N.A HP Total RNA Kit (Omega Bio-tek) as per the manufacturer's instructions. The quality and quantity of the extracted RNA were assessed using a NanoDrop Lite spectrophotometer. One-step qRT-PCR was performed with equal amounts of RNA using the SuperScript III Platinum One-Step qRT-PCR kit with ROX (Invitrogen) and commercially available predesigned PrimeTime qPCR Probe Assays (Integrated DNA Technologies) on a 7500 Fast Real-Time PCR System (Applied Biosystems) or QuantStudio 6 (Thermo Fischer). The relative mRNA expression of gene of interest was calculated by using the comparative threshold ($\Delta\Delta C_t$) method and expressed relative to the values for control cells. Gene expression levels were normalized to cellular *GAPDH* expression. qRT-PCR reactions were performed using a 7500 FAST Real-Time PCR machine (Applied Biosystems).

Enzyme-linked immunosorbent assay (ELISA). Culture media collected from transfected or infected cells were centrifuged to remove cell debris. IFN-β levels in the

culture supernatant were quantified by an enzyme-linked immunosorbent assay (ELISA) using a commercially available ELISA kit (PBL Biomedical Laboratories) following the manufacturer's instructions.

Virus infection and titration. Cells were infected with EMCV, VSV-eGFP, DENV, or ZIKV in DMEM containing 2% (vol/vol) FBS at the indicated MOI. After 1-2 h, the inoculum was replaced with normal cell growth medium. IAV infection was carried out in DMEM supplemented with 0.1% (vol/vol) N-tosyl-L-phenylalanine chloromethyl ketone (TPCK)-treated trypsin (MilliporeSigma) for 2 h, after which cells were washed and the media replaced with supplemented DMEM.

EMCV titration was performed on Vero cells using the Reed-Muench tissue culture infectious dose (TCID50) methodology as previously described (Sparrer et al., 2017). IAV titers were determined by plaque assay on MDCK cells using 2.4% Avicel containing overlay media (FMC BioPolymer) as described previously (Matrosovich et al., 2006).

Generation of PPP1R12C KO mice and in vivo studies. *Ppp1r12c*$^{-/-}$ mice (C57BL/6NJ background) used for this study were generated from ES cell clone 18962A-G1 (Regeneron Pharmaceuticals, Inc.) by the Knockout Mouse Project (KOMP) Repository and the Mouse Biology Program at the University of California Davis. Heterozygote mice were used for breeding and production of *Ppp1r12c*$^{-/-}$ and wild-type (WT) control mice. Mice were validated by genotyping as well as qRT-PCR analysis of *Ppp1r12c* transcript expression.

Confocal microscopy. Infected or treated NHLF cells, grown on 12 mm-glass slides, were fixed with 4% (wt/vol) paraformaldehyde (PFA) in PBS (Santa Cruz) for 20 min at room temperature (RT). Fixed samples were washed three times with PBS, permeabilized and free binding sites blocked with PBS containing 0.05% (vol/vol) Triton-X100 (MilliporeSigma) and 5% (vol/vol) FBS (Gibco) for 30 min at RT. After extensive washing with PBS, cells were incubated overnight at 4 °C with anti-R12C (1:400, custom-made) or anti-RIG-I (1:400, Alme-1, AdipoGen) in PBS containing 1% (vol/vol) FCS (Gibco) on a rocking platform. Cells were washed three times with PBS containing 0.25% Tween20 (MilliporeSigma) and then incubated with the secondary antibodies anti-rabbit Alexa 568 and anti-mouse Alexa 488 (both 1:400, Invitrogen) and, where indicated, also with DAPI (1:1000, MilliporeSigma) and phalloidin-647 (1:200, Invitrogen). Cells were washed three times with PBS containing 0.25% Tween20 and once with ultrapure water, and then mounted using Mowiol mounting medium as previously described (Koepke et al., 2020). Laser scanning confocal images were taken using a Leica SP8 system or a Zeiss LSM 710. Images were analyzed using Fiji (ImageJ).

Quantification and statistical analysis. All data were analyzed using GraphPad Prism software (version 7). Statistical analyses were performed using a two-tailed Student's *t*-test (unpaired) unless otherwise stated, and P values of less than 0.05 were considered significant. Significant differences are denoted by *P <0.05, **P <0.01, and ***P <0.001. Pre-specified effect sizes were not assumed and the number of independent biological replicates (n) is indicated for each figure.

CHAPTER 3

INHIBITION OF IFN-γ-MEDIATED STAT1 ACTIVATION BY NOROVIRUS

Attributions: RAR performed and analyzed all experiments with the exception of the following: SK performed and analyzed Figure 3.1 A-B, Figure 3.2, and Figure 3.4 A-B. Figure 3.5 A and 3.6 were performed by SK and RAR

3.1 Abstract

Human noroviruses are a major cause of acute gastroenteritis, yet we currently have no antivirals or vaccines. Efforts to develop treatments for norovirus infection have been hampered by our lack of understanding of the immune response to norovirus infection and viral strategies to combat it. Using murine norovirus (MNV) as a model, it has been established that an effective innate immune response is critical for controlling MNV infection. Despite the pressure of the innate immune system, MNV is still able to infect mice, suggesting that this virus has mechanisms for antagonizing the host's innate immune response. In this study, we determine that MNV is able to inhibit a type II IFN-induced immune response that is otherwise able to effectively restrict the replication of other RNA viruses. The ability of MNV to actively antagonize IFN-γ-activated antiviral pathways is encoded by the nonstructural protein 5 (NS5). In addition to its role in MNV genome transcription and translation, NS5 also inhibits the activation of the important antiviral factor signal transducer and activator of signaling 1 (STAT1) by preventing its nuclear accumulation. NS5's inhibition of STAT1 nuclear redistribution prevents the

upregulation of specific interferon stimulated genes (ISGs) which are needed for the restriction of several RNA viruses.

3.2 Introduction

Human noroviruses are a significant cause of acute viral gastroenteritis globally for which we currently have no vaccines or therapeutics (Glass et al., 2009; Bartsch et al., 2016; McAtee et al., 2016). One of the reasons it has been so difficult to develop norovirus treatments is due to our incomplete understanding of norovirus infection and corresponding immune response. This knowledge gap persists due largely to the technical challenges associated with studying human noroviruses, particularly the lack of conventional cell culture and small animal models (Papafragkou et al., 2013; Wobus et al. 2006). To circumvent these difficulties, the mouse virus, MNV, can be used as a model to gain insights into norovirus biology *in vitro* and *in vivo* (Wobus et al., 2006).

Using MNV as a model, recent studies have uncovered the importance of the innate immune response in controlling norovirus infection (Biering et al., 2017). Specifically, the antiviral pathways requiring STAT1, which include type I, II, and III IFN responses, are absolutely critical for host control of norovirus infection (Karst et al., 2003; Hwang et al., 2012). The type II IFN response, which is mediated by IFN-γ, restricts MNV replication through a pathway that requires several components of the autophagy machinery, such as Atg5, Atg12, and Atg16l1, as part of a system known as targeting by autophagy (TAG). While the TAG system is necessary for the IFN-γ-dependent antiviral response to inhibit MNV infection, TAG does not play a role in the IFN-induced restriction

of many other RNA viruses including mouse hepatitis virus (MHV) and West Nile virus (WNV) (Biering et al., 2017).

Instead, the replication of other RNA viruses is likely inhibited through a more classical, TAG-independent, type II IFN pathway in which IFN-γ activates JAK-STAT signaling through the type II IFN receptor. After IFN-γ binds to its receptor, STAT1 is phosphorylated within its transactivation domain at tyrosine 701 (Y701) and adopts an interferon stimulating gene (ISG)-activating conformation and is subsequently translocated to the nucleus. Once inside the nucleus, STAT1 can be phosphorylated at an additional site, serine 727 (S727), which is necessary for full STAT1 transcriptional activity. STAT1 then induces the transcription of ISGs by binding to IFN-γ-activated sequences (GAS) within the promotor regions of these genes. Once upregulated, ISGs enact a variety of direct and indirect antiviral activities to restrict the replication of many different RNA viruses.

In this study, we show that MNV inhibits TAG-independent IFN-γ antiviral signaling which restricts the replication of many other RNA viruses. MNV antagonizes this pathway using nonstructural protein 5 (NS5) which encodes the viral protein, genome linked (VPg). NS5 prevents the nuclear accumulation of STAT1 in response to IFN-γ, thereby inhibiting STAT1-mediated ISG upregulation in response to IFN.

3.3 Results

3.3.1 MNV actively inhibits the TAG-independent IFN-γ antiviral pathway

IFN-γ is able to restrict the replication of multiple classes of RNA viruses through diverse mechanisms, including the TAG system. TAG has previously been shown to be critical for IFN-γ to restrict MNV replication (Hwang et al., 2012); however, the importance of TAG for IFN-γ-dependent inhibition of other viruses is still unclear. To determine what, if any, role TAG plays in the restriction of RNA viruses other than MNV, we assessed the ability of IFN-γ to restrict MNV, EMCV, and DENV replication in macrophages lacking Atg5, a critical component of the TAG system. To specifically restrict our studies to the effects of IFN-γ, IFNAR KO bone marrow-derived macrophages (BMDM) were used so that type I IFNs could not contribute to viral restriction. While IFN-γ significantly reduced the number of MNV genome copies in cells with Atg5, in the absence of the TAG system, IFN-γ treatment failed to reduce MNV replication compared to untreated cells (Fig 3.1 A). In contrast, IFN-γ was still able to restrict the replication of other RNA viruses, including EMCV and DENV in the absence of Atg5 (Fig 3.1 B). These data demonstrate that IFN-γ can effectively restrict EMCV and DENV replication and that this mechanism of restriction does not require the TAG system. Interestingly, while MNV was the only virus tested that was inhibited by TAG, MNV was also the only virus that was able to evade TAG-independent IFN-γ restriction.

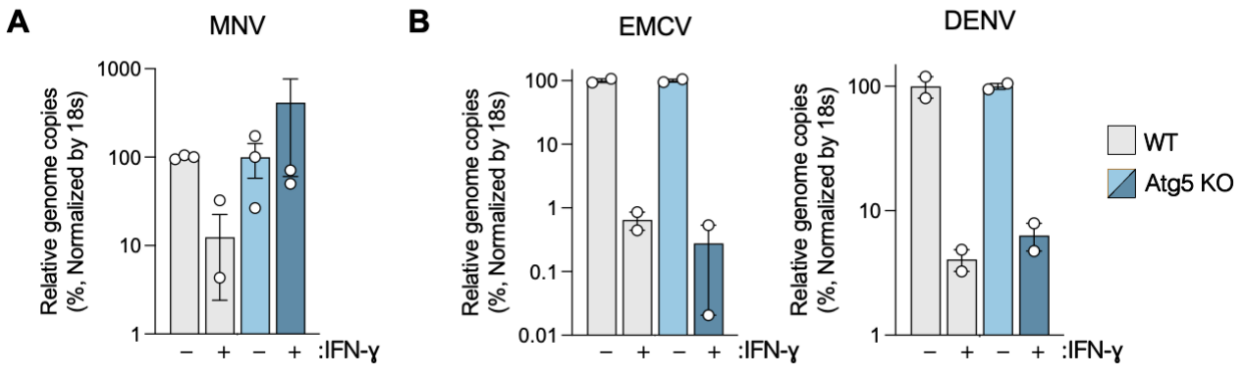

Figure 3.1: IFN-γ-mediated inhibition of several RNA viruses is not dependent on TAG. A-C) qRT-PCR analysis of RNA levels of **A)** MNV (MOI 0.05, 24 h), **B)** EMCV (MOI 0.05, 24 h), or **C)** DENV (MOI 0.5, 72 h) relative to actin (control) in *Ifnar*$^{-/-}$ *Atg5*$^{flox/flox}$ BMDM with or without *LysmCre*, after 24 hour mock-treatment or treatment with 100 U/mL IFN-γ for 24 h.

3.3.2 The MNV protein NS5 antagonizes the IFN-γ-induced antiviral response

We wanted to determine how MNV is able to evade the TAG-independent IFN-γ viral restriction pathway so we began by parsing out if MNV is actively inhibiting the IFN pathway or passively resistant to IFN-γ-induced restriction factors. To do this, we set up coinfection experiments with MNV and EMCV, a virus that is sensitive to IFN-γ treatment independently of TAG. We reasoned that if MNV is passively resistant to IFN-γ, when grown with EMCV, MNV would still be able to evade IFN-γ restriction, but EMCV would not. However, if MNV is actively inhibiting the IFN-γ antiviral pathway, then co-culture of the two viruses should allow both viruses to escape IFN-γ control resulting in higher levels of EMCV replication compared to IFN-γ- treated EMCV monocultures. We measured MNV and EMCV genome copies after mono- or co-infection in the presence or absence of IFN-

γ using qRT-PCR with primers that can specifically detect each viral genome. These infection studies were conducted in *Ifnar*$^{-/-}$ BV-2 cells to prevent the primary viral infection from inducing a Type I IFN response that could restrict the secondary viral infection. The *Ifnar*$^{-/-}$ BV-2 also lacked Atg5 to ensure that MNV replication was not impaired. In contrast to infection with EMCV alone, co-infection of EMCV with MNV reduced the ability of IFN-γ to restrict EMCV infection (Fig 3.2). Because MNV infection increases the escape of not only MNV but also EMCV from the IFN-γ antiviral response, this suggests MNV is actively inhibiting the IFN-induced viral restriction pathway.

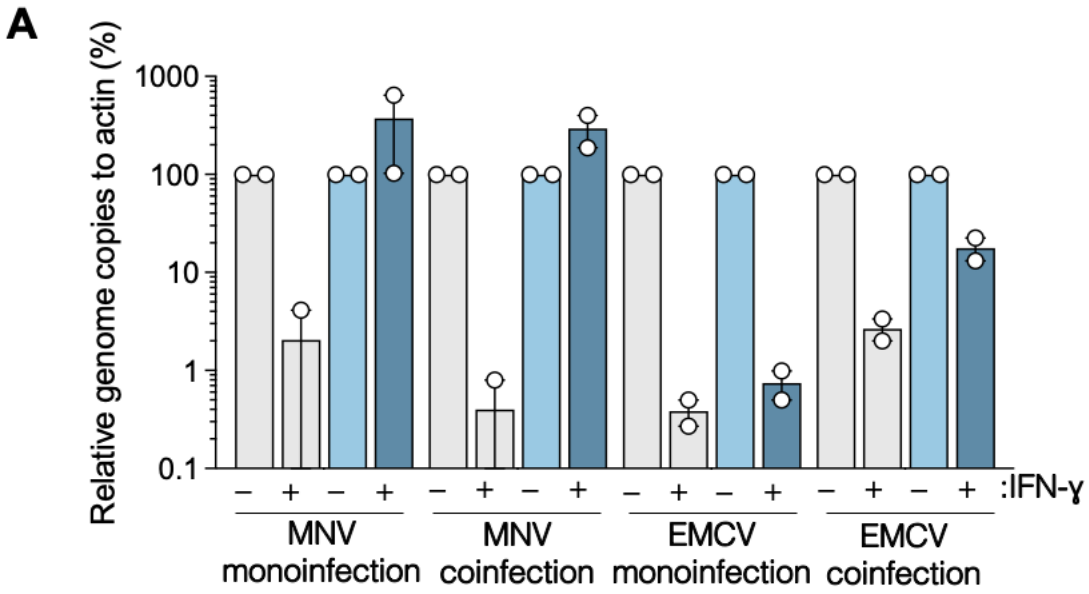

Figure 3.2: MNV actively evades IFN-γ-induced viral restriction. qRT-PCR analysis of MNV and EMCV genome copies relative to actin in *Ifnar*$^{-/-}$ *Atg5*$^{flox/flox}$ BMDM with or without *LysmCcre* expression after monoinfection with MNV (MOI 5, 24 h), or EMCV (MOI 0.05, 12 h), or co-infection with MNV (MOI 5) for 12 h followed by EMCV infection (MOI 0.05) for 12 h, in mock or IFN-γ treated cells (100 U/mL, 24 h).

To understand how MNV is actively inhibiting the TAG-independent IFN-γ response, we screened each of the ten MNV proteins individually to see if any of them

specifically possess activity against the IFN-γ pathway. As a readout for the ability of each MNV protein to inhibit the IFN-dependent antiviral response, we measured the percent of cells expressing each protein that were infected with EMCV and treated with INF-γ. Expression of nine out of the ten MNV proteins had little or no effect on EMCV restriction by IFN-γ (Fig 3.3 A). However, expression of MNV NS5 alone was sufficient to enhance EMCV replication in cells treated with IFN-γ compared to WT cells not expressing any viral proteins (Fig 3.3 A). Furthermore, NS5's inhibition of the IFN-γ response was not dependent on TAG, as Atg5 was absent in the tested cells.

To verify NS5's antagonism of the antiviral response was not an EMCV-specific phenomenon, the replication of DENV2 in IFN-γ-treated cells expressing MNV NS5 was measured by qRT-PCR. In cells not expressing NS5, DENV2 genome replication is inhibited by IFN-γ treatment (Fig 3.3 B). In contrast, expression of MNV NS5 allowed DENV2 to replicate to similar levels regardless FN-γ treatment (Fig 3.3 B). Therefore, MNV NS5 is able to enhance the replication of several RNA viruses, such as EMCV and DENV2, in IFN-γ-treated cells.

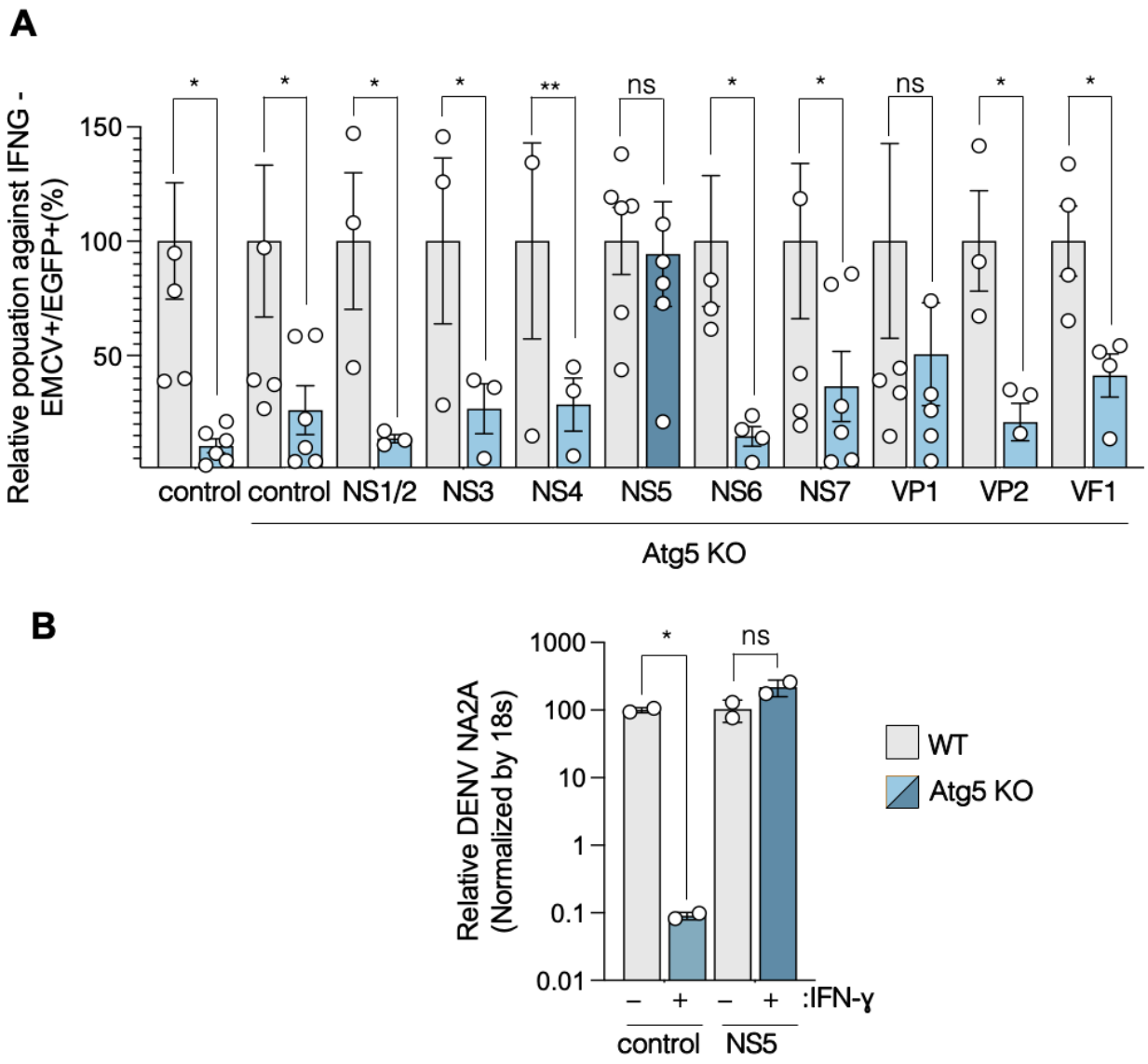

Figure 3.3: Norovirus NS5 inhibits INFγ-mediated viral restriction. A) Percent of *Atg5* KO BV-2 cells stably expressing MNV proteins (NS1/2, NS3, NS4, NS5, NS6 NS7, VP1, VP2, or VF1) infected with EMCV (MOI 5, 6h) relative to mock-treated cells, after 24 h stimulation with 100 U/mL IFN-γ, measured by flow cytometry to detect intracellular J2 (dsRNA) antibody staining in transduced cells (GFP positive). **B)** qRT-PCR analysis of RNA levels of DENV NS2A (MOI 0.1, 24h) relative to actin (control) in *Atg5* KO BV-2 expressing MNV NS5 after mock-treatment or IFN-γ treatment (100 U/mL, 24 h).

To verify that NS5 is facilitating viral replication by directly inhibiting the type II IFN response, we measured the IFN-γ-triggered upregulation of ISGs in cells exogenously

expressing NS5. When NS5 was present, the levels of transcribed ISGs, including *Gbp1*, *Gbp2,* and *Irf8*, were significantly lower than in stimulated cells not expressing NS5 (Fig 3.4 A). Interestingly, the transcription of all ISGs was not sensitive to NS5 expression. The upregulation of several ISGs, including *Irf1*, was not impacted by NS5 expression at all (Fig 3.4 A). This is in agreement with a previously published data set which showed by RNA-seq that a number of IFN-γ-induced genes were downregulated after MNV infection (Biering et al., 2017). When the individual ISGs found in the data set published by Biering et al. were examined, we found a significant overlap between the ISGs downregulated by MNV infection and by NS5 expression alone (Fig 3.4 B). Considered together, these data suggest NS5 facilitates RNA virus replication by inhibiting the selective upregulation of a subset of ISGs.

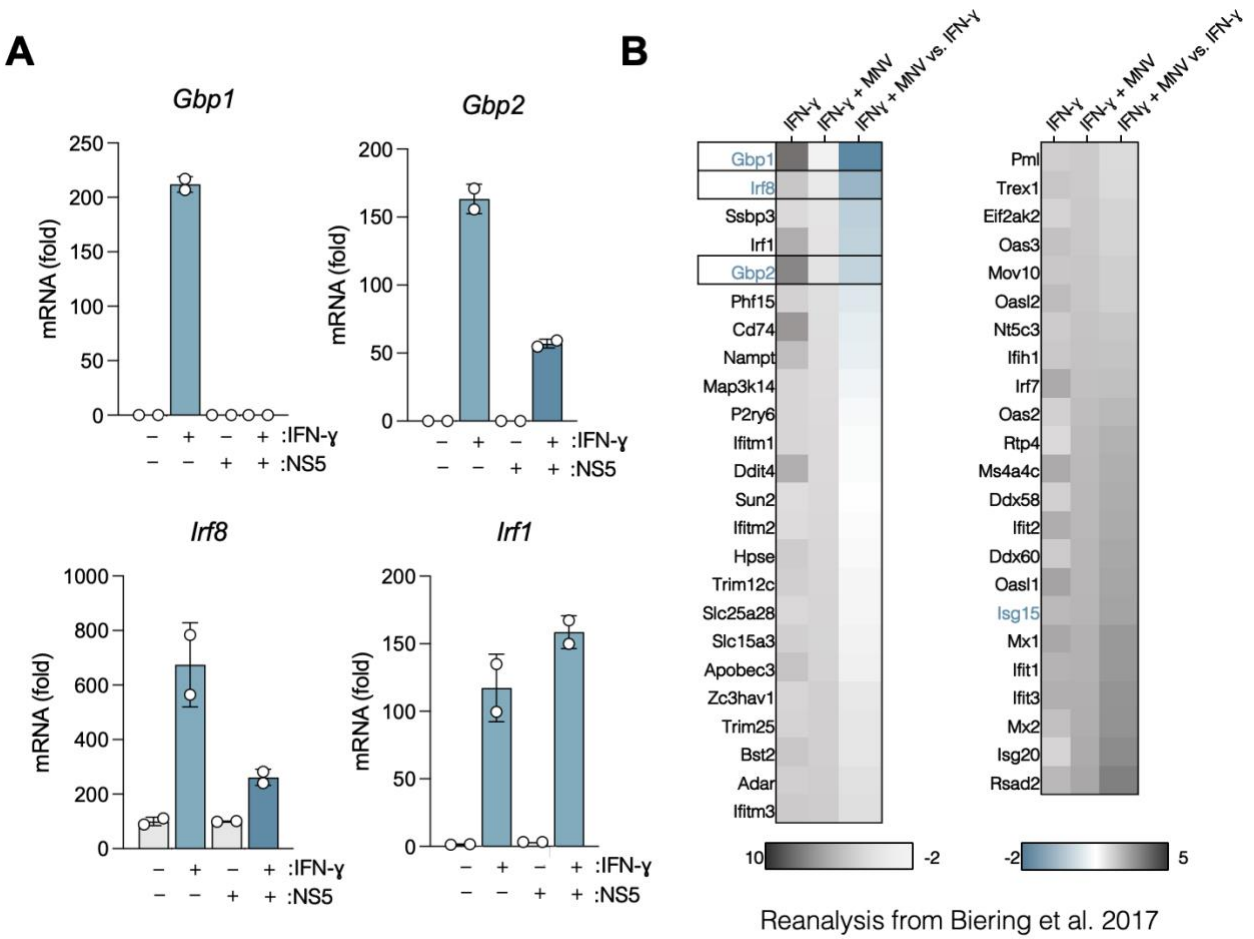

Figure 3.4: NS5 inhibits the induction of a subset of ISGs. A) qRT-PCR analysis of mRNA levels of the indicated ISGs in WT or *Atg5* KO BV-2 with or without NS5 expression after 100 U/mL IFN-γ treatment for 24 h or mock treatment, relative to actin mRNA (control). **B)** Reanalysis of RNA-seq data published in Biering et al., 2017.

3.3.3 Complete STAT1 activation is inhibited in the presence NS5

To determine how MNV NS5 inhibits the restriction of RNA viruses by IFN-γ, we used mass spectrometry to identify NS5 interacting partners in the context of IFN treatment. Previous studies have also used mass spectrometry to determine NS5 interactions; however, none have looked at NS5 protein interactors in the context of IFN-γ treatment or viral infection (Chung et al., 2014; Hosmillo et al., 2019). To isolate NS5-

interacting proteins for identification via mass spectrometry, we pulled-down HA-tagged NS5 or the control protein EGFP from the lysate of BV-2 cells that were treated with IFN-γ or mock-treated. Binding proteins were visualized by Coomassie stain and bands of interest were excised and analyzed by mass spectrometry (Fig 3.5 A). By comparing the subset of proteins that interact with NS5 with or without IFN-γ treatment, we identified candidate proteins that may be potential targets of NS5 as a means of inhibiting IFN-γ signaling. Our mass spectrometry analysis revealed a significant portion of overlap with previously published analyses; we identified more than 2/3 of all previously identified NS5 interacting proteins (Chung et al., 2014; Hosmillo et al., 2019). Most of the previously identified proteins bound to NS5 both with and without IFN-γ stimulation. We repeated this screen twice and found a shortlist of 51 proteins in both screens that interact with NS5 only after IFN-γ treatment (Fig 3.5 B).

We narrowed down the list of 51 candidate proteins by creating a protein-protein interaction network based on tested and predicted associations using STRING in Cytoscape to visualize how the proteins relate to one another (Fig 3.5 C). Of particular interest to us was a cluster of interacting proteins with functions associated with the innate immune response. Among these genes was STAT1, which is a critical component of the signaling cascade downstream of all three types of IFN. Because STAT1 is a critical component of the type II IFN-mediated response, and MNV NS5 inhibits the IFN-γ antiviral response, we chose to follow up on STAT1 as the primary target of NS5 antagonism.

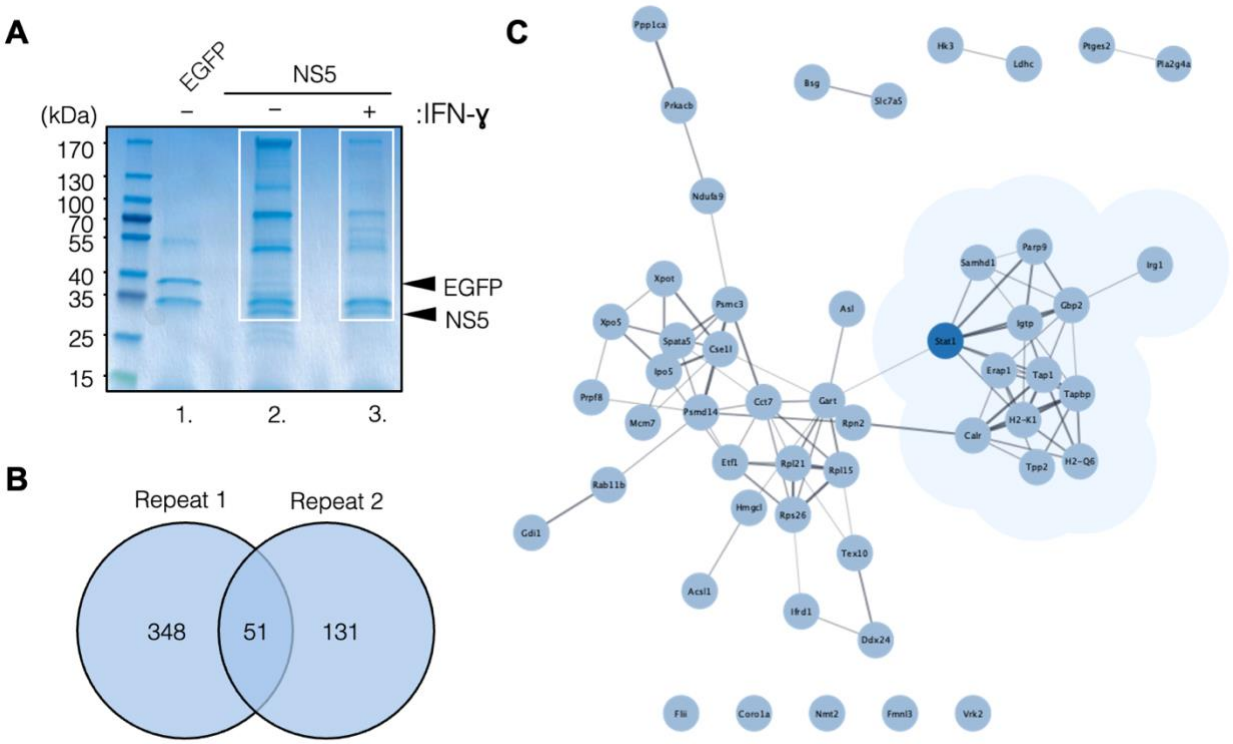

Figure 3.5: Mass spectrometry analysis of NS5 binding partners. A) Coomassie-stained proteins co-immunoprecipitated with HA-tagged EGFP (control) or mock or IFN-γ-treated (100 U/mL, 24h) NS5 purified from BV-2 cells using HA-conjugated sepharose. Arrows denote the bands corresponding to EGFP and NS5. White boxes indicate the gel sections sent for mass spectrometry analysis. **B)** Diagram representing the number of overlapping proteins found by mass spectrometry to bind to NS5 after IFN-γ treatment in two independent experiments. C) Network STING analysis of the 51 proteins identified in both mass spectrometry experiments using Cytoscape.

In order to determine if NS5 is inhibiting the activity of STAT1 in response to IFN-γ, we checked each stage of STAT1 activation in the presence of NS5. The first requirement for STAT1 activity is phosphorylation of the transactivation domain at tyrosine 701 by receptor-associated JAKs (Villarino et al., 2017; Platanias, 2005). STAT1 is also known to be phosphorylated at other sites that contribute to its activity, particularly phosphorylation at serine 727, but this occurs at a later stage of STAT1 activation, and

nuclear localization and tyrosine phosphorylation are prerequisites for this modification (Sadzak et al., 2008; Bancerek et al. 2013). We assessed both the tyrosine and serine phosphorylation of STAT1 by western blot using phosphorylation-specific antibodies in cells stimulated with IFN-γ, in the presence of NS5. INF-γ treatment robustly induced STAT1 phosphorylation at both Y701 and S727. While NS5 expression had little or no effect on the tyrosine phosphorylation of STAT1, NS5 significantly reduced the phosphorylation of STAT1 at S727 in response to IFN-γ (Fig 3.6).

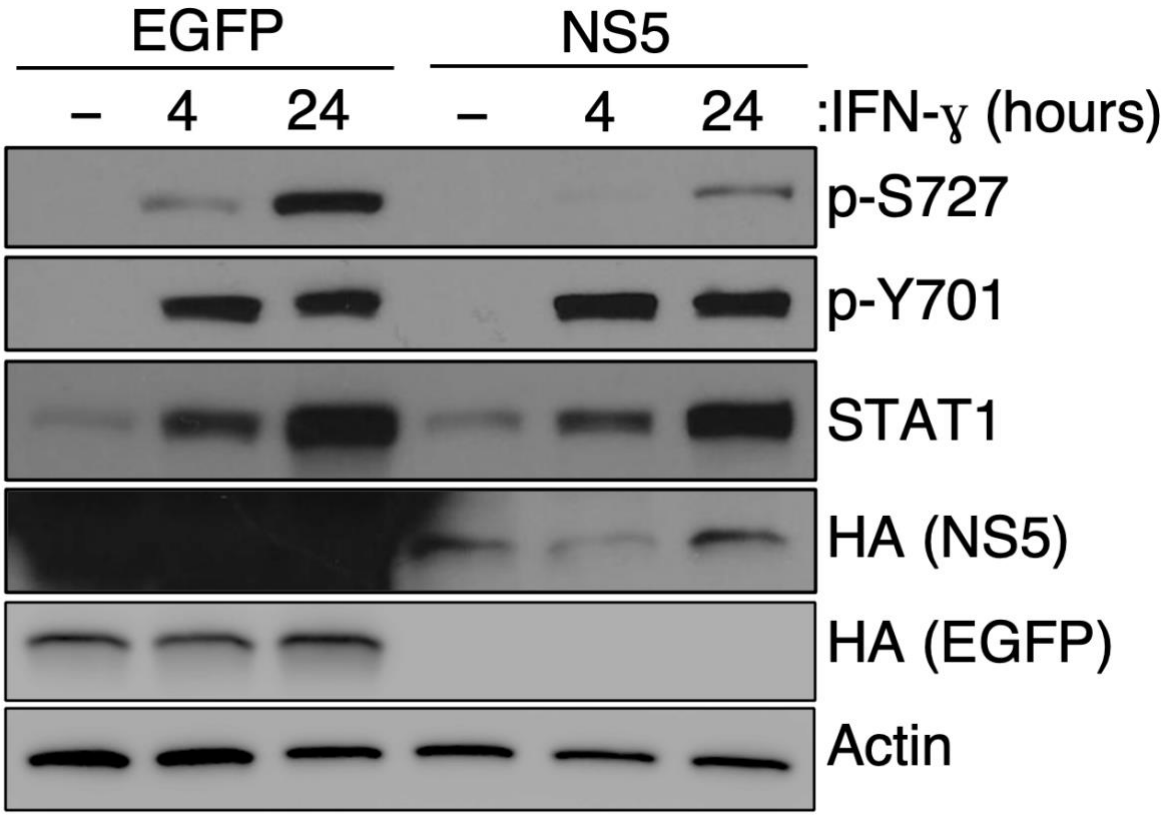

Figure 3.6: Norovirus NS5 inhibits STAT1 serine phosphorylation. Phosphorylation of STAT1 determined by western blot with anti-phospho-Y701-STAT1 and anti-phospho-S727-STAT1 specific antibodies in *Atg16l1* KO BV-2 expressing HA-tagged NS5 or EGFP (control) after treatment with 100 U/mL IFN-γ for the indicated amounts of time.

Phosphorylation of STAT1 at S727 has been shown to be necessary for the complete activation of STAT1 transcriptional activity (Bancerek et al., 2013; Varinou et al., 2003). Because NS5 expression inhibits STAT1 serine phosphorylation we considered the possibility that phosphorylation of STAT1 at S727 may be necessary for viral restriction in response to IFN-γ. To test this theory we generated STAT1 KO BV-2 cells which we then complemented with WT STAT1 or with STAT1 mutants in which S727 was substituted with a non-phosphorylatable alanine residue (S727A), or with glutamic acid (S727E) which mimics constitutively phosphorylated STAT. We then tested the importance of this serine phosphorylation site by assessing EMCV replication in complemented cells after IFN-γ treatment. As expected, after the loss of STAT1, EMCV infection was no longer sensitive to the IFN-γ-induced antiviral response, and complementation of these KO cells with WT STAT1 resulted in the return of IFN-γ-mediated control (Fig 3.7 A, C). We also observed that both STAT1 phosphomutants behaved similarly to WT STAT1; the percentage of cells infected with EMCV was diminished after expression of STAT1 S727A or STAT1 S727E in response to IFN-γ (Fig 3.7 A). In agreement with this finding, we also observed that the production of infectious EMCV particles was inhibited after IFN-γ stimulation in cells expressing WT, S727A, or S727E STAT1 (Fig 3.7 B).

To corroborate this finding and to ensure that there were no off-target effects associated with introducing these mutations into STAT1, we also inhibited STAT1 phosphorylation using siRNA to target the kinases responsible for phosphorylating STAT1 at this site. The kinase that has been most well characterized in terms of phosphorylating STAT1 at S727 is CDK8 in conjunction with CDK19 (Bancerek et al. 2013; Steinparzer et

al., 2019). Using siRNA we targeted CDK8, CDK19, or both together and observed that knockdown of CDK8, with or without the additional knockdown of CDK19, resulted in a marked reduction in STAT1 phosphorylation after IFN-γ stimulation (Fig 3.7 D). However, when we measure EMCV replication in these cells, IFN-γ stimulation was able to inhibit EMCV virion production just as efficiently in cells treated with control siRNA as those lacking CDK8 or CDK8 and CDK19 (Fig 3.7 C). Taken together, these data suggest that while NS5 inhibits STAT1 phosphorylation at S727, phosphorylation at this site is not necessary for IFN-γ to inhibit EMCV replication. Rather, the loss of STAT1 serine phosphorylation is likely an indirect effect of NS5's activity.

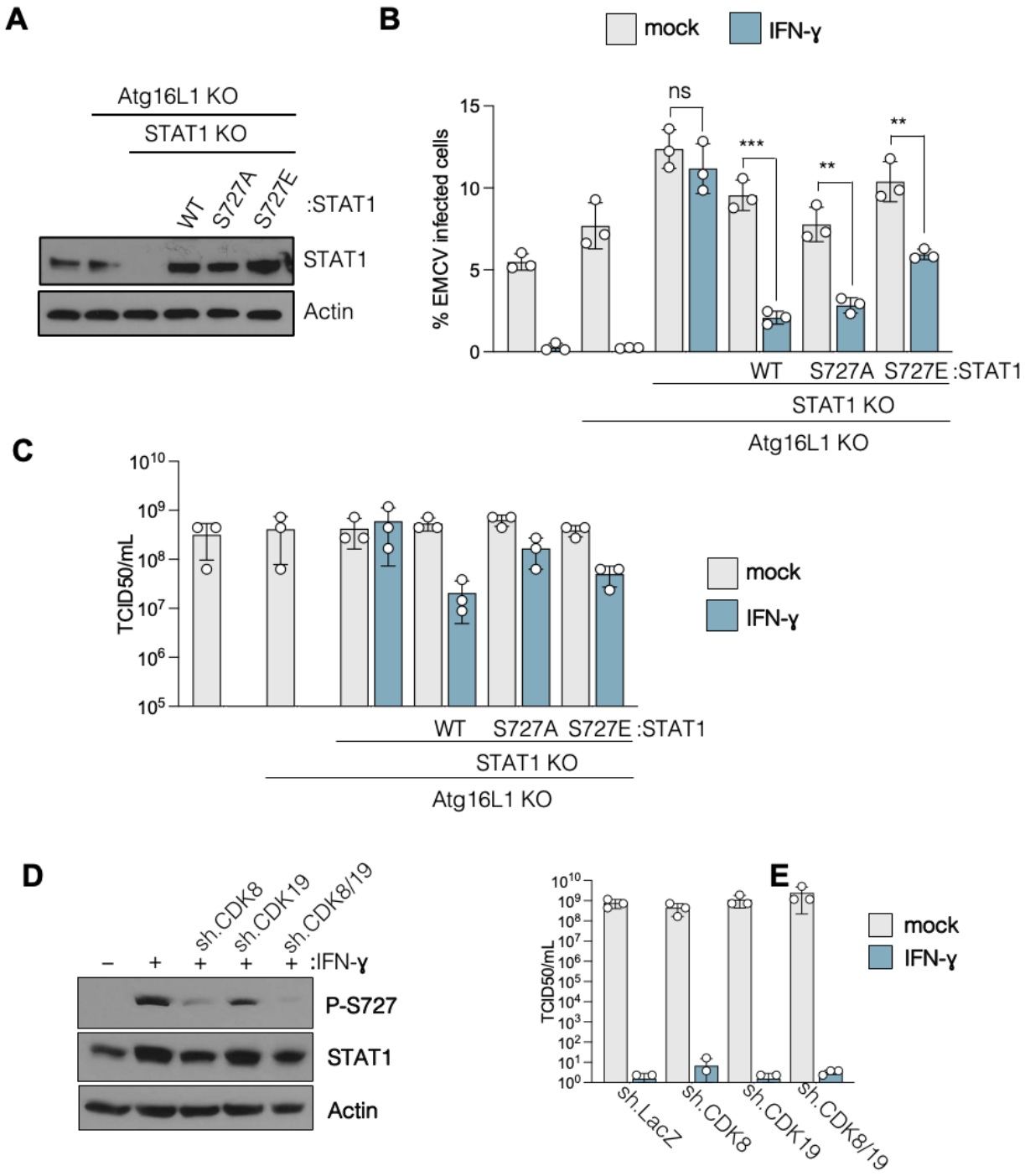

Figure 3.7: Loss of STAT1 serine phosphorylation does not prevent IFN-γ restriction of viral replication. A) Percent of *Atg16l1* KO or *Atg16l1*, *Stat1* double KO BV-2 cells stably expressing STAT1 WT, STAT1 S727A, or STAT1 S727E infected with EMCV (MOI 5, 6h) after 24 h treatment with 100 U/ML IFN-γ relative to mock-treated cells, measured by flow cytometry to detect intracellular J2 (dsRNA) antibody staining.

Figure 3.7 continued: B) EMCV titers for total cellular and extracellular virus in *Atg16l1* KO and *Atg16l1*, *Stat1* double KO BV-2 cells complemented with STAT1 WT, S727A, or S727E and mock-treated or treated with 100 U/mL IFN-γ for 24 h prior to infection at an MOI of 0.01 for 24 h, determined by TCID50 assay. **C)** Representative expression of STAT1 WT, S727A, and S727E in *Atg16l1*, *Stat1* double KO BV-2 cells, determined by western blot using the indicated antibodies. **D)** phosphorylation of STAT1 at S727 determined by western blot with anti-phospho-S727-STAT1 specific antibodies in *Atg16l1* KO BV-2 mock-treated or treated with 100 U/mL IFN-γ for 24 h following knockdown of CDK8, CDK19, or CDK8 and CDK19 by siRNA. **E)** Total cellular end extracellular EMCV titers in *Atg16l1* KO BV-2 mock-treated or treated with 100 U/mL IFN-γ for 24 h after knockdown of CDK8, CDK19, or CDK8 and CDK19 by siRNA, determined by TCID50 assay.

3.3.5 NS5 prevents the nuclear accumulation of STAT1 in response to IFN

Because STAT1 serine phosphorylation is inhibited by NS5 but this phosphorylation site is not critical for restricting EMCV replication, we postulated that a step upstream of STAT1 S727 phosphorylation is targeted by NS5. Phosphorylation of STAT1 at S727 requires tyrosine phosphorylation and nuclear translocation. However, NS5 expression did not prevent STAT1 Y701 phosphorylation (Fig 3.6). Therefore, we examined the nuclear accumulation of STAT1 after MNV infection by immunofluorescence microscopy. In uninfected BV-2 cells, STAT1 is distributed evenly throughout the cytoplasm and nucleus but then becomes concentrated in the nucleus after IFN-γ stimulation (Fig 3.8 A, B). In contrast, infection of IFN-γ-treated cells with MNV reduced the accumulation of STAT1 within the nucleus (Fig 3.8 A, B). While MNV infection did not entirely exclude STAT1 from the nucleus, our data strongly suggest that MNV inhibits the nuclear concentration of STAT1 which is critical for its antiviral function. Additionally, this data implies that either MNV inhibition of STAT1 nuclear localization is 'leaky,' or only inhibits the accumulation of a specific subset of STAT1 within the nuclear, which may explain why the upregulation of only some ISGs is inhibited by NS5.

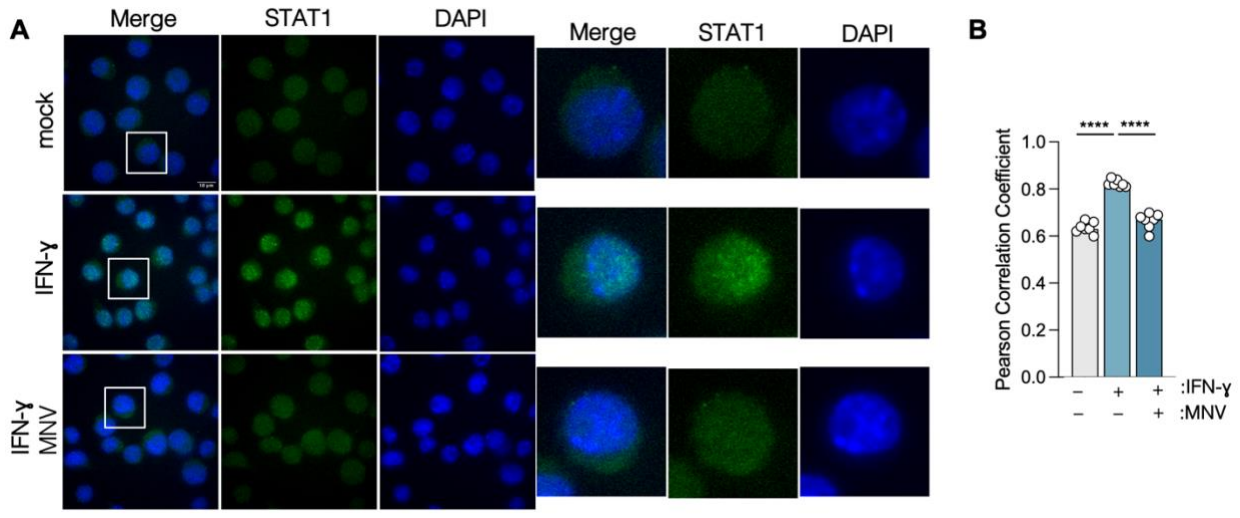

Figure 3.8: Norovirus infection inhibits nuclear accumulation of STAT1. A) Representative images from immunofluorescent microscopy experiments showing the colocalization of STAT1 (green) with the nuclear marker DAPI (blue) in *Atg161* KO BV-2 cells treated with 100 U/mL IFN-γ or mock-treated for 6 h prior to infection with MNV (MOI 5, 16h). Scale Bar, 10 μm. **B)** Pearson Correlation Coefficients for data represented in A), determined by Coloc2 plugin in ImageJ.

We have shown that MNV infection robustly prevents the nuclear accumulation of STAT1. However, to determine if STAT1 localization during viral infection is dysregulated specifically by the activity of NS5 we evaluated the distribution of STAT1 in uninfected cells expressing NS5. While expression of the control protein EGFP did not inhibit STAT1 redistribution to the nucleus after IFN-γ treatment, NS5 expression alone was sufficient to prevent STAT1 nuclear accumulation (Fig 3.9 A, B). Based on these data, we can specifically attribute the impairment in STAT1 nuclear accumulation during MNV infection to the activity of NS5.

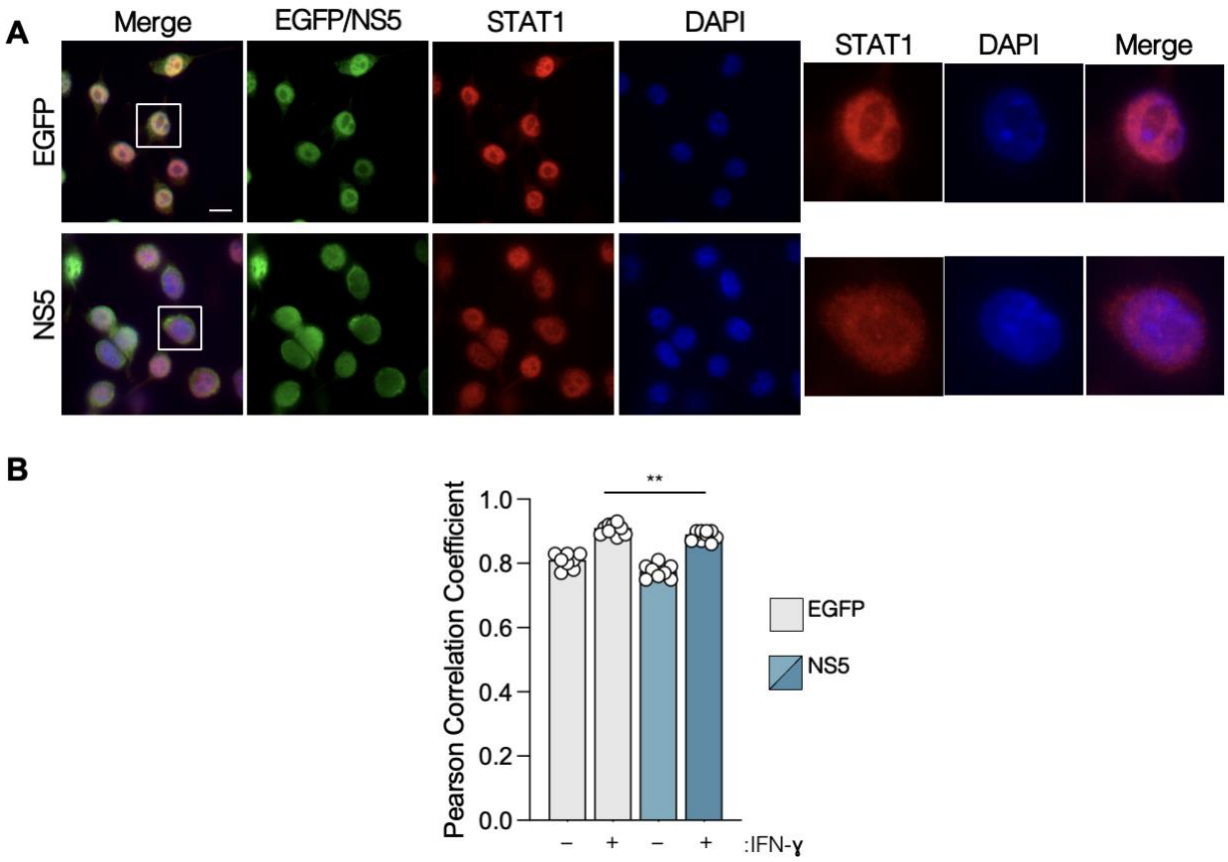

Figure 3.9: NS5 inhibits nuclear accumulation of STAT1. A) Representative images of STAT1 (red) colocalization with the nuclear marker DAPI (blue) in *Atg16l1* KO BV-2 cells expressing EGFP or NS5 (green) and treated with 100 U/mL IFN-γ or mock-treated for 24 h. Scale Bar, 10 µm. **B)** Pearson Correlation Coefficients for data represented in A), determined by the Coloc2 plugin in ImageJ.

The fully active form of STAT1 is located within the nucleus and both serine and tyrosine phosphorylated. Because NS5 does not completely exclude STAT1 from the nucleus, we wanted to determine the location of the phosphorylated versions of STAT1. Using immunofluorescence microscopy, we observed that NS5 expression also prevented the nuclear accumulation of tyrosine phosphorylated STAT1 (Fig 3.9 A, C). This data suggests that NS5 has an effect, particularly on the active forms of STAT1.

When we observed the localization of serine phosphorylated STAT1, even in mock-treated samples, S727 phosphorylated STAT1 was predominantly in the nucleus; however, IFN-γ treatment resulted in an increase in the signal intensity of serine phosphorylated STAT1. This is in agreement with previously published data suggesting that S727 phosphorylation only occurs after the nuclear translocation of STAT1 (Sadzak et al., 2008). We also did not observe a significant decrease in the colocalization of phospho-S727 STAT1 with the nuclear DAPI marker after NS5 expression and type II IFN treatment, although the overall levels of serine phosphorylated STAT1 were lower (Fig 3.9 B, C). This data corroborates our hypothesis that NS5 does not directly inhibit STAT1 serine phosphorylation, but rather inhibits STAT1 nuclear accumulation which indirectly prevents the phosphorylation of STAT1 at S727, which can only occur in the nucleus. This suggests that NS5 expression results in less STAT1 getting to the nucleus overall but does not prevent the phosphorylation of STAT1 once inside the nucleus.

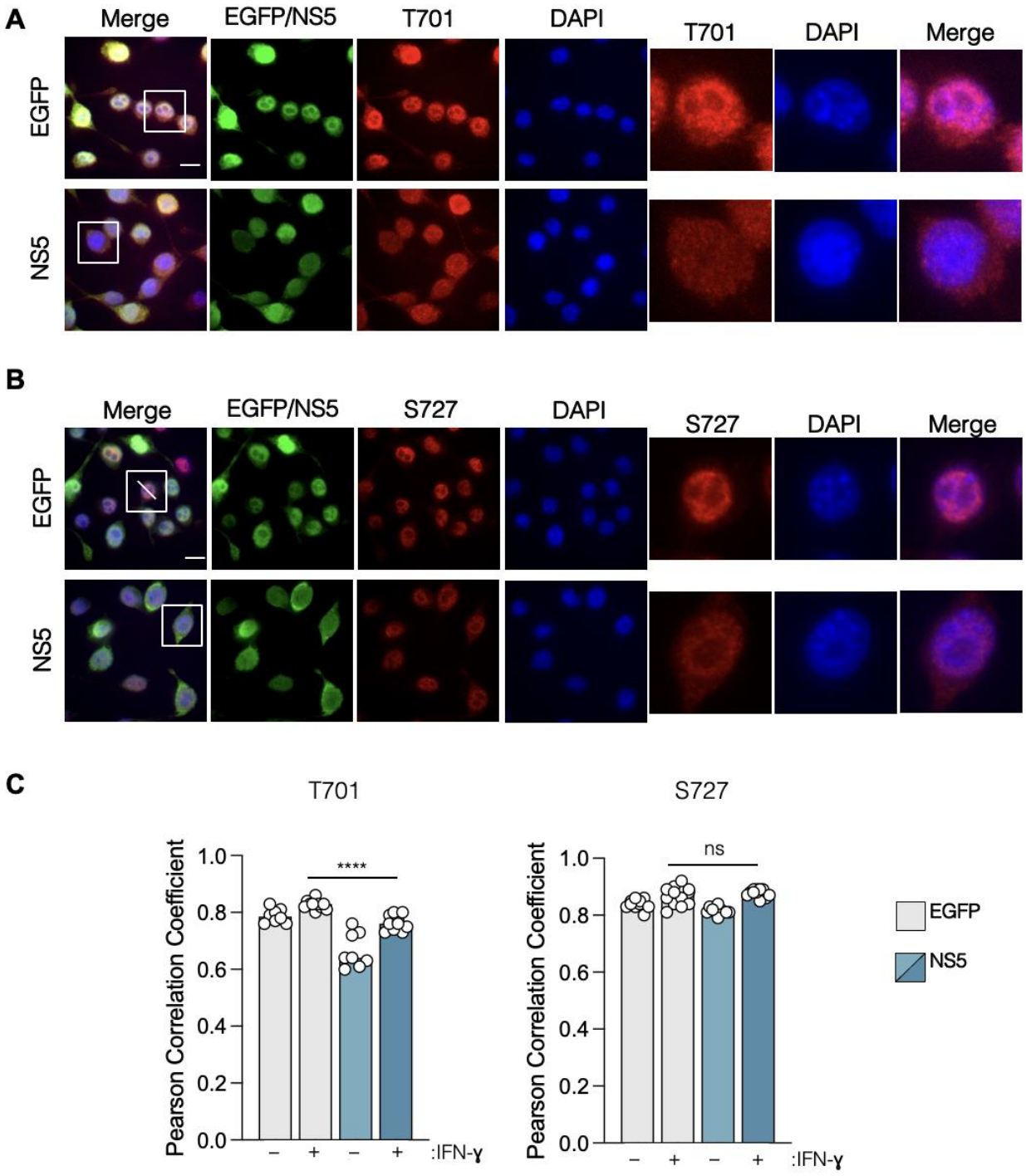

Figure 3.10: NS5 inhibits nuclear accumulation of tyrosine phosphorylated STAT1. **A)** Representative images of Y701 phosphorylated STAT1 (red) colocalization with the nuclear marker DAPI (blue) in *Atg16l1* KO BV-2 cells expressing EGFP or NS5 (green) and treated with 100 U/mL IFN-γ or mock-treated for 24 h. Scale Bar, 10 µm. **B)** Representative images of S727 phosphorylated STAT1 (red) colocalization with the nuclear marker DAPI (blue) in *Atg16l1* KO BV-2 cells expressing EGFP or NS5 (green) and treated with 100 U/mL IFN-γ or mock-treated for 24 h. Scale Bar, 10 µm.

Figure 3.10 continued: C) Pearson Correlation Coefficients for data represented in A) and B), determined by the Coloc2 plugin in ImageJ.

3.4 Discussion

The outcome of viral infection is the net result of the interaction between the host immune defenses and the viral strategies to antagonize them. For noroviruses, the innate branch of the immune response is primarily responsible for controlling infection. However, despite an innate antiviral response, MNV is still able to infect and replicate within the gut of mice with intact immune systems but without causing detectable disease. MNV is able to avoid restriction by the immune system through the action of virally encoded factors that inhibit an effective antiviral response. For the first time, we have characterized here the anti-immune function of one of MNV's proteins, NS5.

NS5 encodes MNV's VPg, which has essential roles in the virus lifecycle facilitating transcription and translation. NS5 also modulates host cell cycle progression in a manner independent of genome linkage (McSweeny et al., 2021). Here we demonstrate that MNV NS5 inhibits the type II IFN response to viral infection. It has not yet been determined which molecular features present in NS5 are required for this protein's antagonistic function. Additional investigation of the activity of NS5 mutants with targeted disruptions of key functional domains would significantly enhance our understanding of the NS5's function.

When expressed alone, NS5 is sufficient to allow viral escape from INF-γ-induced antiviral pathways. NS5 antagonizes the IFN-γ response by blocking STAT1 serine phosphorylation and nuclear accumulation. However, only nuclear accumulation of

STAT1 is critical for the inhibition of EMCV replication, as this blockade prevents the upregulation of several critical ISGs. What remains unclear is if NS5 inhibits STAT1 nuclear accumulation by preventing STAT1 import or by enhancing the export of STAT1, and the molecular details of this action. Further mechanistic studies will be needed to determine which specific nuclear import/export factors are modulated by MNV infection.

In summary, the TAG-independent type II IFN response is critical for controlling the replication of several RNA viruses. MNV has developed a strategy to escape this immune pathway utilizing the virally encoded protein NS5. NS5 specifically impedes the activation of STAT1 by preventing its nuclear accumulation and therefore its transcriptional activity inside the nucleus.

3.5 Materials and Methods

Cell Lines. Human embryonic kidney cells (HEK293T; ATCC), mouse microglial cells (BV-2), and *Atg5* KO BV-2 (a gernerous gift from Dr. Robert C. Orchard, UT Southwestern) were cultured in Dulbecco's modified Eagle media (DMEM; Gibco) supplemented with 10% (vol/vol) fetal bovine serum (FBS; Gemini), 1% (vol/vol) penicillin-streptomycin (Millipore Sigma), and 0.1mM non-essential amino acids (NEAA; Gibco) under standard culture conditions.

Primary Cells. Murine bone marrow derived macrophages (BMDMs) were isolated from *Atg5*$^{flox/flox}$, *Atg5*$^{flox/flox}$*+/-LysMcre*, *Ifnar*$^{-/-}$*Atg5*$^{flox/flox}$, and *Ifnar*$^{-/-}$*Atg5*$^{flox/flox}$*+/-LysMcre. Atg5*$^{flox/flox}$*+/-LysMcre* C57BL/6 mice provided by Dr. Herbert W. Virgin, Washington

University in St. Louis, USA, as previously described (Hwang et al., 2012). Briefly, bone marrows were isolated from the femurs and tibias of 6-12 week-old male mice and plated in non-tissue culture-treated 10-cm dishes in 10 mL of BMDM media (DMEM, 10% (vol/vol) FBS, 5% (vol/vol) horse serum (Life Technology), 0.1mM NEAA, 1 mM sodium pyruvate (Mediatech), 2 mM L-glutamine (Mediatech), 10% L929 conditioned media containing macrophage colony-stimulating factor (M-CSF; Stanley and Heard, 1977)). An additional 10 mL of BMDM media was added four days later. On the 12th day after isolation (D12), BMDMs were detached from the dish using ice-cold 0.02% ethylenediaminetetraacetic acid (EDTA; Sigma-Aldrich) in Dulbecco's phosphate-buffered saline (DPBS; Gibco), and allowed to rest for three days in tissue culture treated multi-well plates prior to any experiments. The remaining D12 BMDMs were frozen in BMDM media containing 10% dimethylsulfoxide (DMSO; VWR).

Cell Culture. All cells were cultured at 37 °C in a humidified 5% CO2 atmosphere. Commercially obtained cells were authenticated by the vendor (ATCC). The knockout BV/-2 cells generated in this study were validated by western blot. All cell lines used in this study were regularly checked for the presence of mycoplasma using the MycoAlert Mycoplasma Detection Kit (Lonza).

Generation of CRISPR knockout cells. *Atg16l1* KO BV-2 cells were generated using CRISPR/Cas9. The *Atg16l1* specific sgRNA, 5'-ACC AGG AAC TGG TCA CCA G-3' was cloned into pLentiCRISPR v.2 vector (Addgene) containing the sgRNA scaffold and Cas9.

The CRISPR vector was packaged into lentiviral particles in HEK293T cells with second-generation lentiviral packaging mix (abm) using Lentifectin (abm). WT BV-2 cells were transduced with lentivirus containing the *Atg16l1*-targeting sgRNA, and KO cells were selected with 3 mg/mL Puromycin (Sigma-Aldrich). Loss of *Atg16l1* was confirmed at the protein level by western blot.

Stat1 was specifically targeted in BV-2 cells using the CRIPSR guide (sgRNA) 5'- GAG GAG GTC ATG GAA GCG G-3' cloned into the pLentiCRISPR v.2 vector. The CRISPR vector was packaged into lentiviral particles in HEK293T cells with second-generation lentiviral packaging mix using Lentifectin. Parental *Atg16l1* KO BV-2 cells were transduced with lentivirus containing the *Stat1*-targeting sgRNA, and KO cells were selected with 300 μg/mL Hygromycin B. Loss of *Stat1* was confirmed at the protein level by western blot.

Expression constructs.

MNV-1 NS5 and EGFP were subcloned from pCW3P3 (Thackray et al., 2007) and pENTR-EGFP (Biering et al., 2017) respectively, into pHAGE-N-Flag-HA (pHNHF) (Behrends et al., 2010) using Gateway cloning. The MNV gene expression constructs were generated by subcloning each gene from the plasmid pCW3P3 using the following primer sets: NS1/2, 5'-TAG AGC TAG AGC TAG ATG AGG ATG GCA ACG CCA TC-3' and 5'-CTG CCC TCA GCG GCC AAT TCG GCC TGC CAT TCC CC-3'; NS3, 5'-TAG AGC TAG AGC TAG ATG GGG CCC TTC GAC CTT GCT-3' and 5'-CTG CCC TCA GCG GCC AAC TGG AGG CCG AAA TCA TCA T-3'; NS4, 5'-TAG AGC TAG AGC TAG ATG

AAC AAG GTC TAT GAC TTT GAT G-3’ and 5’-CTG CCC TCA GCG GCC AAC TCA GAG TGG TAC CAC CCA-3’; NS5, 5’-TAG AGC TAG AGC TAG ATG GGA AAG AAG GGC AAG AAC AAG-3’ and 5’-CTG CCC TCA GCG GCC AAC TCA AAG TTG ATC TTC TCG CC-3’; NS6, 5’-TAG AGC TAG AGC TAG ATG GCC CCA GTC TCC ATC TGG T-3’ and 5’-CTG CCC TCA GCG GCC AAC TGG AAC TCC AGA GCC TCA A-3’; NS7, 5’-TAG AGC TAG AGC TAG ATG GGA CCC CCC ATG CTT CCC-3’ and 5’-CTG CCC TCA GCG GCC AAC TCA TCC TCA TTC ACA AAG ACT G-3’; VP1, 5’-TAG AGC TAG AGC TAG ATG AGG ATG AGT GAT GGC GC-3’ and 5’-CTG CCC TCA GCG GCC AAT TGT TTG AGC ATT CGG CCT GT-3’; VP2, 5’-TAG AGC TAG AGC TAG ATG GCT GGT GCT CTT TTT GGA-3’ and 5’-CTG CCC TCA GCG GCC AAT GCC CTG CTA CTC CCG ATC T-3’; VF1, 5’-TAG AGC TAG AGC TAG ATG GCG CAG CGC CAA AA-3’ and 5’-CTG CCC TCA GCG GCC AAG GTA GAC AAA ATT GAA ATC AGC C-3’. MNV genes were inserted into pCDH-MCS-T2A-copGFP-MSCV (System Biosciences; hereafter referred to as ‘c274’) between the restriction sites NheI and Not1 via In-Fusion assembly (Takara Bio).

c274-STAT1 WT, c274-STAT1 S727A, and c274-STAT1 S727E, were generated by subcloning the STAT1 from eGFP STAT1 WT (Addgene # 12301), eGFP STAT1 S727A (Addgene # 12305), or eGFP STAT1 S727E (Addgene # 12304) respectively using the forward primer 5’-ATA CTA GAG CTA GAG CTC AGA TCT ATG TCT CAG TGG TAC GA-3’ and the reverse primers 5’-CTG CCC TCA GCG GCC GCT ACT GTG TTC ATC ATA CTG TCG AAT TCT-3’. STAT1 genes were inserted into the c274 vector using the NheI and NotI restriction sites.

The sequence of all constructs was confirmed as correct by DNA sequencing.

Lentiviral production and transduction. All lentiviral pseudoparticles were generated in HEK293T cells using pHAGE-N-Flag-HA (pHNHF), pCDH-MCS-T2A-copGFP-MSCV (C274), and pLentiCRISPR v.2 lentiviral vectors. Vectors were transiently transfected into cells along with using second generation packaging mix (abm) using Lentifectin transfection reagent (abm). Twenty-four hours after transfection, cell culture media was replaced and at 48 hours post transfection lentiviral particles were collected and filtered through 0.45μm PVDF syringe filters (Millipore). For lentiviral transductions, filtered particles were incubated with target cells for at least 24 hours prior to antibiotic selection (puromycin, 5 μg/mL, Sigma-Aldrich; Hygromycin B, 300 μg/mL, Invitrogen) Expression of all transduced constructs were validated by western blot.

Viruses. MNV was produced from an infectious cDNA clone containing the genome of MNV-1.CW3. Viral particles were produced in 293T cells transfected with the MNV-1.CW3 plasmid for 48 h (P0) and then amplified in BV-2 cells (P1 and P2) for 36-48 h, or until more than 90% cytopathic effect (CPE) was observed. Infected BV-2 cells were lysed via a freeze-thaw cycle, and cellular debris was removed by centrifugation for 20min at 3000 rpm at 4C. Viral particles were then concentrated by ultracentrifugation at 26,500 rpm for 3 hours at 4°C. Encephalomyocarditis virus (EMCV; strain K) was obtained from Dr. Marco Colonna (Washington University in St. Louis). The strain 16681 was used for all DENV2 infections.

Viral infection and interferon treatment. All cells were seeded 24 hours prior to infection. Where applicable, cells were treated with 100 U of IFN-γ (Peprotech) or 100 U of IFN-β (PBL) for the specified amount of time. Infections were performed at the indicated times and MOIs in normal culture media for 30 minutes at room temperature with rocking. After the initial 30-minute infection, the inoculum was removed and cells were washed once with DPBS before adding fresh cell culture media and returning cells to 37°C for the remaining duration of the infection.

Viral coinfection. *Ifnar*$^{-/-}$ *Atg5*$^{flox/flox}$ and *Ifnar*$^{-/-}$ *Atg5*$^{flox/flox}$ *LysMCre*$^{+/-}$ BMDM were treated with 100 U IFN-γ for 24 hours prior to viral infection. Treated cells were initially infected with MNV at an MOI of 5 for 12 hours before infection with EMCV (MOI 0.05) for an additional 12 hours. TRI reagent (Sigma-Aldrich) was used to extract RNA from cell lysates according to the protocol provided by the manufacturer. MNV and EMCV replication was assessed by two-step qRT-PCR using virus-specific primers as described below.

qRT-PCR. RNA for analysis was extracted from cells using either TRI reagent or the NucleoSpin 96-well RNA extraction kit from Macherey-Nagel, per the manufacturer's instructions. For two-step qRT-PCR, cDNA was reverse transcribed from RNA samples using IMPROM-II reverse transcriptase (Promega) with random hexamers according to the manufacturer's protocol. Taq polymerase (lab-made and column purified), dNTP mixture (Thomas Scientific), and SYBR-green reagent (Life technology) were used to

quantify RNA levels in conjunction with the following specific primer sets targeting the following: MNV, 5'-AGC TCA GGA TGG TCT CGG AT-3' and 5'-TCA AGA GCA AGG TCG AAG GG-3'; ECMV, F 5'-GAC GCT TGA AGA CGT TGT CTT CTT A-3' and 5'-CCC TAC CTC ACG GAA TGG GGC AAA G-3'; actin, 5'-GCC TTC CTT CTT GGG TAT GG-3' and 5'-GCA CTG TGT TGG CAT AGA GG-3'; Gbp1, 5'- AAA CCA GGA GGC TAC TAC CTT TTT-3' and 5'- GTA TTT TCT CAG CAT CAC TTC AGC-3'; Gbp2, 5'-ACC TGG AAC ATT CCC TGA CC-3' and 5'-ACA GCT CCT CCT CCC GCA GAG-3'; Irf1, 5'-ACA CTA AGA GCA AAA CCA AGA G-3' and 5'-TTT CCA TAT CCA AGT CCT GA-3'; Irf8, 5'-CAA TCA GGA GGT GGA TGC TTC C-3' and 5'-GTT CAG AGC ACA GCG TAA CCT C-3'.

One-step qRT-PCR was performed using SuperScript III Platinum One-Step qRT-PCR kit with ROX with commercially available predesigned PrimeTime qPCR Probe Assays (IDT) and premixed primer-probe targeting 18s (Thermo Fisher). All qPCRs were performed using an Applied Biosystems StepOnePlus Real-Time PCR system. Relative RNA values were normalized to 18s or actin threshold values and calculated using the comparative threshold ($\Delta\Delta C_t$) method and expressed in comparison to control cells.

Flow Cytometry. For flow cytometry analysis, cells were fixed with 4% (wt/vol) paraformaldehyde (PFA) in distilled water for 15 minutes at room temperature and then permeabilized with 0.2% Triton-X 100 (vol/vol; Acros Organics) diluted in PBS for 10 minutes. Cells were blocked in a solution of 2% FBS and 0.5% saponin for 30 minutes. To detect EMCV infection, fixed and permeabilized cells were stained with J2 antibody (Millipore; 1:125) targeting double-stranded RNA and Alexa Fluor® 647 Donkey Anti-

Mouse IgG (H+L) (jackson immunoResearch; 1:1000) as secondary antibody. Cells were analyzed with a BD LSRFortessa benchtop analyzer and data analysis was conducted using FlowJo (FlowJo, LLC).

TCID50 assay. Total MNV and EMCV infectious virions were assessed in cells infected at the indicated time points after infection with the indicated MOIs. Virions from cells and media were obtained by lysing cells via a single freeze-thaw cycle at -80°C. Infectious particles were then quantified using the Reed-Muench tissue culture infectious dose 50 (TCID50) method. Briefly, infected lysates were serially diluted 20- or 50-fold in standard media. Dilutions were added to BV-2 cells in eight technical replicates per sample for each dilution. Cells were incubated with viral dilutions for 5 days before being assessed for cytopathic effect (CPE) to calculate the TCID50/mL in the original samples. The limit of detection for this assay equals the 50% CPE for the lowest dilution.

Western Blot. Cells were lysed at the indicated times in lysis buffer (50 mM Tris-HCL pH 8, 150 mM NaCl, 1% (vol/vol) IGEPAL, 2 mM EDTA) with cOmpleat protease inhibitor cocktail (Sigma-Aldrich) for 20 minutes on ice. Cellular debris was removed by centrifugation at 16,100 g for 20 min at 4°C. The cleared lysate, whole cell lysate (WLC), was combined with concentrated Laemmli buffer and heated for 5 min at 95°C. Proteins were separated via SDS-PAGE on 4-20% mini-Protean TGX precast gradient gels (BioRad) and then transferred to polyvinylidene difluoride (PVDF) membranes. Specific proteins were visualized with the indicated antibodies (STAT1, cell signaling, 1:1000;

phosphor-S727-STAT1, cell signaling, 1:2000; phosphor-Y701-STAT1, cell signaling, 1:1000; HA.11, 1:1000; actin, 1:2000;).

Mass spectrometry analysis. To identify NS5 binding partners, BV-2 cells expressing either EGFP or NS5 in the presence or absence of IFN- γ were lysed in cell lysis buffer. After removing cellular debris by centrifugation, cell lysates were precleared by a two-hour incubation with Sepharose beads. EGFP and NS5 were then immunoprecipitated from the lysates via HA-conjugated Sepharose beads at 4°C for approximately 16 hours. Non-interacting proteins were removed by washing the HA beads three times with cell lysis buffer. The immunoprecipitated proteins were then resolved on pre-cast gradient gels by gel electrophoresis. EGFP or NS5 and their associated proteins were visualized by staining the gels with ProtoBlue Safe (National Diagnostics) colloidal Coomassie stain overnight, before destaining in purified water. Gel sections were excised and sent for mass spectrometry analysis at Harvard Taplin Biological Mass Spectrometry Facility, Boston. STRING network analysis was performed in Cytoscape.

Immunofluorescence microscopy. BV-2 cells were grown of 12 mm glass coverslips and then treated or infected as indicated. Before analysis, cells were fixed for 20 minutes at room temperature with 4% (wt/vol) PFA. Fixes cells were permeabilized in 0.2% (vol/vol) Triton-X 100 (vol/vol) and then incubated with blocking solution (10% goat serum, 0.05% (vol/vol) saponin in PBS) for 30 minutes. Cells were incubated with the following primary antibodies; anti-STAT1 (1:250), anti-phospho-S727-STAT1 (1:500), anti-

phospho-Y701-STAT1 (1:250), and anti-HA.11 (1:200), overnight at 4°C in blocking solution. Mouse- or rabbit-specific Alexa Fluor conjugated secondary antibodies (1:400) were incubated with coverslips for 30 minutes at room temperature. Coverslips were mounted on slides with ProLong Gold antifade mountant with DAPI (Invitrogen). Images of each slide were acquired using Slidebook software and Olympus DSU Spinning Disc Confocal with a 100X NA 1.45 oil-immersion TIRFM objective. Exposure times and thresholds were kept constant for each experiment. Pearson correlation coefficients were calculated in ImageJ using the coloc2 plugin.

Quantification and statistical analysis. Data are displayed as mean ± standard deviation or standard error as indicated. All data were analyzed using GraphPad Prism software (version 9). Statistical significance was determined using a two-tailed Student's *t*-test (unpaired). P values of less than or equal to 0.05 were marked as not significant (ns). Significant differences are denoted by *P <0.05, **P <0.01, ***P <0.001 and **** P <0.0001. The number of independent biological replicates (n) is indicated for each figure.

CHAPTER 4

CONCLUSIONS

4.1 Overview of Results

In this dissertation, I have presented evidence that R12C is a critical regulator of RLR activation that detects viral infection by sensing changes in actin cytoskeleton dynamics. R12C is necessary for the RLRs to induce the production of IFNs during infection. Due to the reduction of RLR-induced IFN, ISG upregulation is also hampered in the absence of R12C. Importantly, the defect in ISG production in cells lacking R12C supports higher levels of viral replication compared to replication in cells with R21C.

R12C contributes to the RLR pathway by physically mediating the interaction between RIG-I or MDA5 and PP1. The formation of a complex that includes RLR, PP1, and R12C results in the dephosphorylation of the CARD domains of RIG-I and MDA5, promoting their downstream signaling activity.

Targeting of PP1 to the RLRs by R12C is dependent on the localization of R12C within the cell. During viral infection, normal actin dynamics are perturbed which triggers the translocation of R12C from filamentous actin to the cytoplasm where the RLRs reside. The redistribution of R12C is sufficient to induce the dephosphorylation of RIG-I and MDA5 even in the absence of an RNA ligand.

I have also presented data pertaining to an unrelated project describing the inhibition of TAG-independent IFN-γ immunity by MNV. While other RNA viruses are susceptible to the TAG-independent type II response, MNV actively evades this innate immune pathway. MNV evasion is due to the activity of NS5, which inhibits the

upregulation of a specific set of ISGs which also allows other RNA viruses to escape IFN-γ control.

MNV NS5 inhibits the type II IFN response by interfering with the activation of STAT1. NS5 inhibits serine phosphorylation of STAT1; however, STAT1 serine phosphorylation is not necessary for IFN-γ control of EMCV. Instead, NS5 indirectly inhibits STAT1 phosphorylation as a result of inhibiting STAT1 nuclear accumulation.

4.2 Concluding remarks and perspectives

4.2.1 Regulation of R12C activity in actin dynamics and innate immune signaling

The work presented here extends our understanding of how RLRs are activated to include more than one signal. Here we present a model where perturbation of the actin cytoskeleton during infection acts as a trigger for R12C to promote RLR activation. However, we still do not have a complete understanding of how R12C detects virus-induced actin changes. The RLRs have a helicase domain which binds to specific features of stimulatory RNA, inducing conformational changes and ATPase activity, but we do not have an analogous understanding of how R12C's localization and activity are regulated in response to viral infection.

In uninfected cells, R12C functions as part of the regulatory circuit controlling the phosphorylation of non-muscle myosin. R12C's ability to target PP1 to myosin light chain is itself also dependent on phosphorylation. Phosphorylation of R12C at T560 and S452 regulate its ability to target PP1's activity toward the cytoskeleton (Tan et al., 2001; Ito et

al., 2004; Banko et al., 2011). It has not yet been tested if the same phosphatases and kinases that control R12Cs myosin targeting ability also regulate R12C's activity toward the RLRs but it would provide a convenient link between actin dynamics and the RLR pathway. Because R12C dissociates from filamentous actin after viral infection, it is tempting to speculate that R12C's activity with respect to myosin is inhibited either directly or indirectly during viral infection as part of the process of enhancing actin dynamics. Furthermore, it would be interesting to determine if this 'inactive' form of R12C enhances the targeting of PP1 toward the RLRs.

However, if R12C's function in the RLR pathways is regulated by the same circuits that regulate its activity toward the cytoskeleton then the question arises, how does R12C distinguish between normal actin remodeling in a healthy call and viral perturbations during infection? It may be that to some degree R12C does not distinguish between normal and abnormal changes in the actin cytoskeleton and the RLRs are primarily kept inactive in uninfected cells due to the lack of an appropriate RNA ligand. However, this is unlikely because both RIG-I and MDA5 are predominantly phosphorylated in uninfected cells. On the other hand, R12C activation with respect to the RLR pathway may not be as simple as being triggered by general or non-specific changes in actin dynamics. Additional research is needed to more specifically define the trigger that induced R12C's targeting of PP1 to the RLRs in order to answer this question.

4.2.2 Actin perturbation as a potential regulator of multiple sensors in response to infection with diverse pathogens

Dynamic phosphorylation of innate immune sensors—RLRs, cGAS, and NOD-like receptors—has emerged as a key regulatory mechanism by which phosphorylation keeps these receptors inactive and phosphatase-dependent dephosphorylation prompts their activation (Li et al., 2021; Niu et al., 2021; Spalinger et al., 2016; Tang et al., 2021; Wies et al., 2013; Zhong et al., 2020). How the activity of phosphatases upstream of these sensors is coordinated to achieve rapid and specific PRR activation has remained elusive. Here, we show that subcellular redistribution of F-actin-residing R12C during virus infection induces the formation of an active PP1-R12C-RLR complex, which dephosphorylates the RLRs. These findings uncover key molecular events upstream of RLR activation and provide evidence for a direct link between the regulation of the cytoskeleton and innate immunity.

Cellular cytoskeleton components have increasingly been recognized as key mediators of host defenses, such as B-cell-mediated adaptive immunity (Mostowy and Shenoy, 2015; Randow et al., 2013; Tolar, 2017). Because the RLRs are not the only immune sensors that are regulated by switching between phosphorylated and dephosphorylated states, we think it warrants further study to determine if virus-induced actin changes may function more broadly in the activation of other PRRs.

Actin remodeling during infection is not restricted just to RNA viruses, or even viral pathogens alone. Bacterial pathogens also promote changes in the host's cytoskeleton as part of their lifecycle and these changes have also been associated with an immune response (Keestra et al., 2013; Bielig et al., 2014; Legrand-Poels et al., 2007). It is worth

investigating the role of actin dynamics in RLR activation during infection with other pathogens, such as specific DNA viruses sensed by RLRs (Rehwinkel and Gack, 2020) or perhaps certain bacteria.

4.2.3 Implications of different types of virus-induced actin rearrangement of the activation of RLRs

Many studies have shown that viruses usurp the actin cytoskeleton for processes critical to the viral lifecycle, which are highly beneficial for the virus despite contributing to an antiviral response. Whereas viruses such as HIV induce dynamic actin remodeling to facilitate viral entry (Wang et al., 2012; Yoder et al., 2008), other viruses use the actin cytoskeleton for intracellular trafficking or viral egress (Döhner and Sodeik, 2005; Taylor et al., 2011). The types of actin remodeling induced during infection are diverse and have distinct mechanisms. Therefore, it remains unclear if all virus-induced actin reorganizations initiate the formation of R12C-PP1-RLR complexes and if they induce RLR dephosphorylation to the same degree. Because the exact mechanism(s) that trigger the relocalization of R12C from F-actin to RLRs and key molecules mediating this process remain to be identified, it is difficult to speculate. Future studies are needed to address how different types of virus-induced actin cytoskeleton changes and their relative timing during infection impact the effectiveness of host immune responses and contribute to the outcome of viral infection.

4.2.4 RLR dephosphorylation by R12C in autoimmune disorders and vaccine development

One consequence of having more than one signal for RLR activation is it creates new opportunities for dysregulation which can result in autoimmune/proinflammatory diseases. Since we have established a new link between the actin cytoskeleton and RLR activation, we could speculate that individuals with mutations in the actin-regulatory proteins that determine R12C activity might result in a decreased threshold for RLR activation if R12C is constitutively targeting PP1 to the RLRs. In fact, there is already documentation of cases in which autoimmune disorders have been traced back to genes involved primarily in cytoskeleton remodeling, although no one has yet examined the role of R12C specifically in autoimmune disease (Moulding et al., 2013; Papa et al., 2020)

Conversely, we hypothesize that employing R12C activation could be an effective strategy for improving some vaccines. In instances where effective vaccination requires initial activation of an RLR-mediated innate immune response, such as the MDA5 response to the SARS CoV-2 mRNA vaccine (Li et al., 2022), triggering actin remodeling could be used as an adjuvant to boost the RLR response.

4.2.5 Not all ISGs are created equal: only a subset of ISGs are needed for viral restriction

Our results presented here indicate that MNV, like many other viruses, actively antagonizes the host innate immune response by targeting one of the key signaling components of these pathways; STAT1. Many viruses completely inhibit STAT1 activity

by preventing phosphorylation/inducing dephosphorylation of critical residues or blocking the translocation of all STAT1 to the nucleus. MNV also inhibits the nuclear accumulation of STAT1 but does not completely block all STAT1 nuclear translocation. It seems likely that MNV NS5 is inhibiting the nuclear accumulation of a specific subset of the total STAT1 pool but the identity of this STAT1 subset remains unclear at the moment. What we do know is that the partial blockade of STAT1 nuclear concentration prevents the upregulation of some, but not all, IFN-γ-induced ISGs.

Despite the fact that many ISGs with well-characterized antiviral functions are highly expressed in cells when NS5 is present, NS5 expression is still sufficient to inhibit the type II IFN response to a degree that allows for MNV and EMCV replication. As a group, ISGs have many different functions which can directly or indirectly impact the viral life cycle. Our interpretation of this data is that not all of these functions are necessary for inhibiting the replication of a particular virus in a given cell type. By specifically inhibiting critical ISGs, but not the class of ISGs as a whole, MNV can escape the host's innate immune system. At the same time, inhibiting only a small set of ISGs may also prevent unwanted changes in beneficial host cell processes due to larger-scale changes in host transcription. One potential drawback of this strategy is that, while it works for MNV and EMCV, selective inhibition of STAT1 function by NS5 may not be sufficient to allow pathogens that are sensitive to different types of to evade the immune system.

Alternatively, the IFN-γ-induced ISGs that are not inhibited by NS5 may still inhibit MNV replication, but this could be a mechanism to ‘tune’ the overall level of MNV infection. In mice where ISG expression is prevented due to the complete lack of STAT1, MNV infection is lethal (Karst et al., 2003). This is in contrast to MNV infection in

immunocompetent mice which is prevalent among research mice but entirely asymptomatic and usually self-limiting (Thackray et al., 2007; Karst et al., 2003). Perhaps the benefit of not entirely ablating STAT1 signaling is host survival, which could potentially enhance viral transmission. In addition, hosts that don't succumb to MNV infection represent an opportunity for persistent infection and long-term fecal shedding of virions which has been described for some strains of MNV (Karst & Tibbetts, 2016; Thackray et al., 2007).

4.2.6 The potential regulation of STAT1 by human noroviruses

One of the primary motivations for understanding how MNV interacts with the innate immune system is to develop theories that can be tested on the more difficult-to-study human noroviruses. Because human and mouse noroviruses, and more specifically these viruses VPgs, are highly similar, they may both use the same mechanism to antagonize the TAG-independent type II IFN response. While human noroviruses can be challenging to grow in cell culture models, the biochemical activity of human norovirus NS5 can be tested in human cells using the same assays described in this body of work.

REFERENCES

Acharya, Dhiraj, Rebecca Reis, Meta Volcic, Guan Qun Liu, May K. Wang, Bing Shao Chia, Rayhane Nchioua, et al. “Actin Cytoskeleton Remodeling Primes RIG-I-like Receptor Activation.” *Cell* 185, no. 19 (September 2022): 3588-3602.e21. https://doi.org/10.1016/j.cell.2022.08.011.

Bancerek, Joanna, Zachary C. Poss, Iris Steinparzer, Vitaly Sedlyarov, Thaddäus Pfaffenwimmer, Ivana Mikulic, Lars Dölken, et al. “CDK8 Kinase Phosphorylates Transcription Factor STAT1 to Selectively Regulate the Interferon Response.” *Immunity* 38, no. 2 (February 2013): 250–62. https://doi.org/10.1016/J.IMMUNI.2012.10.017.

Banko, Max R., Jasmina J. Allen, Bethany E. Schaffer, Erik W. Wilker, Peiling P. Tsou, Jamie L. White, Judit Villén, et al. “Chemical Genetic Screen for AMPKα2 Substrates Uncovers a Network of Proteins Involved in Mitosis.” *Molecular Cell* 44, no. 6 (2011): 878–92. https://doi.org/10.1016/j.molcel.2011.11.005.

Barretto, N., D. Jukneliene, K. Ratia, Z. Chen, A. D. Mesecar, and S. C. Baker. “The Papain-Like Protease of Severe Acute Respiratory Syndrome Coronavirus Has Deubiquitinating Activity.” *Journal of Virology* 79, no. 24 (2005): 15189–98. https://doi.org/10.1128/jvi.79.24.15189-15198.2005.

Bartsch, Sarah M., Benjamin A. Lopman, Sachiko Ozawa, Aron J. Hall, and Bruce Y. Lee. “Global Economic Burden of Norovirus Gastroenteritis.” *PLOS ONE* 11, no. 4 (April 2016): e0151219–e0151219. https://doi.org/10.1371/JOURNAL.PONE.0151219.

Baum, Alina, and Adolfo García-Sastre. “Differential Recognition of Viral RNA by RIG-I.” *Http://Dx.Doi.Org/10.4161/Viru.2.2.15481* 2, no. 2 (2011): 166–69. https://doi.org/10.4161/VIRU.2.2.15481.

Begitt, Andreas, Mathias Droescher, Thomas Meyer, Christoph D. Schmid, Michelle Baker, Filipa Antunes, Markus R. Owen, Ronald Naumann, Thomas Decker, and Uwe Vinkemeier. “STAT1-Cooperative DNA Binding Distinguishes Type 1 from Type 2 Interferon Signaling.” *Nature Immunology 2014 15:2* 15, no. 2 (January 2014): 168–76. https://doi.org/10.1038/ni.2794.

Bielig, Harald, Katja Lautz, Peter R. Braun, Maureen Menning, Nikolaus Machuy, Christine Brügmann, Sandra Barisic, et al. “The Cofilin Phosphatase Slingshot Homolog 1 (SSH1) Links NOD1 Signaling to Actin Remodeling.” *PLOS Pathogens* 10, no. 9 (September 2014): e1004351–e1004351. https://doi.org/10.1371/JOURNAL.PPAT.1004351.

Biering, Scott B., Jayoung Choi, Rachel A. Halstrom, Hailey M. Brown, Wandy L. Beatty, Sanghyun Lee, Broc T. McCune, et al. “Viral Replication Complexes Are Targeted by LC3-Guided Interferon-Inducible GTPases.” *Cell Host & Microbe* 22, no. 1 (July 2017): 74-85.e7. https://doi.org/10.1016/J.CHOM.2017.06.005.

Chan, Martin C.W., Y. P. Wong, and Wai K. Leung. “Cell Culture Assay for Human Noroviruses.” *Emerging Infectious Diseases* 13, no. 7 (2007): 1117–1117. https://doi.org/10.3201/EID1307.070131.

Chan, Ying Kai, and Michaela U. Gack. “A Phosphomimetic-Based Mechanism of Dengue Virus to Antagonize Innate Immunity.” *Nature Immunology* 17, no. 5 (2016): 523–30. https://doi.org/10.1038/ni.3393.

Chang, Kyeong Ok, Stanislav V. Sosnovtsev, Gaël Belliot, Adriene D. King, and Kim Y. Green. “Stable Expression of a Norwalk Virus RNA Replicon in a Human Hepatoma Cell Line.” *Virology* 353, no. 2 (September 2006): 463–73. https://doi.org/10.1016/J.VIROL.2006.06.006.

Chaudhry, Yasmin, Arabinda Nayak, Marie Eve Bordeleau, Junichi Tanaka, Jerry Pelletier, Graham J. Belsham, Lisa O. Roberts, and Ian G. Goodfellow. “Caliciviruses Differ in Their Functional Requirements for EIF4F Components.” *Journal of Biological Chemistry* 281, no. 35 (September 2006): 25315–25. https://doi.org/10.1074/jbc.M602230200.

Chen, Xiaomin, Uwe Vinkemeier, Yanxiang Zhao, David Jeruzalmi, James E. Darnell, and John Kuriyan. “Crystal Structure of a Tyrosine Phosphorylated STAT-1 Dimer Bound to DNA.” *Cell* 93, no. 5 (May 1998): 827–39. https://doi.org/10.1016/S0092-8674(00)81443-9.

Chhabra, Preeti, Miranda de Graaf, Gabriel I. Parra, Martin Chi Wai Chan, Kim Green, Vito Martella, Qiuhong Wang, et al. “Updated Classification of Norovirus Genogroups and Genotypes.” *Journal of General Virology* 100, no. 10 (September 2019): 1393–1406. https://doi.org/10.1099/JGV.0.001318/CITE/REFWORKS.

Chung, Liliane, Dalan Bailey, Eoin N. Leen, Edward P. Emmott, Yasmin Chaudhry, Lisa O. Roberts, Stephen Curry, Nicolas Locker, and Ian G. Goodfellow. “Norovirus Translation Requires an Interaction between the C Terminus of the Genome-Linked Viral Protein VPg and Eukaryotic Translation Initiation Factor 4G.” *Journal of Biological Chemistry* 289, no. 31 (August 2014): 21738–50. https://doi.org/10.1074/jbc.M114.550657.

Cohen, Patricia T W. “Protein Phosphatase 1--Targeted in Many Directions.” *Journal of Cell Science* 115, no. Pt 2 (2002): 241–56.

Davies, Colin, and Vernon K. Ward. “Expression of the NS5 (VPg) Protein of Murine Norovirus Induces a G1/S Phase Arrest.” *PLOS ONE* 11, no. 8 (August 2016): e0161582–e0161582. https://doi.org/10.1371/JOURNAL.PONE.0161582.

Dixit, Evelyn, and Jonathan C. Kagan. “Intracellular Pathogen Detection by RIG-I-Like Receptors.” *Advances in Immunology* 117 (2013): 99–125. https://doi.org/10.1016/B978-0-12-410524-9.00004-9.

Du, Yijun, Jingshan Bi, Jiyu Liu, Xing Liu, Xiangju Wu, Ping Jiang, Dongwan Yoo, et al. “3C pro of Foot-and-Mouth Disease Virus Antagonizes the Interferon Signaling Pathway by Blocking STAT1/STAT2 Nuclear Translocation.” *Journal of Virology* 88, no. 9 (May 2014): 4908–20. https://doi.org/10.1128/JVI.03668-

13/ASSET/1D2D89EE-6BE8-49EB-98DC-EF17EBD65095/ASSETS/GRAPHIC/ZJV9990989200010.JPEG.

Duizer, Erwin, Kellogg J. Schwab, Frederick H. Neill, Robert L. Atmar, Marion P.G. Koopmans, and Mary K. Estes. “Laboratory Efforts to Cultivate Noroviruses.” *Journal of General Virology* 85, no. 1 (January 2004): 79–87. https://doi.org/10.1099/VIR.0.19478-0/CITE/REFWORKS.

Eto, Masumi, Jason A. Kirkbride, and David L. Brautigan. “Assembly of MYPT1 with Protein Phosphatase-1 in Fibroblasts Redirects Localization and Reorganizes the Actin Cytoskeleton.” *Cell Motility and the Cytoskeleton* 62, no. 2 (2005): 100–109. https://doi.org/10.1002/cm.20088.

Fagerlund, Riku, Krister Melé, Leena Kinnunen, and Ilkka Julkunen. “Arginine/Lysine-Rich Nuclear Localization Signals Mediate Interactions between Dimeric STATs and Importin ÃŽÂ±5*.” *Journal of Biological Chemistry* 277, no. 33 (2002): 30072–78. https://doi.org/10.1074/jbc.M202943200.

Fujioka, Yoichiro, Masumi Tsuda, Asuka Nanbo, Tomoe Hattori, Junko Sasaki, Takehiko Sasaki, Tadaaki Miyazaki, and Yusuke Ohba. “A Ca2+-Dependent Signalling Circuit Regulates Influenza A Virus Internalization and Infection.” *Nature Communications* 4 (2013): 1–13. https://doi.org/10.1038/ncomms3763.

Gack, Michaela U., Estanislao Nistal-Villán, Kyung-Soo Inn, Adolfo García-Sastre, and Jae U. Jung. “Phosphorylation-Mediated Negative Regulation of RIG-I Antiviral Activity.” *Journal of Virology* 84, no. 7 (April 2010): 3220–29. https://doi.org/10.1128/JVI.02241-09/ASSET/000E8576-1921-4806-A7F7-E0BBFA629AFA/ASSETS/GRAPHIC/ZJV9990930130007.JPEG.

Glass, Roger I., Umesh D. Parashar, and Mary K. Estes. “Norovirus Gastroenteritis.” *Https://Doi.Org/10.1056/NEJMra0804575* 361, no. 18 (October 2009): 1776–85. https://doi.org/10.1056/NEJMRA0804575.

Goodfellow, Ian. “The Genome-Linked Protein VPg of Vertebrate Viruses — a Multifaceted Protein.” *Current Opinion in Virology* 1, no. 5 (November 2011): 355–62. https://doi.org/10.1016/J.COVIRO.2011.09.003.

Goodfellow, Ian, Yasmin Chaudhry, Ioanna Gioldasi, Andreas Gerondopoulos, Alessandro Natoni, Louisette Labrie, Jean François Laliberté, and Lisa Roberts. “Calicivirus Translation Initiation Requires an Interaction between VPg and EIF4E.” *EMBO Reports* 6, no. 10 (October 2005): 968–72. https://doi.org/10.1038/SJ.EMBOR.7400510.

Goubau, Delphine, Safia Deddouche, and Caetano Reis e Sousa. “Cytosolic Sensing of Viruses.” *Immunity* 38, no. 5 (2013): 855–69. https://doi.org/10.1016/j.immuni.2013.05.007.

Grassie, Michael E., Lori D. Moffat, Michael P. Walsh, and Justin A. MacDonald. “The Myosin Phosphatase Targeting Protein (MYPT) Family: A Regulated Mechanism for Achieving Substrate Specificity of the Catalytic Subunit of Protein Phosphatase

Type 1δ." *Archives of Biochemistry and Biophysics* 510, no. 2 (2011): 147–59. https://doi.org/10.1016/j.abb.2011.01.018.

Hartmann, G. "Nucleic Acid Immunity." *Advances in Immunology* 133 (January 2017): 121–69. https://doi.org/10.1016/BS.AI.2016.11.001.

Heroes, Ewald, Bart Lesage, Janina Görnemann, Monique Beullens, Luc Van Meervelt, and Mathieu Bollen. "The PP1 Binding Code: A Molecular-Lego Strategy That Governs Specificity." *FEBS Journal* 280, no. 2 (2013): 584–95. https://doi.org/10.1111/j.1742-4658.2012.08547.x.

Hirano, Katsuya, Brigitte C. Phan, and David J. Hartshorne. "Interactions of the Subunits of Smooth Muscle Myosin Phosphatase." *Journal of Biological Chemistry* 272, no. 6 (1997): 3683–88. https://doi.org/10.1074/jbc.272.6.3683.

Hoeve, Johanna ten, Maria de Jesus Ibarra-Sanchez, Yubin Fu, Wei Zhu, Michel Tremblay, Michael David, and Ke Shuai. "Identification of a Nuclear Stat1 Protein Tyrosine Phosphatase." *Molecular and Cellular Biology* 22, no. 16 (August 2002): 5662–68. https://doi.org/10.1128/MCB.22.16.5662-5668.2002.

Hornung, Veit, Hiroki Kato, Hendrik Poeck, Shizuo Akira, Karl-klaus Conzelmann, and Martin Schlee. "5'-Triphosphate RNA Is the Ligand for RIG-I." *Science* 314 (2006): 994–97. https://doi.org/10.1126/science.1132505.

Horvath, Curt M. "Weapons of STAT Destruction." *European Journal of Biochemistry* 271, no. 23–24 (December 2004): 4621–28. https://doi.org/10.1111/J.1432-1033.2004.04425.X.

Hosmillo, Myra, Jia Lu, Michael R. McAllaster, James B. Eaglesham, Xinjie Wang, Edward Emmott, Patricia Domingues, et al. "Noroviruses Subvert the Core Stress Granule Component G3BP1 to Promote Viral VPg-Dependent Translation." *ELife* 8 (August 2019). https://doi.org/10.7554/ELIFE.46681.

Humphries, Ashley C., and Michael Way. "The Non-Canonical Roles of Clathrin and Actin in Pathogen Internalization, Egress and Spread." *Nature Reviews Microbiology* 11, no. 8 (2013): 551–60. https://doi.org/10.1038/nrmicro3072.

Hwang, Seungmin, Nicole S. Maloney, Monique W. Bruinsma, Gautam Goel, Erning Duan, Lei Zhang, Bimmi Shrestha, et al. "Nondegradative Role of Atg5-Atg12/ Atg16L1 Autophagy Protein Complex in Antiviral Activity of Interferon Gamma." *Cell Host & Microbe* 11, no. 4 (April 2012): 397–409. https://doi.org/10.1016/J.CHOM.2012.03.002.

Ito, Masaaki, Takeshi Nakano, Ferenc Erd‹ di, and David J Hartshorne. "Myosin Phosphatase: Structure, Regulation and Function." Vol. 259. Molecular and Cellular Biochemistry, 2004.

Jiang, Fuguo, Anand Ramanathan, Matthew T. Miller, Guo Qing Tang, Michael Gale, Smita S. Patel, and Joseph Marcotrigiano. "Structural Basis of RNA Recognition and Activation by Innate Immune Receptor RIG-I." *Nature 2011 479:7373* 479, no. 7373 (September 2011): 423–27. https://doi.org/10.1038/nature10537.

Jones, Melissa K., Katrina R. Grau, Veronica Costantini, Abimbola O. Kolawole, Miranda De Graaf, Pamela Freiden, Christina L. Graves, et al. “Human Norovirus Culture in B Cells.” *Nature Protocols 2015 10:12* 10, no. 12 (October 2015): 1939–47. https://doi.org/10.1038/nprot.2015.121.

Kapikian, Albert Z., Richard G. Wyatt, Raphael Dolin, Thomas S. Thornhill, Anthony R. Kalica, and Robert M. Chanock. “Visualization by Immune Electron Microscopy of a 27-Nm Particle Associated with Acute Infectious Nonbacterial Gastroenteritis.” *Journal of Virology* 10, no. 5 (November 1972): 1075–81. https://doi.org/10.1128/JVI.10.5.1075-1081.1972.

Karst, Stephanie M., and Scott A. Tibbetts. “Recent Advances in Understanding Norovirus Pathogenesis.” *Journal of Medical Virology* 88, no. 11 (November 2016): 1837–43. https://doi.org/10.1002/JMV.24559.

Karst, Stephanie M., Christiane E. Wobus, Margarita Lay, John Davidson, and Herbert W. Virgin IV. “STAT1-Dependent Innate Immunity to a Norwalk-like Virus.” *Science* 299, no. 5612 (March 2003): 1575–78. https://doi.org/10.1126/SCIENCE.1077905/SUPPL_FILE/KARST.SOM.PDF.

Kato, Hiroki, Osamu Takeuchi, Eriko Mikamo-Satoh, Reiko Hirai, Tomoji Kawai, Kazufumi Matsushita, Akane Hiiragi, Terence S. Dermody, Takashi Fujita, and Shizuo Akira. “Length-Dependent Recognition of Double-Stranded Ribonucleic Acids by Retinoic Acid–Inducible Gene-I and Melanoma Differentiation–Associated Gene 5.” *The Journal of Experimental Medicine* 205, no. 7 (2008): 1601–10. https://doi.org/10.1084/jem.20080091.

Kawai, Taro, and Shizuo Akira. “The Role of Pattern-Recognition Receptors in Innate Immunity: Update on Toll-like Receptors.” *Nature Immunology 2010 11:5* 11, no. 5 (April 2010): 373–84. https://doi.org/10.1038/ni.1863.

Keestra, A. Marijke, Maria G. Winter, Josef J. Auburger, Simon P. Fräßle, Mariana N. Xavier, Sebastian E. Winter, Anita Kim, et al. “Manipulation of Small Rho GTPases Is a Pathogen-Induced Process Detected by NOD1.” *Nature 2013 496:7444* 496, no. 7444 (March 2013): 233–37. https://doi.org/10.1038/nature12025.

Khromov, Alexander, Nandini Choudhury, Andra S. Stevenson, Avril V. Somiyo, and Masumi Eto. “Phosphorylation-Dependent Autoinhibition of Myosin Light Chain Phosphatase Accounts for Ca2+sensitization Force of Smooth Muscle Contraction.” *Journal of Biological Chemistry* 284, no. 32 (2009): 21569–79. https://doi.org/10.1074/jbc.M109.019729.

Kimura, Kazushi, Masaaki Ito, Mutsuki Amano, Kazuyasu Chihara, Yuko Fukata, Kazushi Kimura, Masaaki Ito, and Mutsuki Amano. “Regulation of Myosin Phosphatase by Rho and Rho-Associated Kinase (Rho- Kinase) Masato Nakafuku , Bunpei Yamamori , Jianhua Feng , Takeshi Nakano , Katsuya Okawa , Akihiro Iwamatsu and Kozo Kaibuchi Published by : American Association for the Advancemen” 273, no. 5272 (2018): 245–48.

Koga, Yasuhiko, and Mitsuo Ikebe. “A Novel Regulatory Mechanism of Myosin Light Chain Phosphorylation via Binding of 14-3-3 to Myosin Phosphatase.” *Molecular Biology of the Cell* 19 (2008): 1062–71. https://doi.org/10.1091/mbc.E07.

Koo, Hoonmo L., Frederick H. Neill, Mary K. Estes, Flor M. Munoz, Arlin Cameron, Herbert L. DuPont, and Robert L. Atmar. “Noroviruses: The Most Common Pediatric Viral Enteric Pathogen at a Large University Hospital After Introduction of Rotavirus Vaccination.” *Journal of the Pediatric Infectious Diseases Society* 2, no. 1 (March 2012): 57–60. https://doi.org/10.1093/JPIDS/PIS070.

Korrodi-Gregório, Luís, Sara L.C. Esteves, and Margarida Fardilha. “Protein Phosphatase 1 Catalytic Isoforms: Specificity toward Interacting Proteins.” *Translational Research* 164, no. 5 (2014): 366–91. https://doi.org/10.1016/j.trsl.2014.07.001.

Kumar, Amrita, Jin Hyang Kim, Priya Ranjan, Maureen G. Metcalfe, Weiping Cao, Margarita Mishina, Shivaprakash Gangappa, et al. “Influenza Virus Exploits Tunneling Nanotubes for Cell-to-Cell Spread.” *Scientific Reports* 7 (2017): 1–14. https://doi.org/10.1038/srep40360.

Lazear, Helen M., John W. Schoggins, and Michael S. Diamond. “Shared and Distinct Functions of Type I and Type III Interferons.” *Immunity* 50, no. 4 (April 2019): 907–23. https://doi.org/10.1016/J.IMMUNI.2019.03.025.

Leen, Eoin N., K. Y. Rex Kwok, James R. Birtley, Peter J. Simpson, Chennareddy V. Subba-Reddy, Yasmin Chaudhry, Stanislav V. Sosnovtsev, et al. “Structures of the Compact Helical Core Domains of Feline Calicivirus and Murine Norovirus VPg Proteins.” *Journal of Virology* 87, no. 10 (May 2013): 5318–30. https://doi.org/10.1128/JVI.03151-12/ASSET/4421B588-34B6-4404-87CE-B84C655130DF/ASSETS/GRAPHIC/ZJV9990976380008.JPEG.

Legrand-Poels, Sylvie, Gaelle Kustermans, Françoise Bex, Elisabeth Kremmer, Thomas A. Kufer, and Jacques Piette. “Modulation of Nod2-Dependent NF-KB Signaling by the Actin Cytoskeleton.” *Journal of Cell Science* 120, no. 7 (April 2007): 1299–1310. https://doi.org/10.1242/JCS.03424.

Levy, David E., and J. E. Darnell. “STATs: Transcriptional Control and Biological Impact.” *Nature Reviews Molecular Cell Biology 2002 3:9* 3, no. 9 (2002): 651–62. https://doi.org/10.1038/nrm909.

Li, Chunfeng, Audrey Lee, Lilit Grigoryan, Prabhu S. Arunachalam, Madeleine K.D. Scott, Meera Trisal, Florian Wimmers, et al. “Mechanisms of Innate and Adaptive Immunity to the Pfizer-BioNTech BNT162b2 Vaccine.” *Nature Immunology 2022 23:4* 23, no. 4 (March 2022): 543–55. https://doi.org/10.1038/s41590-022-01163-9.

Liu, Guan Qun, Jung Hyun Lee, Zachary M. Parker, Dhiraj Acharya, Jessica J. Chiang, Michiel van Gent, William Riedl, et al. “ISG15-Dependent Activation of the Sensor MDA5 Is Antagonized by the SARS-CoV-2 Papain-like Protease to Evade Host Innate Immunity.” *Nature Microbiology 2021 6:4* 6, no. 4 (March 2021): 467–78. https://doi.org/10.1038/s41564-021-00884-1.

Liu, Helene Minyi, Yueh Ming Loo, Stacy M. Horner, Gregory A. Zornetzer, Michael G. Katze, and Michael Gale. “The Mitochondrial Targeting Chaperone 14-3-3ε Regulates a RIG-I Translocon That Mediates Membrane Association and Innate Antiviral Immunity.” *Cell Host and Microbe* 11, no. 5 (2012): 528–37. https://doi.org/10.1016/j.chom.2012.04.006.

Liu, Siqi, Xin Cai, Jiaxi Wu, Qian Cong, Xiang Chen, Tuo Li, Fenghe Du, et al. “Phosphorylation of Innate Immune Adaptor Proteins MAVS, STING, and TRIF Induces IRF3 Activation.” *Science* 347, no. 6227 (March 2015). https://doi.org/10.1126/SCIENCE.AAA2630/SUPPL_FILE/LIU.SM.REVISION.1.PDF.

Liu, Su Yang, David Jesse Sanchez, Roghiyh Aliyari, Sun Lu, and Genhong Cheng. “Systematic Identification of Type I and Type II Interferon-Induced Antiviral Factors.” *Proceedings of the National Academy of Sciences of the United States of America* 109, no. 11 (March 2012): 4239–44. https://doi.org/10.1073/PNAS.1114981109/SUPPL_FILE/ST05.DOCX.

Loo, Yueh-Ming, and Michael Gale. “Immunity Review Immune Signaling by RIG-I-like Receptors,” 2011. https://doi.org/10.1016/j.immuni.2011.05.003.

Mao, Xiang, Zhiyong Ren, Gregory N. Parker, Holger Sondermann, Michael A. Pastorello, Wei Wang, John S. McMurray, Borries Demeler, James E. Darnell, and Xiaomin Chen. “Structural Bases of Unphosphorylated STAT1 Association and Receptor Binding.” *Molecular Cell* 17, no. 6 (March 2005): 761–71. https://doi.org/10.1016/J.MOLCEL.2005.02.021.

Marsh, Mark, and Ari Helenius. “Virus Entry: Open Sesame.” *Cell* 124, no. 4 (2006): 729–40. https://doi.org/10.1016/j.cell.2006.02.007.

Mboko, Wadzanai P., Preeti Chhabra, Marta Diez Valcarce, Veronica Costantini, and Jan Vinjé. “Advances in Understanding of the Innate Immune Response to Human Norovirus Infection Using Organoid Models.” *The Journal of General Virology* 103, no. 1 (2022). https://doi.org/10.1099/JGV.0.001720.

McAtee, Casey L., Rachel Webman, Robert H. Gilman, Carolina Mejia, Caryn Bern, Sonia Apaza, Susan Espetia, et al. “Burden of Norovirus and Rotavirus in Children after Rotavirus Vaccine Introduction, Cochabamba, Bolivia.” *The American Journal of Tropical Medicine and Hygiene* 94, no. 1 (January 2016): 212–212. https://doi.org/10.4269/AJTMH.15-0203.

McBride, Kevin M., Gregg Banninger, Christine McDonald, and Nancy C. Reich. “Regulated Nuclear Import of the STAT1 Transcription Factor by Direct Binding of Importin-α.” *The EMBO Journal* 21, no. 7 (April 2002): 1754–63. https://doi.org/10.1093/EMBOJ/21.7.1754.

McBride, Kevin M., and Nancy C. Reich. “The Ins and Outs of STAT1 Nuclear Transport.” *Science’s STKE* 2003, no. 195 (August 2003). https://doi.org/10.1126/STKE.2003.195.RE13/ASSET/BBCCB982-9695-4D99-82F5-252B2DF3421A/ASSETS/GRAPHIC/1952003RE13F4.JPEG.

McCartney, Stephen A., Larissa B. Thackray, Leonid Gitlin, Susan Gilfillan, Herbert W. Virgin IV, and Marco Colonna. “MDA-5 Recognition of a Murine Norovirus.” *PLOS Pathogens* 4, no. 7 (July 2008): e1000108–e1000108. https://doi.org/10.1371/JOURNAL.PPAT.1000108.

McFadden, Nora, Dalan Bailey, Guia Carrara, Alicia Benson, Yasmin Chaudhry, Amita Shortland, Jonathan Heeney, et al. “Norovirus Regulation of the Innate Immune Response and Apoptosis Occurs via the Product of the Alternative Open Reading Frame 4.” *PLOS Pathogens* 7, no. 12 (December 2011): e1002413–e1002413. https://doi.org/10.1371/JOURNAL.PPAT.1002413.

McSweeney, Alice M., Vivienne L. Young, and Vernon K. Ward. “Norovirus Vpg Binds Rna through a Conserved N-Terminal k/r Basic Patch.” *Viruses* 13, no. 7 (July 2021): 1282–1282. https://doi.org/10.3390/V13071282/S1.

Mercer, Jason, and Ari Helenius. “Virus Entry by Macropinocytosis.” *Nature Cell Biology* 11, no. 5 (2009): 510–20. https://doi.org/10.1038/ncb0509-510.

Mercer, Jason, Mario Schelhaas, and Ari Helenius. “Virus Entry by Endocytosis.” *Https://Doi.Org/10.1146/Annurev-Biochem-060208-104626* 79 (June 2010): 803–33. https://doi.org/10.1146/ANNUREV-BIOCHEM-060208-104626.

Meyer, Thomas, Andreas Begitt, Inga Lo, È Dige, Marleen Van Rossum, and Uwe Vinkemeier. “Constitutive and IFN-γ-Induced Nuclear Import of STAT1 Proceed through Independent Pathways.” *The EMBO Journal* 21, no. 3 (February 2002): 344–54. https://doi.org/10.1093/EMBOJ/21.3.344.

Meylan, Etienne, Jürg Tschopp, and Michael Karin. “Intracellular Pattern Recognition Receptors in the Host Response.” *Nature 2006 442:7098* 442, no. 7098 (July 2006): 39–44. https://doi.org/10.1038/nature04946.

Moorhead, Greg B. G., Laura Trinkle-Mulcahy, and Annegret Ulke-Lemée. “Emerging Roles of Nuclear Protein Phosphatases.” *Nature Reviews Molecular Cell Biology* 8, no. 3 (2007): 234–44. https://doi.org/10.1038/nrm2126.

Moreno, Julian Eduardo, and B Videla. “Rastreando Ausencias: La Hipótesis Del Abandono Del Uso de Los Recursos Marinos En El Momento Ecuestre En La Patagonia Continental.” *Magallania* 36, no. 2 (2008): 91–104. https://doi.org/10.1016/j.tibs.2010.03.002.

Moulding, Dale A., Julien Record, Dessislava Malinova, and Adrian J. Thrasher. “Actin Cytoskeletal Defects in Immunodeficiency.” *Immunological Reviews* 256, no. 1 (November 2013): 282–99. https://doi.org/10.1111/IMR.12114.

Mulder, Jacqueline, Aafke Ariaens, Dick van den Boomen, and Wouter H. Moolenaar. “P116Rip Targets Myosin Phosphatase to the Actin Cytoskeleton and Is Essential for RhoA/ROCK-Regulated Neuritogenesis.” *Molecular Biology of the Cell* 15, no. 12 (2004): 5516–27. https://doi.org/10.1091/mbc.E04-04-0275.

Mulder, Jacqueline, Mieke Poland, Martijn F.B.G. Gebbink, Jero Calafat, Wouter H. Moolenaar, and Onno Kranenburg. “P116Rip Is a Novel Filamentous Actin-Binding

Protein." *Journal of Biological Chemistry* 278, no. 29 (2003): 27216–23. https://doi.org/10.1074/jbc.M302399200.

Nair, Jayasree S., Christopher J. DaFonseca, Agneta Tjernberg, Wei Sun, James E. Darnell, Brian T. Chait, and J. Jillian Zhang. "Requirement of Ca2+ and CaMKII for Stat1 Ser-727 Phosphorylation in Response to IFN-γ." *Proceedings of the National Academy of Sciences* 99, no. 9 (April 2002): 5971–76. https://doi.org/10.1073/PNAS.052159099.

Najjar, I., and R. Fagard. "STAT1 and Pathogens, Not a Friendly Relationship." *Biochimie* 92, no. 5 (May 2010): 425–44. https://doi.org/10.1016/J.BIOCHI.2010.02.009.

Netzler, Natalie E., Daniel Enosi Tuipulotu, and Peter A. White. "Norovirus Antivirals: Where Are We Now?" *Medicinal Research Reviews* 39, no. 3 (May 2018): 860–86. https://doi.org/10.1002/MED.21545.

Paludan, Søren R., and Andrew G. Bowie. "Immune Sensing of DNA." *Immunity* 38, no. 5 (May 2013): 870–80. https://doi.org/10.1016/J.IMMUNI.2013.05.004.

Papa, Riccardo, Federica Penco, Stefano Volpi, and Marco Gattorno. "Actin Remodeling Defects Leading to Autoinflammation and Immune Dysregulation." *Frontiers in Immunology* 11 (January 2020): 3335–3335. https://doi.org/10.3389/FIMMU.2020.604206/BIBTEX.

Papafragkou, Efstathia, Joanne Hewitt, Geun Woo Park, Gail Greening, and Jan Vinjé. "Challenges of Culturing Human Norovirus in Three-Dimensional Organoid Intestinal Cell Culture Models." *PLOS ONE* 8, no. 6 (June 2013): e63485–e63485. https://doi.org/10.1371/JOURNAL.PONE.0063485.

Park, Sungwoo, Jayoung Choi, Scott B. Biering, Erin Dominici, Lelia E. Williams, and Seungmin Hwang. "Targeting by AutophaGy Proteins (TAG): Targeting of IFNG-Inducible GTPases to Membranes by the LC3 Conjugation System of Autophagy." *Autophagy* 12, no. 7 (July 2016): 1153–67. https://doi.org/10.1080/15548627.2016.1178447/SUPPL_FILE/KAUP_A_1178447_SM1407.ZIP.

Peisley, Alys, Bin Wu, Hui Xu, Zhijian J. Chen, and Sun Hur. "Structural Basis for Ubiquitin-Mediated Antiviral Signal Activation by RIG-I." *Nature 2014 509:7498* 509, no. 7498 (March 2014): 110–14. https://doi.org/10.1038/nature13140.

Peisley, Alys, Bin Wu, Hui Yao, Thomas Walz, and Sun Hur. "RIG-I Forms Signaling-Competent Filaments in an ATP-Dependent, Ubiquitin-Independent Manner." *Molecular Cell* 51, no. 5 (September 2013): 573–83. https://doi.org/10.1016/J.MOLCEL.2013.07.024.

Perng, Yi Chieh, and Deborah J. Lenschow. "ISG15 in Antiviral Immunity and Beyond." *Nature Reviews Microbiology* 16, no. 7 (2018): 423–39. https://doi.org/10.1038/s41579-018-0020-5.

Pichlmair, A, O Schulz, C P Tan, T I Naslund, P Liljestrom, F Weber, and C Reis e Sousa. “RIG-I-Mediated Antiviral Response to Single-Stranded RNA Bearing 5’-Phosphates.” *Science* 314, no. November (2006): 997–1002.

Pilz, Andreas, Katrin Ramsauer, Hamid Heidari, Michael Leitges, Pavel Kovarik, and Thomas Decker. “Phosphorylation of the Stat1 Transactivating Domain Is Required for the Response to Type I Interferons.” *EMBO Reports* 4, no. 4 (April 2003): 368–73. https://doi.org/10.1038/SJ.EMBOR.EMBOR802.

Platanias, Leonidas C. “Mechanisms of Type-I- and Type-II-Interferon-Mediated Signalling.” *Nature Reviews Immunology 2005 5:5* 5, no. 5 (May 2005): 375–86. https://doi.org/10.1038/nri1604.

Ploubidou, Aspasia, and Michael Way. “Viral Transport and the Cytoskeleton.” *Current Opinion in Cell Biology* 13, no. 1 (February 2001): 97–105. https://doi.org/10.1016/S0955-0674(00)00180-0.

Radtke, Kerstin, Katinka Döhner, and Beate Sodeik. “The Voyage Starts.” *Cellular Microbiology* 8, no. 3 (2006): 387–400. https://doi.org/10.1111/j.1462-5822.2005.00679.x.

Ran, F. Ann, Patrick D. Hsu, Jason Wright, Vineeta Agarwala, David A. Scott, and Feng Zhang. “Genome Engineering Using the CRISPR-Cas9 System.” *Nature Protocols* 8, no. 11 (2013): 2281–2308. https://doi.org/10.1038/nprot.2013.143.

Ratia, Kiira, Kumar Singh Saikatendu, Bernard D. Santarsiero, Naina Barreto, Susan C. Baker, Raymond C. Stevens, and Andrew D. Mesecar. “Severe Acute Respiratory Syndrome Coronavirus Papain-like-Protease: Structure of a Viral Deubiquitinating Enzyme.” *Proceedings of the National Academy of Sciences of the United States of America* 103, no. 15 (2006): 5717–22. https://doi.org/10.1073/pnas.0510851103.

Rehwinkel, Jan, and Michaela U. Gack. “RIG-I-like Receptors: Their Regulation and Roles in RNA Sensing.” *Nature Reviews Immunology 2020 20:9* 20, no. 9 (March 2020): 537–51. https://doi.org/10.1038/s41577-020-0288-3.

Reikine, Stephanie, Jennifer B. Nguyen, and Yorgo Modis. “Pattern Recognition and Signaling Mechanisms of RIG-I and MDA5.” *Frontiers in Immunology* 5, no. JUL (July 2014): 342–342. https://doi.org/10.3389/FIMMU.2014.00342/BIBTEX.

Rengachari, Srinivasan, Silvia Groiss, Juliette M. Devos, Elise Caron, Nathalie Grandvaux, and Daniel Panne. “Structural Basis of STAT2 Recognition by IRF9 Reveals Molecular Insights into ISGF3 Function.” *Proceedings of the National Academy of Sciences of the United States of America* 115, no. 4 (January 2017): E601–9. https://doi.org/10.1073/PNAS.1718426115/SUPPL_FILE/PNAS.201718426SI.PDF.

Riddick, Nadeene, Ken Ichi Ohtani, and Howard K. Surks. “Targeting by Myosin Phosphatase-RhoA Interacting Protein Mediates RhoA/ROCK Regulation of Myosin Phosphatase.” *Journal of Cellular Biochemistry* 103, no. 4 (2008): 1158–70. https://doi.org/10.1002/jcb.21488.

Roberts, Kari L., Balaji Manicassamy, and Robert A. Lamb. “Influenza A Virus Uses Intercellular Connections To Spread to Neighboring Cells.” *Journal of Virology* 89, no. 3 (2015): 1537–49. https://doi.org/10.1128/JVI.03306-14.

Rossman, J. S., G. P. Leser, and R. A. Lamb. “Filamentous Influenza Virus Enters Cells via Macropinocytosis.” *Journal of Virology* 86, no. 20 (2012): 10950–60. https://doi.org/10.1128/JVI.05992-11.

Sadzak, Iwona, Melanie Schiff, Irene Gattermeier, Reingard Glinitzer, Ines Sauer, Armin Saalmüller, Edward Yang, Barbara Schaljo, and Pavel Kovarik. “Recruitment of Stat1 to Chromatin Is Required for Interferon-Induced Serine Phosphorylation of Stat1 Transactivation Domain.” *Proceedings of the National Academy of Sciences of the United States of America* 105, no. 26 (July 2008): 8944–49. https://doi.org/10.1073/PNAS.0801794105/SUPPL_FILE/0801794105SI.PDF.

Sanchez, Jacint G., Konstantin M.J. Sparrer, Cindy Chiang, Rebecca A. Reis, Jessica J. Chiang, Matthew A. Zurenski, Yueping Wan, Michaela U. Gack, and Owen Pornillos. “TRIM25 Binds RNA to Modulate Cellular Anti-Viral Defense.” *Journal of Molecular Biology*, no. xxxx (2018): 1–14. https://doi.org/10.1016/j.jmb.2018.10.003.

Schroder, Kate, Paul J. Hertzog, Timothy Ravasi, and David A. Hume. “Interferon-γ: An Overview of Signals, Mechanisms and Functions.” *Journal of Leukocyte Biology* 75, no. 2 (February 2003): 163–89. https://doi.org/10.1189/JLB.0603252.

Sekimoto, Toshihiro, Naoko Imamoto, Koichi Nakajima, Toshio Hirano, and Yoshihiro Yoneda. “Extracellular Signal-Dependent Nuclear Import of Stat1 Is Mediated by Nuclear Pore-Targeting Complex Formation with NPI-1, but Not Rch1.” *The EMBO Journal* 16, no. 23 (December 1997): 7067–77. https://doi.org/10.1093/EMBOJ/16.23.7067.

Shi, Yigong. “Serine/Threonine Phosphatases: Mechanism through Structure.” *Cell* 139, no. 3 (2009): 468–84. https://doi.org/10.1016/j.cell.2009.10.006.

Skaug, Brian, and Zhijian J. Chen. “Emerging Role of ISG15 in Antiviral Immunity.” *Cell* 143, no. 2 (2010): 187–90. https://doi.org/10.1016/j.cell.2010.09.033.

Snowden, Joseph S., Daniel L. Hurdiss, Oluwapelumi O. Adeyemi, Neil A. Ranson, Morgan R. Herod, and Nicola J. Stonehouse. “Dynamics in the Murine Norovirus Capsid Revealed by High-Resolution Cryo-EM.” *PLOS Biology* 18, no. 3 (2020): e3000649–e3000649. https://doi.org/10.1371/JOURNAL.PBIO.3000649.

Sodeik, Beate. “Mechanisms of Viral Transport in the Cytoplasm.” *Trends in Microbiology* 8, no. 10 (October 2000): 465–72. https://doi.org/10.1016/S0966-842X(00)01824-2.

Steinparzer, Iris, Vitaly Sedlyarov, Jonathan D. Rubin, Kevin Eislmayr, Matthew D. Galbraith, Cecilia B. Levandowski, Terezia Vcelkova, et al. “Transcriptional Responses to IFN-γ Require Mediator Kinase-Dependent Pause Release and Mechanistically Distinct CDK8 and CDK19 Functions.” *Molecular Cell* 76, no. 3 (November 2019): 485-499.e8. https://doi.org/10.1016/J.MOLCEL.2019.07.034.

Straub, Timothy M., Kerstin Höner Zu Bentrup, Patricia Orosz-Coghlan, Alice Dohnalkova, Brooke K. Mayer, Rachel A. Bartholomew, Catherine O. Valdez, et al. “In Vitro Cell Culture Infectivity Assay for Human Noroviruses.” *Emerging Infectious Diseases* 13, no. 3 (2007): 396–396. https://doi.org/10.3201/EID1303.060549.

Suela, Traian. “Letter to the Editor Deubiquitination , a New Function of the Severe Acute Respiratory Syndrome.” *Journal of Virology* 79, no. 7 (2005): 4550–51. https://doi.org/10.1128/JVI.79.7.4550.

Sugai, Akihiro, Hiroki Sato, Ikuyo Takayama, Misako Yoneda, and Chieko Kai. “Nipah and Hendra Virus Nucleoproteins Inhibit Nuclear Accumulation of Signal Transducer and Activator of Transcription 1 (STAT1) and STAT2 by Interfering with Their Complex Formation.” *Journal of Virology* 91, no. 21 (November 2017): 1136–53. https://doi.org/10.1128/JVI.01136-17/ASSET/CDFCD4F2-34E2-4C05-9576-FA02C62AAEA5/ASSETS/GRAPHIC/ZJV9991830440005.JPEG.

Surks, Howard K., Christopher T. Richards, and Michael E. Mendelsohn. “Myosin Phosphatase-Rho Interacting Protein: A New Member of the Myosin Phosphatase Complex That Directly Binds RhoA.” *Journal of Biological Chemistry* 278, no. 51 (2003): 51484–93. https://doi.org/10.1074/jbc.M305622200.

Tan, Ivan, Chong Han Ng, Louis Lim, and Thomas Leung. “Phosphorylation of a Novel Myosin Binding Subunit of Protein Phosphatase 1 Reveals a Conserved Mechanism in the Regulation of Actin Cytoskeleton.” *Journal of Biological Chemistry* 276, no. 24 (2001): 21209–16. https://doi.org/10.1074/jbc.M102615200.

Taylor, Matthew P., Orkide O. Koyuncu, and Lynn W. Enquist. “Subversion of the Actin Cytoskeleton during Viral Infection.” *Nature Reviews Microbiology* 9, no. 6 (2011): 427–39. https://doi.org/10.1038/nrmicro2574.

Terrak, Mohammed, Frederic Kerff, Knut Langseimo, Terence Tao, and Roberto Dominguez. “Structural Basis of Protein Phosphatase 1 Regulation.” *Nature* 429, no. 6993 (2004): 780–84. https://doi.org/10.1038/nature02582.

Tessier, Tanner M., Mackenzie J. Dodge, Martin A. Prusinkiewicz, and Joe S. Mymryk. “Viral Appropriation: Laying Claim to Host Nuclear Transport Machinery.” *Cells 2019, Vol. 8, Page 559* 8, no. 6 (June 2019): 559–559. https://doi.org/10.3390/CELLS8060559.

Thackray, Larissa B., Christiane E. Wobus, Karen A. Chachu, Bo Liu, Eric R. Alegre, Kenneth S. Henderson, Scott T. Kelley, and Herbert W. Virgin. “Murine Noroviruses Comprising a Single Genogroup Exhibit Biological Diversity despite Limited Sequence Divergence.” *Journal of Virology* 81, no. 19 (October 2007): 10460–73. https://doi.org/10.1128/JVI.00783-07/SUPPL_FILE/LEGEND_TO_FIGURE_S1.DOC.

Thorne, Lucy G., and Ian G. Goodfellow. “Norovirus Gene Expression and Replication.” *Journal of General Virology* 95, no. PART 2 (February 2014): 278–91. https://doi.org/10.1099/VIR.0.059634-0/CITE/REFWORKS.

Tolomeo, Manlio, Andrea Cavalli, and Antonio Cascio. “STAT1 and Its Crucial Role in the Control of Viral Infections.” *International Journal of Molecular Sciences 2022, Vol. 23, Page 4095* 23, no. 8 (April 2022): 4095–4095. https://doi.org/10.3390/IJMS23084095.

Uddin, Shahab, Antonella Sassano, Dilip K. Deb, Amit Verma, Beata Majchrzak, Arshad Rahman, Asrar B. Malik, Eleanor N. Fish, and Leonidas C. Platanias. “Protein Kinase C-δ (PKC-δ) Is Activated by Type I Interferons and Mediates Phosphorylation of Stat1 on Serine 727.” *Journal of Biological Chemistry* 277, no. 17 (April 2002): 14408–16. https://doi.org/10.1074/jbc.M109671200.

Varinou, Louisa, Katrin Ramsauer, Marina Karaghiosoff, Thomas Kolbe, Klaus Pfeffer, Mathias Müller, and Thomas Decker. “Phosphorylation of the Stat1 Transactivation Domain Is Required for Full-Fledged IFN-γ-Dependent Innate Immunity.” *Immunity* 19, no. 6 (December 2003): 793–802. https://doi.org/10.1016/S1074-7613(03)00322-4.

Vashist, Surender, Dalan Balley, Akos Putics, and Ian Goodfellow. “Model Systems for the Study of Human Norovirus Biology.” *Future Virology* 4, no. 4 (2009): 353–353. https://doi.org/10.2217/FVL.09.18.

Velasco, Guillermo, Chris Armstrong, Nick Morrice, Sheelagh Frame, and Philip Cohen. “Phosphorylation of the Regulatory Subunit of Smooth Muscle Protein Phosphatase 1M at Thr850 Induces Its Dissociation from Myosin.” *FEBS Letters* 527, no. 1–3 (2002): 101–4. https://doi.org/10.1016/S0014-5793(02)03175-7.

Venkataraman, Thiagarajan, Maikel Valdes, Rachel Elsby, Shigeru Kakuta, Gisela Caceres, Shinobu Saijo, Yoichiro Iwakura, and Glen N. Barber. “Loss of DExD/H Box RNA Helicase LGP2 Manifests Disparate Antiviral Responses.” *The Journal of Immunology* 178, no. 10 (May 2007): 6444–55. https://doi.org/10.4049/JIMMUNOL.178.10.6444.

Vicente-Manzanares, Miguel, Xuefei Ma, Robert S. Adelstein, and Alan Rick Horwitz. “Non-Muscle Myosin II Takes Centre Stage in Cell Adhesion and Migration.” *Nature Reviews. Molecular Cell Biology* 10, no. 11 (November 2009): 778–778. https://doi.org/10.1038/NRM2786.

Villarino, Alejandro V., Yuka Kanno, and John J. O’Shea. “Mechanisms and Consequences of Jak–STAT Signaling in the Immune System.” *Nature Immunology 2017 18:4* 18, no. 4 (March 2017): 374–84. https://doi.org/10.1038/ni.3691.

Virshup, David M., and Shirish Shenolikar. “From Promiscuity to Precision: Protein Phosphatases Get a Makeover.” *Molecular Cell* 33, no. 5 (March 2009): 537–45. https://doi.org/10.1016/J.MOLCEL.2009.02.015.

Wack, Andreas, Ewa Terczyńska-Dyla, and Rune Hartmann. “Guarding the Frontiers: The Biology of Type III Interferons.” *Nature Immunology 2015 16:8* 16, no. 8 (July 2015): 802–9. https://doi.org/10.1038/ni.3212.

Wang, Yuxin, Qiaoling Song, Wei Huang, Yuxi Lin, Xin Wang, Chenyao Wang, Belinda Willard, et al. “A Virus-Induced Conformational Switch of STAT1-STAT2 Dimers

Boosts Antiviral Defenses." *Cell Research 2020 31:2* 31, no. 2 (August 2020): 206–18. https://doi.org/10.1038/s41422-020-0386-6.

Wenta, Nikola, Holger Strauss, Stefanie Meyer, and Uwe Vinkemeier. "Tyrosine Phosphorylation Regulates the Partitioning of STAT1 between Different Dimer Conformations." *Proceedings of the National Academy of Sciences of the United States of America* 105, no. 27 (July 2008): 9238–43. https://doi.org/10.1073/PNAS.0802130105/SUPPL_FILE/0802130105SI.PDF.

Wies, Effi, May K. Wang, Natalya P. Maharaj, Kan Chen, Shenghua Zhou, Robert W. Finberg, and Michaela U. Gack. "Dephosphorylation of the RNA Sensors RIG-I and MDA5 by the Phosphatase PP1 Is Essential for Innate Immune Signaling." *Immunity* 38, no. 3 (March 2012): 437–49. https://doi.org/10.1016/J.IMMUNI.2012.11.018.

Wobus, Christiane E., Larissa B. Thackray, and IV Herbert W. Virgin. "Murine Norovirus: A Model System To Study Norovirus Biology and Pathogenesis." *Journal of Virology* 80, no. 11 (June 2006): 5104–5104. https://doi.org/10.1128/JVI.02346-05.

Yoneyama, Mitsutoshi, and Takashi Fujita. "Structural Mechanism of RNA Recognition by the RIG-I-like Receptors." *Immunity* 29, no. 2 (August 2008): 178–81. https://doi.org/10.1016/J.IMMUNI.2008.07.009.

Yoneyama, Mitsutoshi, Mika Kikuchi, Kanae Matsumoto, Tadaatsu Imaizumi, Makoto Miyagishi, Kazunari Taira, Eileen Foy, et al. "Shared and Unique Functions of the DExD/H-Box Helicases RIG-I, MDA5, and LGP2 in Antiviral Innate Immunity." *The Journal of Immunology* 175, no. 5 (September 2005): 2851–58. https://doi.org/10.4049/JIMMUNOL.175.5.2851.

Yu, Qin, Kun Qu, and Yorgo Modis. "Cryo-EM Structures of MDA5-DsRNA Filaments at Different Stages of ATP Hydrolysis." *Molecular Cell* 72, no. 6 (December 2018): 999-1012.e6. https://doi.org/10.1016/J.MOLCEL.2018.10.012.

Zhang, Jue J., Yingming Zhao, Brian T. Chait, Wyndham W. Lathem, Marion Ritzi, Rolf Knippers, and James E. Darnell. "Ser727-Dependent Recruitment of MCM5 by Stat1α in IFN-γ-Induced Transcriptional Activation." *The EMBO Journal* 17, no. 23 (December 1998): 6963–71. https://doi.org/10.1093/EMBOJ/17.23.6963.

Zhao, Chen, Mark N. Collins, Tien Ying Hsiang, and Robert M. Krug. "Interferon-Induced ISG15 Pathway: An Ongoing Virus-Host Battle." *Trends in Microbiology* 21, no. 4 (2013): 181–86. https://doi.org/10.1016/j.tim.2013.01.005.

Zhao, Chen, Haripriya Sridharan, Ran Chen, Darren P. Baker, Shanshan Wang, and Robert M. Krug. "Influenza B Virus Non-Structural Protein 1 Counteracts ISG15 Antiviral Activity by Sequestering ISGylated Viral Proteins." *Nature Communications* 7 (2016): 1–12. https://doi.org/10.1038/ncomms12754.

Zhong, Minghao, Melissa A. Henriksen, Kenji Takeuchi, Olaf Schaefer, Bin Liu, Johanna Ten Hoeve, Zhiyong Ren, et al. "Implications of an Antiparallel Dimeric Structure of Nonphosphorylated STAT1 for the Activation-Inactivation Cycle." *Proceedings of the National Academy of Sciences of the United States of America* 102, no. 11

(March 2005): 3966–71. https://doi.org/10.1073/PNAS.0501063102/ASSET/6A530139-543D-45EB-A046-0370457465C2/ASSETS/GRAPHIC/ZPQ0120577350004.JPEG.

Züst, Roland, Luisa Cervantes-Barragan, Matthias Habjan, Reinhard Maier, Benjamin W. Neuman, John Ziebuhr, Kristy J. Szretter, et al. “Ribose 2’-O-Methylation Provides a Molecular Signature for the Distinction of Self and Non-Self MRNA Dependent on the RNA Sensor Mda5.” *Nature Immunology* 12, no. 2 (2011): 137–43. https://doi.org/10.1038/ni.1979.